Regulation of the NF-κB p65 subunit by phosphorylation and ubiquitination

Inaugural-Dissertation

zur
Erlangung des Doktorgrades
der Naturwissenschaften
-Dr. rer. nat.-

vorgelegt von

Hui Geng
aus China

angefertigt am Institut für Biochemie
Fachbereich Medizin und dem Fachbereich Biologie
Justus-Liebig-Universität Giessen

Giessen, April 2008

Gutachter: **Prof. Dr. Michael Martin**

Professur für Immunologie
Fachbereich Biologie und Chemie
Justus-Liebig-Universität Giessen

Gutachter: **Prof. Dr. M. Lienhard Schmitz**

Institut für Biochemie
Fachbereich Medizin
Justus-Liebig-Universität Giessen

To my parents
Meinen Eltern
致我父母

Table of contents

Abbreviations

ABIN	A20-binding inhibitor of NF-κB
Ac	acetylation
ATM	ataxia telangiectasia-mutated
BAFF	B cell-activating factor of the TNF family
Bcl	B cell lymphoma
C-terminus	carboxy-terminus
CaMKIV	calmodulin-dependent kinase IV
CBP	CREB-binding protein
CC	coiled-coil
CCDN-1	cyclin D1
CCL-2	chemokine (C-C-motif) ligand 2
C/EBP	CCAAA/enhancer-binding protein
ChIP	chromatin immunoprecipitation
CHX	cycloheximide
cIAP	cellular inhibitor of apoptosis
CKII	casein kinase II
COMMD1	copper metabolism gene MURR1 domain-containing 1
COX-2	cyclooxygenase 2
CREB	cAMP responsive element-binding protein
CSF-2	colony stimulating factor 2
Cul	cullin
CXCL	chemokine (C-X-C motif) ligand
CYLD	cylindromatosis protein
DD	death domain
DUB	de-ubiquitinating enzyme
E1	ubiquitin-activating enzyme
E2	ubiquitin-conjugating enzyme
E3	ubiquitin ligase

E.coli	*escherichia coli*
ECS^{SOCS1}	elongin B/C, cullin-2 and SOCS1-containing multisubunit complex
EMSA	electrophoretic mobility shift assay
ERK	extracellular signal-regulated kinase
FOXO3a	forkhead box transcription factor
GAPDH	glyceraldehyde-3-phosphate dehydrogenase
GFP	green fluorescent protein
GRR	glycine-rich region
GSK3β	glycogen synthase kinase 3 beta
GST	glutathione S-transferase
HA	hemagglutinin
HAT	histone acetyltransferase
HDAC	histone deacetylase
HECT	homologous to E6-associated protein C-terminus
HIF-2α	hypoxia-induced factor 2 alpha
His	histidine
HLH	helix-loop-helix
IB	immunoblotting
ICAM-1	intercellular adhesion molecule 1
IFN	interferon
IκB	inhibitor of NF-κB
IKK	IκB kinase
IL	interleukin
Iono	ionomycin
IP	immunoprecipitation
IP-10	interferon gamma-inducible protein 10
IRF	interferon regulatory factor
JNK	c-Jun N-terminal kinase
KA	kinase assay
LPS	lipopolysaccharide

LTβ	lymphotoxin beta
Lys	lysine
LZ	leucine zipper
MAPK	mitogen-activated protein kinase
MEF	mouse embryonic fibroblast
MIP-2	macrophage inflammatory protein 2
MMP	matrix metalloproteinase
MSK1	mitogen- and stress-activated protein kinase 1
MYC	myelocytomatosis viral oncogene homolog
N	tyrosine nitration
N-terminus	amino-terminus
NAK	NF-κB-activiting kinase
NAP1	NAK-associated protein 1
NBD	NEMO-binding domain
NEMO	NF-κB essential modulator
NES	nuclear export signal
NF-κB	nuclear factor κB
NFKBIA	inhibitor of NF-κB alpha
NIK	NF-κB-inducing kinase
NLS	nuclear localization signal
P	phosphorylation
PCAF	p300/CBP-associated factor
PDLIM2	PDZ-LIM domain-containing protein 2
PI3K	phosphatidylinositol 3' kinase
PIDD	p53-inducible death domain-containing protein
Pin1	peptidyl-prolyl cis-trans isomerase 1
PKAc	protein kinase A catalytic subunit
PKCθ	protein kinase C theta
PLCγ	phospholipase C gamma
PMA	phorbol-12-myristate-13-acetate

PML	promyelocytic leukemia
Pr	proline isomerization
Pro	proline
RANTES	regulated upon activation, normal T-cell expressed and secreted
RHD	Rel homology domain
RING	really interesting new gene
RIP	receptor-interacting protein
rRNA	ribosomal RNA
RSK1	p90 ribosomal S6 kinase 1
SAA	serum amyloid A
$SCF^{\beta\text{-}TrCP}$	Skp1, Cul1 and β-TrCP-containing multisubunit E3 complex
SDS-PAGE	sodium dodecyl sulfate-polyacrylamide gel electrophoresis
Ser	serine
shRNA	small hairpin RNA
SMRT	silencing mediator for retinoic acid and thyroid hormone receptor
SOCS1	suppressor of cytokine signaling 1
SUMO	small ubiquitin-like modifier
T2K	TRAF2-associated kinase
TAB	TAK1 binding protein
TAD	transactivation domain
TAFII31	TATA-binding protein-associated factor II31
TAK1	transforming growth factor beta-activated kinase 1
TANK	TRAF associated NF-κB activator
TBK1	TANK-binding kinase 1
TCR	T cell receptor
Thr	threonine
TLR	Toll-like receptor
Tm	melting temperature
TNF	tumour necrosis factor
TRAF	TNF receptor-associated factor

β-TrCP	beta-transducin repeat-containing protein
TTP	tristetraprolin
Tyr	tyrosine
Ub	ubiquitination
UV	ultraviolet
VCAM-1	vascular cell adhesion molecule 1
VEGF	vascular endothelial growth factor
wt	wildtype
ZF	zinc finger

Publications

The following publication and manuscripts are based on this study.

Publication:

1. Mattioli I*, **Geng H***, Sebald A, Hodel M, Bucher C, Kracht M, Schmitz ML. Inducible phosphorylation of NF-kappa B p65 at serine 468 by T cell costimulation is mediated by IKKepsilon. *J Biol Chem. 2006 Mar 10; 281(10):6175-83.* (* Equally contributing authors)

Manuscripts:

1. **Geng H**, Wittwer T, Dittrich-Breiholz O, Kracht M, Schmitz ML. Phosphorylation of NF-κB p65 at serine 468 controls its COMMD1-dependent ubiquitination and target gene specific proteasomal elimination. *Submitted*

2. Buss H, Doerrie A, **Geng H**, Kaldis P, Wait R, Saklatvala J, Schmitz ML, Kracht M. Identification of cyclin-dependent kinase (CDK) 6 as a novel p65 NF-κB kinase. *Manuscript in preparation*

Summary

The inducible transcription factor NF-κB regulates a wide variety of target genes and plays a key role in many biological processes. While all NF-κB activation pathways share a critical step involving proteasome-mediated degradation of inhibitory proteins and the release of DNA-binding subunits, NF-κB itself is also regulated by post-translational modification of the DNA-binding subunits. This second level of regulation is required to determine the specificity and to control the amplitude as well as duration of the transcriptional response. This study identified IKKε as a novel p65 kinase mediating inducible phosphorylation at Ser 468 and also Ser 536 in response to T cell costimulation. In costimulated T cells, multiple experimental approaches revealed an important role of IKKε for p65 phosphorylation at Ser 468, whereas Ser 536 phosphorylation also occurred in the absence of this kinase. These results also provide a mechanistic clue that helps to explain the relevance of IKKε for the expression of a subset of NF-κB target genes without affecting IKK activity. The functional role of these phosphorylation sites was tested in reconstitution experiments. Gene arrays and real-time PCR analyses showed that the effect of Ser 468 phosphorylation depends on the individual target gene. While some genes show strict dependency on the integrity of this phosphorylation site, other genes are expressed at even higher rates when the phosporylatable serine is replaced by an alanine. The latter finding can be explained by an increased stability of the mutated p65 protein, which is largely refractory to ubiquitination and proteasome-dependent elimination. Further experiments showed that TNF-induced p65 phosphorylation at Ser 468 controls its ability to associate with COMMD1 and Cullin-2, components of a multisubunit ubiquitin ligase complex. These proteins in turn mediate p65 ubiquitination and allow for proteasome-dependent degradation of this transcription factor. ChIP assays revealed that phosphorylation of p65 at Ser 468 leads to ubiquitin/proteasome-dependent removal of chromatin-bound p65, thus contributing to the selective termination of late NF-κB-dependent gene expression.

Zusammenfassung

Der induzierbare Transkriptionsfaktor NF-κB reguliert zahlreiche Zielgene und spielt bei unterschiedlichen biologischen Prozessen eine zentrale Rolle. NF-κB kann durch verschiedene Signalwege aktiviert werden, die letztlich durch einen Proteasomen-vermittelten Schritt zur Generierung von freien, DNA-bindenden Untereinheiten führen. Die Aktivität der DNA-bindenden Untereinheiten kann durch posttranslationale Modifikation weiter gesteuert werden. Diese zweite Regulationsebene beeinflusst die Spezifität, Amplitude und Dauer der transkriptionellen Aktivierung. In dieser Studie wurde die Serin/Threonin Kinase IKKε als eine neue Kinase für die NF-κB p65 Untereinheit identifiziert, welche in costimulierten T Zellen für die induzierbare Phosphorylierung an den Serinen 536 und 468 verantwortlich ist. Unterschiedliche experimentelle Strategien zeigten die Wichtigkeit von IKKε für die induzierbare Serin 468 Phosphorylierung, während das C-terminale Serin 536 auch von anderen Kinasen modifiziert werden konnte. Diese Ergebnisse erlauben auch ein mechanistisches Verständnis von früheren Studien, welche in IKKε$^{-/-}$ defizienten Zellen eine intakte IκBα Degradation und DNA-Bindung, aber Defekte in der induzierbaren Expression von selektiven NF-κB Zielgenen gemessen hatten. Die funktionelle Rolle dieser Phosphorylierungen wurde durch Rekonstitutionsexperimente untersucht. Gene array und real-time PCR Experimente zeigten, dass die funktionellen Konsequenzen der p65 Serin 468 Phosphorylierung vom individuellen Zielgen abhängen. Während die Expression einiger Gene die Intaktheit dieser Phosphorylierungsstelle benötigen, war die Expression anderer Gene davon unbeeinflusst und weitere Gene zeigten sogar eine verstärkte Expression. Der letztere Befund kann molekular dadurch erklärt werden, dass die TNF-induzierte p65 Serin 468 Phosphorylierung die Bindung des Transkriptionsfaktors an COMMD1 und Cullin-2 erlaubt, zwei Komponenten eines Multi-Protein Ubiquitin E3 Ligase Komplexes. Die anschliessende Polyubiquitinierung von p65 führt zum proteasomalen Abbau des

Transkriptionsfaktors und stellt somit in selektiver Weise die Termination einzelner Gene während der späten NF-κB Antwort sicher.

1 Introduction

1.1 NF-κB and IκB proteins

In mammals, the transcription factor nuclear factor kappa B (NF-κB) family consists of five different DNA-binding subunits: p65 (RelA), RelB, c-Rel, p50/p105 (NF-κB1) and p52/p100 (NF-κB2) (Baldwin, 1996). Both p50 and p52 are generated through proteasome-dependent processing of their precursors p105 and p100, respectively (Betts and Nabel, 1996; Palombella et al., 1994; Xiao et al., 2001). In most cell types, NF-κB subunits exist as hetero- or homodimers bound to the inhibitory IκB proteins, which retain the complex mainly in the cytoplasm (Karin and Ben-Neriah, 2000). All Rel proteins share a conserved motif, the Rel homology domain (RHD) that is located at the N-terminus and consists of approximately 300 amino acids. The RHD is responsible for dimerization, DNA-binding, nuclear localization and interaction with IκBs (Siebenlist et al., 1994; Verma et al., 1995). NF-κB family members p65, RelB and c-Rel contain C-terminal transactivation domains (TADs), which mediate transcription of NF-κB target genes (Fig. 1.1). The p65 subunit bears two TADs in its C-terminal portion and induces gene activation (Schmitz and Baeuerle, 1991). The p50 and p52 subunits are transcriptionally inactive, but can trigger gene expression when complexed as heterodimers with p65, c-Rel or RelB (Bours et al., 1993; Franzoso et al., 1992). The IκB family contains seven members: IκBα, IκBβ, IκBε, IκBγ, IκBζ, and also the precursor proteins p100 and p105 (Fig. 1.1) (Ghosh et al., 1998; Hayden and Ghosh, 2008). IκB proteins are characterized by the presence of five-to-seven ankyrin repeats, which mediate binding to the dimerization domain of NF-κB and mask the nuclear localization sequence (NLS) of NF-κB, thus preventing the nuclear import of this transcription factor (Huxford et al., 1998; Jacobs and Harrison, 1998). IκBα, IκBβ, and IκBε contain N-terminal regulatory regions, which allow NF-κB activation through stimulus-induced phosphorylation, ubiquitination and subsequent degradation of the inhibitory proteins (Brown et al., 1995; DiDonato et al., 1996; Whiteside and Israel, 1997).

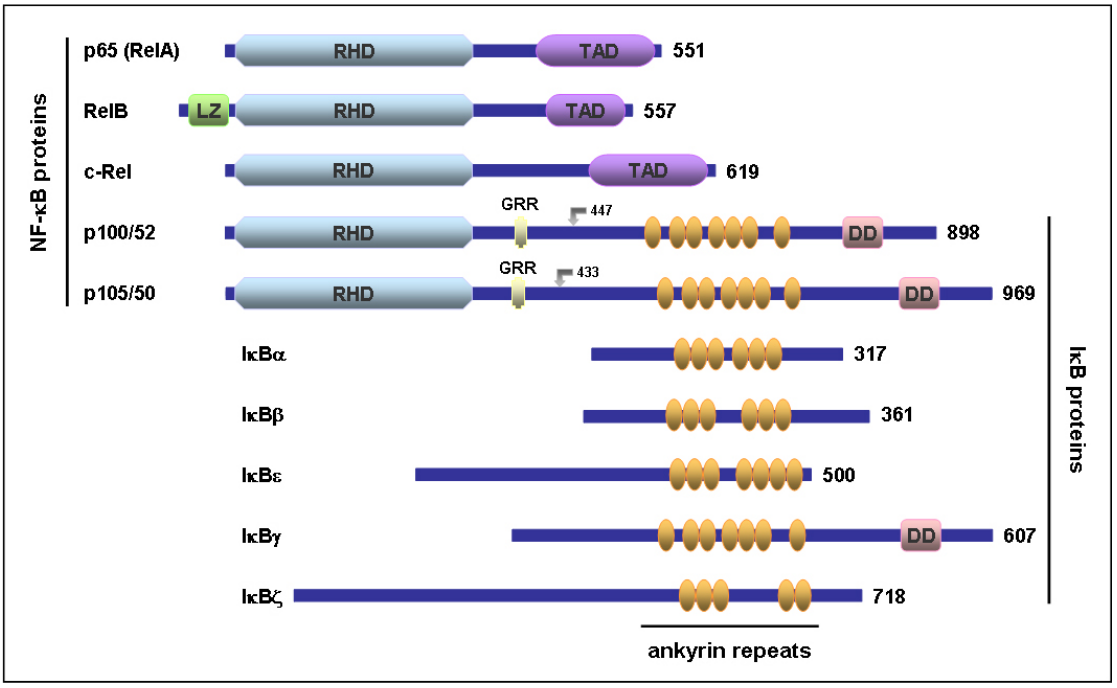

Fig. 1.1 Architecture of NF-κB and IκB family members.

NF-κB and IκB proteins are shown. The number of amino acids in each human protein is indicated on the right. The NF-κB DNA-binding subunits share one N-terminal RHD and RelB bears a LZ at its N terminus. p65, RelB and c-Rel contain one or several C-terminal TADs. Cleavage sites on p105/p50 and p100/p52 are marked at residues 433 and 447, respectively. All IκB proteins share five-to-seven ankyrin repeats. Abbreviations: DD, death domain; GRR, glycine-rich region; LZ, leucine zipper; RHD, Rel homology domain; TAD, transactivation domain.

1.2 NF-κB activation pathways

This transcription factor can be activated by a wide range of stimuli, including pro-inflammatory cytokines, Toll-like receptors, T cell receptor, B cell receptor and DNA damage (Hayden et al., 2006). NF-κB activation is considered to occur through three major pathways, the canonical (classical), alternative (non-canonical) and atypical pathways (Fig. 1.2) (Janssens and Tschopp, 2006). All NF-κB activating events rely on sequentially activated kinases, which mediate the generation of DNA-binding dimers in a proteasome-dependent manner (Viatour et al., 2005). Once in the nucleus, NF-κB can bind to DNA and regulate the transcription of a broad variety of genes, encoding pro-inflammatory cytokines (e.g., TNF-α and IL-1), chemokines (e.g., IL-8 and RANTES), adhesion molecules (e.g., ICAM-1 and

VCAM-1), acute-phase proteins (e.g., SAA) and inducible effector enzymes (e.g., COX-2) (Ghosh and Karin, 2002; Jimi and Ghosh, 2005). NF-κB target genes not only contribute to the innate and adaptive immune responses, but also serve to control cell survival and proliferation. Therefore, NF-κB participates in a number of biological processes, including inflammation, immunity, proliferation, development, apoptosis as well as oncogenesis (Kim et al., 2006; Perkins, 2007).

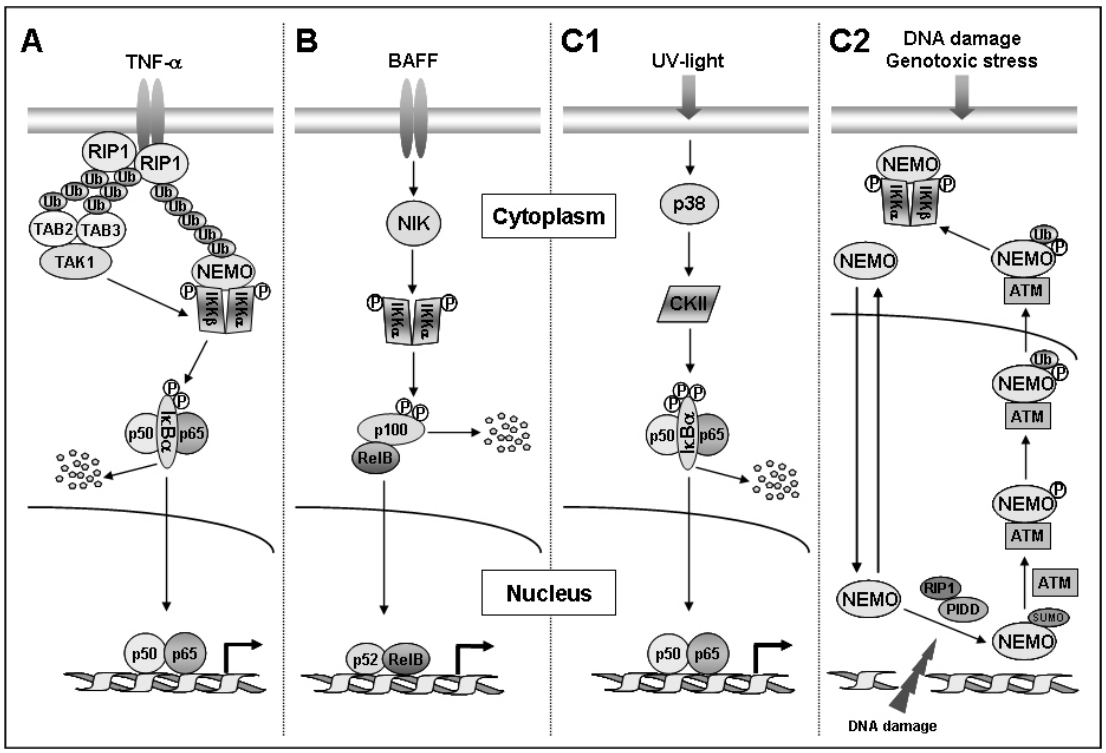

Figure 1.2 Schematic representations of major NF-κB activating pathways.

(A) Canonical NF-κB activation by TNF-α. Activation of NF-κB takes place near the plasma membrane and the interaction of NEMO with Lys 63 polyubiquitinylated RIP1 is the critical step, which activates the IKK complex that leads to the liberation of the p50/p65 heterodimer. (B) Alternative NF-κB activation pathway. NIK and IKKα are activated to phosphorylate the p100 precursor, followed by p100 processing and the generation of a p52/RelB dimer. (C1) UV-triggered activation of NF-κB. Signals proceed via a p38 MAP kinase and CKII to phosphorylate IκBα and then to release NF-κB. (C2) NF-κB activation pathway by genotoxic stress. DNA damage causes nuclear localization of free NEMO via SUMO-1 attachment. Subsequent ATM-dependent phosphorylation and ubiquitination of NEMO allows its retrograde transport to the nucleus where it mediates IKK activation. Abbreviations: ATM, ataxia telangiectasia-mutated; BAFF, B cell-activating factor of the TNF family; CKII, casein kinase II; IκB, inhibitor of NF-κB; IKK, IκB kinase; NEMO, NF-κB essential modulator; NIK, NF-κB-inducing kinase; P, phosphorylation; PIDD, p53-inducible death domain-containing protein; RIP, receptor-interacting protein; SUMO, small ubiquitin-like modifier; TAB, TAK1 binding protein; TAK1, transforming growth factor beta-activated kinase 1; TNF, tumour necrosis factor; Ub, ubiquitination; UV, ultraviolet.

1.2.1 Canonical NF-κB activation

The canonical pathway allows NF-κB activation via stimulation by pro-inflammatory cytokines, T cell costimulation and Toll-like receptors (Fig. 1.2 A). In unstimulated cells, IκB-associated NF-κB dimers are mainly localized in the cytoplasm (Birbach et al., 2002; Li and Verma, 2002). The most abundant combination of NF-κB in this pathway is the heterodimer between p50 and p65 complexed to IκBα. In this NF-κB·IκB complex, the nuclear localization sequence of p50 is exposed, whereas the NLS of p65 is masked by IκBα (Nolan et al., 1991). IκBα contains a strong nuclear export signal (NES), which dominates the NLS of p50 to keep most p50/p65 dimers in the cytoplasm (Arenzana-Seisdedos et al., 1997; Huang et al., 2000). Stimulation of cells by TNF-α initiates a signal cascade resulting in the activation of the IκB kinase (IKK) complex (Bonizzi and Karin, 2004). The IKK complex consists of two kinases IKKα/IKK1 and IKKβ/IKK2, as well as the NF-κB essential modulator (NEMO) (Delhase et al., 1999). In this activated IKK complex, IKKβ plays a central role to phosphorylate IκBα at Ser 32 and Ser 36 (Chen et al., 1995; DiDonato et al., 1996; Sizemore et al., 2002), allowing its ubiquitination at Lys 21 and Lys 22 by the $SCF^{\beta\text{-}TrCP}$ complex and subsequent degradation by the 26S proteasome (Hatakeyama et al., 1999; Scherer et al., 1995; Yaron et al., 1998). This leads to an unmasking of the p65 NLS and allows NF-κB nuclear entry, as well as DNA-binding, which can then activate target gene transcription (Israel, 1995).

1.2.2 Alternative NF-κB activation

The second, alternative pathway (Fig 1.2 B) is activated by a subset of NF-κB inducers, including lymphotoxin-β, BAFF and CD40 ligand. This pathway occurs predominantly in B cells, where the p52/RelB heterodimer is the major NF-κB dimer (Claudio et al., 2002; Coope et al., 2002; Dejardin et al., 2002). The alternative NF-κB pathway is NEMO-independent and relies solely on the sequential activation of NIK and IKKα (Regnier et al., 1997; Xiao et al., 2001), which induces the

processing of p100 to p52. The liberated p52 forms a functional heterodimer with RelB, translocates into the nucleus to regulate gene expression (Ling et al., 1998; Senftleben et al., 2001; Xiao et al., 2001).

1.2.3 Atypical NF-κB activation

The so-called "atypical pathways" refer to those pathways that do not belong to the former two categories. Atypical stimuli, such as DNA damage, oxidative stress, doxorubicin or UV-light, trigger these pathways, as they all mediate a slow and weak NF-κB signal (Janssens and Tschopp, 2006). The involvement of IKKs in the atypical NF-κB pathways is a matter of debate. While the groups of Verma and Karin have demonstrated an IKK-independent, atypical NF-κB activation which is induced by doxorubicin or ultraviolet light (Kato et al., 2003; Tergaonkar et al., 2003), others report on the requirement of IKK signaling in response to genotoxic stress, oxidative insult or DNA damage (Huang et al., 2003; Janssens et al., 2005).

UV-triggered NF-κB activation (Fig. 1.2 C1) employs a p38 MAPK-dependent mechanism that finally leads to the activation of CKII. This kinase phosphorylates IκBα at multiple serine residues within the C-terminus, but not at Ser 32/36 (Kato et al., 2003). The phosphorylated IκBα is then recognized and degraded by the 26 S proteasome. This event also allows NF-κB release and induced transcription of target genes.

The so-called IKK-dependent, genotoxic stress-induced pathway (Fig. 1.2 C2) is based on sequential modifications of NEMO. Upon cellular stress, NEMO is sumoylated within the nucleus, followed by phosphorylation and ubiquitination in an ATM-dependent manner. Ubiquitinated NEMO then translocates back to the cytoplasm, activates the IKK complex and thus induces NF-κB activation (Huang et al., 2003; Janssens et al., 2005).

1.3 Regulation of NF-κB activity by post-translational modifications

Following degradation of IκBs, the liberated NF-κB dimers move to the nucleus, and bind to promoter and enhancer regions of which typically bear κB sites with the consensus sequence GGGRNWYYCC (N represents any base, R represents a purine; W represents an adenine or a thymine and Y represents a pyrimidine) (Hoffmann et al., 2006). However, systematic analyses of NF-κB binding sites on chromosome 22 also revealed atypical NF-κB binding sites (Martone et al., 2003; Udalova et al., 2002). The DNA-binding specificity and affinity are determined by the composition of NF-κB dimers (Saccani et al., 2003; Wietek and O'Neill, 2007).

NF-κB transcriptional activity can be regulated through differential interactions with either co-activators, such as CBP and p300 or co-repressor proteins, for instance histone deacetylases (HDACs) (Campbell and Perkins, 2006). The induction, amplitude and duration of the NF-κB response are codetermined by post-translational modifications of this transcription factor. From all NF-κB subunits, most information on post-translational modifications has been obtained for the p65 subunit, which is known to be modified by phosphorylation, acetylation, prolyl isomerization, nitrosylation and ubiquitination (Fig. 1.3) (Perkins and Gilmore, 2006).

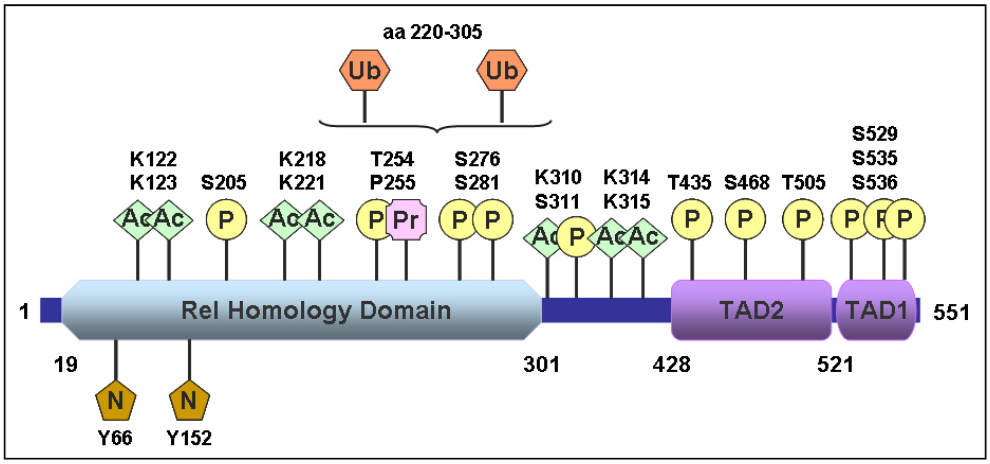

Figure 1.3 Schematic diagram of p65 post-translational modifications motifs

Amino acid numbering corresponds to the human p65 protein. TAD1 and TAD2 represent the subdomains of p65 transactivation domains. Abbreviations: Ac, acetylation; K, lysine; N, tyrosine nitration; P, phosphorylation; P, proline; Pr, proline isomerization; S, serine; T, threonine; Ub, ubiquitination; Y, tyrosine.

1.3.1 Phosphorylation of p65

Phosphorylation is the best characterized p65 post-translational modification pattern. To date, eight serine and three threonine residues have been mapped as p65 phosphorylation sites (Fig. 1.3) (Neumann and Naumann, 2007; Perkins, 2006; Viatour et al., 2005). These phosporylations occur either in the cytoplasm or in the nucleus, and are mediated by various protein kinases. Some sites can be modified in a stimulus- and/or cell type-specific fashion by several kinases (Chen and Greene, 2004). Furthermore, p65 phosphorylation at these individual sites leads to different effects, as summarized in Table 1.1.

Table 1.1 Phosphorylation of p65 and the responsible kinases

Site	Location	Kinase	Function	Reference
Ser 205	RHD	unknown	Transcriptional activity	Anrather et al., 2005
Ser 276	RHD	PKAc MSK1	Transcriptional activity Coactivator binding Transcriptional activity	Zhong et al., 1998 Zhong et al., 1998 Vermeulen et al., 2003
Ser 281	RHD	unknown	Transcriptional activity	Anrather et al., 2005
Ser 311	RHD	PKCζ	Transcriptional activity	Duran et al., 2003
Ser 468	TAD2	GSK3β IKKβ IKKε	Transcriptional activity Transcriptional activity Transcriptional activity	Buss et al., 2004a Schwabe and Sakurai, 2005 Mattioli et al., 2006
Ser 529	TAD1	CKII	Transcriptional activity	Wang et al., 2000
Ser 535	TAD1	CaMKIV	Transcriptional activity	Bae et al., 2003
Ser 536	TAD1	IKKα IKKβ IKKε TBK1 RSK1	Transcriptional activity and stabilization Transcriptional activity and nuclear import Transcriptional activity Nuclear localization Affinity to IκBα	Jiang et al., 2003 Lawrence et al., 2005 Sakurai et al., 1999 Mattioli et al., 2004b Buss et al., 2004b Fujita et al., 2003 Bohuslav et al., 2004
Thr 254	RHD	unknown	Stabilization and nuclear localization	Ryo et al., 2003
Thr 435	TAD2	unknown	Transcriptional activity	Yeh et al., 2004
Thr 505	TAD2	ATR ChK1	Transcriptional activity Transcriptional activity	Campbell et al., 2006 Campbell et al., 2006

From all these known p65 phosphorylation sites, Ser 276, Ser 468 and Ser 536 are the best studied ones, which will be discussed here in detail.

Ser 276

This phosphorylation site is located within the N-terminal RHD, and can be mediated by two kinases: the catalytic subunit of protein kinase A (PKAc) and mitogen- and stress-activated protein kinase 1 (MSK1) (Vermeulen et al., 2003; Zhong et al., 1998). LPS triggers PKAc-mediated p65 Ser 276 phosphorylation in the cytoplasm. In the unphosphorylated state, p65 shows an intramolecular interaction between the C-terminal region and the N-terminal portion. Ser 276 phosphorylation weakens this intramolecular association and induces a conformational change, which creates an additional binding site for histone acetyltransferases (HATs), such as CBP and p300 (Zhong et al., 1998). MSK1-triggerd Ser 276 phosphorylation takes place within the nucleus in response to TNF treatment (Vermeulen et al., 2003). While Ser 276 is phosphorylated by two different kinases in distinct cellular compartments, both phosphorylation events allow enhanced NF-κB transcriptional activity through increased CBP/p300 recruitment and displacement of inhibitory p50/HDAC1 complexes from the DNA (Zhong et al., 2002). In addition, Ser 276-phosphorylated p65 can also associate with RelB in the nucleus. This heterodimer does not bind to consensus κB sites, thus serving to dampen RelB activity in response to TNF (Jacque et al., 2005).

Ser 468

The p65 Ser 468 is a recently discovered phosphorylation site within TAD2 (Mattioli et al., 2004a). This serine residue is inducibly phosphorylated in response to TNF, IL-1β as well as T cell costimulation and is targeted by three kinases: glycogen synthase kinase 3β (GSK3β), IKKβ and IKKε (Buss et al., 2004a; Mattioli et al., 2006; Schwabe and Sakurai, 2005). While basal Ser 468 phosphorylation is mediated by GSK3β (Buss et al., 2004a), cytokine-triggered phosphorylation of this site is mediated by IKKβ (Schwabe and Sakurai, 2005). IKKε can be activated in response

to T cell costimulation to mediate Ser 468 phosphorylation (Mattioli et al., 2006), showing that the involved kinase is determined by the stimulus. Ser 468-phosphorylated p65 is located predominantly within the nucleus (Mattioli et al., 2006), suggesting a role for this specific phosphorylation in nuclear p65-mediated effects. Ser 468 phosphorylation has been described as both enhancing and repressing p65 transcriptional activity. GSK3β-mediated basal phosphorylation down-regulates p65 basal activity (Buss et al., 2004a). TNF-α- or IL-1β-induced, IKKβ-dependent phosphorylation negatively affects p65-mediated transactivation (Schwabe and Sakurai, 2005), whereas IKKε-triggered phosphorylation upon T cell costimulation shows a positive impact on p65 activity (Mattioli et al., 2006).

Ser 536

The evolutionarily conserved Ser 536 is located within the C-terminal TAD1 and can be phosphorylated by multiple kinases, including IKKα/β, IKKε, TBK1 and the p90 ribosomal S6 kinase 1 (RSK1) via various signaling pathways (Bohuslav et al., 2004; Buss et al., 2004b; Fujita et al., 2003; Jiang et al., 2003; O'Mahony et al., 2004; Sakurai et al., 1999). In most cases, these phosphorylations enhance p65 transactivation. The requirements for IKKα and IKKβ seem to depend on the employed stimuli. While TNF-α-mediated p65 phosphorylation relies on IKKβ (Sakurai et al., 1999), IKKα plays a central role in response to the oncoprotein Tax (O'Mahony et al., 2004). In lymphotoxin-β-stimulated cells, IKKα phosphorylates p65 at Ser 536 in a NIK kinase-dependent manner (Jiang et al., 2003). Ser 536 phosphorylation also occurs in response to T cell costimulation and serves to control p65 nuclear import (Mattioli et al., 2004b). In addition to IKKα and IKKβ, IL-1-induced phosphorylation of p65 at Ser 536 can be mediated by the IKK homologous kinases IKKε and TBK1 (Buss et al., 2004b). Ser 536 can also be phosphorylated by IKKε in costimulated T cells (Mattioli et al., 2006) or in cancer cell lines (Adli and Baldwin, 2006). Furthermore, Ser 536 phosphorylation is triggered by DNA damaging agents via the RSK1 (Bohuslav et al., 2004). This phosphorylation event results in a reduced affinity between p65 and IκBα and thus

facilitates NF-κB release. Additionally, a recent study revealed that Ser 536 phosphorylation can enhance LPS-induced p65 destabilization (Lawrence et al., 2005), thus displaying that p65 phosphorylation can serve many functions. Along with this line, Ser 536 phosphorylation is found to couple p65 to TATA-binding protein-associated factor II31 (TAFII31)-dependent transcription (Buss et al., 2004b) and the oscillatory phosphorylation of p65 Ser 536 functions as a consequence of its shuttling between the cytoplasm and nucleus (Nelson et al., 2004).

1.3.2 Acetylation of p65

Acetylation, like phosphorylation, is also important for regulating nuclear NF-κB activity. The transcriptional coactivators p300, CBP and the p300/CBP-associated factor (PCAF) have been identified as p65 interactors and to acetylate this transcription factor at a number of lysine residues. These inducible p65 acetylations can also occur upon TNF, IL-1 or PMA stimulation. Site-specific acetylation has distinct functional consequences on p65 activity, thus serving as another molecular mechanism to promote the specificity of NF-κB target gene expression (Fig. 1.3; Table 1.2) (Chen and Greene, 2004; Neumann and Naumann, 2007; Perkins, 2006).

Table 1.2 Acetylation of p65 and the corresponding enzymes

Site	Location	Enzyme	Function	Reference
Lys 122	RHD	p300, PCAF	Inhibiting DNA binding	Kiernan et al., 2003
Lys 123	RHD	p300, PCAF	Inhibiting DNA binding	Kiernan et al., 2003
Lys 218	RHD	CBP/p300	Unknown	Chen et al., 2002
Lys 221	RHD	CBP/p300	Promoting DNA binding, Inhibiting IκBα binding	Chen et al., 2002
Lys 310	RHD	CBP/p300	Enhancing transactivation	Chen et al., 2002
Lys 314	RHD	p300	Transcriptional activity	Buerki et al., 2008
Lys 315	RHD	p300	Transcriptional activity	Buerki et al., 2008

Acetylated Lys 310 and phosphorylated Ser 311 are directly adjacent to each other, implying a possible functional relationship between these two types of modification.

A functional link between phosphorylation and acetylation has been demonstrated for two phosphorylation sites: phosphorylation of Ser 276 or Ser 536 increases the binding to p300, which in turn mediates p65 acetylation at Lys 310 (Chen et al., 2005). Lys 310 acetylation is required for the full transcriptional activity of p65, and this modification can be deacetylated by corepressor complexes that result in decreased p65 activity (Chen et al., 2002; Yeung et al., 2004).

1.3.3 Other post-translational p65 modifications

Besides phosphorylation and acetylation, p65 is also subject to prolyl isomerization, tyrosine nitration and ubiquitination. Upon TNF-α stimulation, p65 is phosphorylated at Thr 254, and thus creates a pThr-Pro motif with the neighboring Pro 255 residue. This pThr-Pro motif allows interaction with the peptidyl-prolyl isomerase Pin1, which induces prolyl isomerization of p65 and inhibits p65 interaction with IκBα. This Pin1-induced conformational change results in an increased nuclear accumulation of p65 and enhanced stability of this transcription factor (Ryo et al., 2003).

A current study has indicated that p65 can be nitrated at Tyr 66 and Tyr 152 in response to NO treatment. This modification induces the p65 dissociation from p50 and association with IκBα, which allows more p65 to be exported, and results in a repression of NF-κB activity (Park et al., 2005). Ubiquitination of p65 will be discussed in more detail in section 1.6.

1.4 IKK complex and IKK-related kinases

1.4.1 IKK complex

Inducible activation of NF-κB signaling mainly occurs through IKK-mediated IκB phosphorylation. The core IKK complex contains three components: two catalytic kinase subunits, IKKα/IKK1 and IKKβ/IKK2 (DiDonato et al., 1997; Mercurio et al.,

1997), as well as a non-enzymatic regulatory NEMO subunit (Rothwarf et al., 1998; Yamaoka et al., 1998).

IKKα and IKKβ are homologous and both contain an N-terminal kinase domain followed by a conserved leucine zipper, a C-terminal putative helix-loop-helix motif and a NEMO binding domain (Fig 1.4) (May et al., 2002; Zandi et al., 1997). The leucine zipper is involved in homodimer and heterodimer formation, and the helix-loop-helix region can intramolecularly associate with the kinase domain. Activation of IKKs can be achieved via phosphorylation within the activation loop, which contains two inducibly phosphorylated serines at residues 176/180 (IKKα) and 177/181 (IKKβ) (Delhase et al., 1999; Ling et al., 1998; Mercurio et al., 1997). IKK activity is proposed to be regulated through trans-autophosphorylation within the complex (Karin and Delhase, 2000; Tegethoff et al., 2003). The kinase activity of both IKKα and IKKβ can also be inactivated through mutation of Lys 44 in the predicted ATP-binding site (Zandi et al., 1997). Both IKK kinases are required for NF-κB activation and can phosphorylate IκBα at Ser 32 and Ser 36 (Woronicz et al., 1997; Zandi et al., 1998). Although there is a high homology between IKKα and IKKβ, these two kinases have distinct functions. IKKβ is the primary target for pro-inflammatory stimuli and is the major IKK catalytic subunit for NF-κB canonical activation, which depends on IκBα phosphorylation (Delhase et al., 1999; Sizemore et al., 2002). This kinase also participates in a negative feedback loop in the TCR-induced NF-κB activation through phosphorylating Bcl10 (Lobry et al., 2007; Wegener et al., 2006). In contrast, IKKα plays a unique role in the alternative NF-κB activation pathway, which involves phosphorylation and processing of p100 to p52 (Senftleben et al., 2001). Sequence analyses reveal that only IKKα bears a nuclear localization sequence (Sil et al., 2004), suggesting a possible role for this kinase in the transcription of target genes within the nucleus. Consistent with this line, IKKα contributes to the termination of inflammatory transcriptional responses in macrophages by promoting the nuclear degradation of both p65 and c-Rel (Lawrence et al., 2005; Li et al., 2005). In addition to phosphorylating the CBP coactivator

(Huang et al., 2007), IKKα is also required to stimulate derepression of the SMRT/HDAC3 complex from the NF-κB heterodimer, allowing p300 to bind and acetylate p65 subunit (Hoberg et al., 2006).

NEMO is the third core component of the IKK complex, and is required for formation of this complex. IKKα and IKKβ interact with NEMO through their C-terminal NEMO-binding domain (May et al., 2002; Yamaoka et al., 1998). NEMO is primarily a helical protein with large stretches of coiled-coil structures, as well as a leucine zipper and a zinc finger at its C terminus (Fig 1.4) (Rothwarf et al., 1998). Although it is not required for activation of the IKKα-dependent alternative pathway, NEMO is absolutely essential for activation of the IKK complex, serving as an adaptor between the bound catalytic subunits and upstream activators (Hacker and Karin, 2006). Current studies have revealed that NEMO inducibly binds to Lys 63-linked polyubiquitin chains, which is the key event in NF-κB activation as it allows recruitment of upstream kinases, such as TAK1 (Ea et al., 2006; Wu et al., 2006). Cells lacking NEMO or bearing inactivating point mutations fail to activate the IKK complex by any activators of the canonical pathway (Makris et al., 2002; Rudolph et al., 2000; Yamaoka et al., 1998). Furthermore, sequential modifications of nuclear NEMO is implicated in mediating NF-κB activation by genotoxic stress (Huang et al., 2003; Janssens et al., 2005).

Additionally, several current studies have shown that IKKs are involved in some further NF-κB-independent pathways, including the regulation of transcription activity by hypoxia-inducible factors 2α (HIF-2α) or forkhead transcription factor FOXO3a and the modulation of mRNA stability (Bracken et al., 2005; Gringhuis et al., 2005; Hu et al., 2004). NEMO associates with HIF-2α and facilitates its recruitment to CBP/p300, thus inducing HIF-2α transcription activity (Bracken et al., 2005). The activated IKK complex binds and phosphorylates FOXO3a, allowing ubiquitination and proteasomal degradation of this transcription factor. This event results in the promotion of cell proliferation and tumorigenesis (Hu et al., 2004). In

addition, IKKβ, along with PKCδ, contributes to the regulation of mRNA stability through phosphorylation of the chaperone 14-3-3β complexed with tristetraprolin (TTP) (Gringhuis et al., 2005).

1.4.2 IKK-related kinases: IKKε and TBK1

Based on sequence similarity to the classical IKK kinases, two additional members of the IKK family have been identified: IKKε/IKKi and TBK1/NAK/T2K (Peters et al., 2000; Pomerantz and Baltimore, 1999; Shimada et al., 1999; Tojima et al., 2000). Like IKKα and IKKβ, the IKK-related kinases consist of an N-terminal catalytic kinase domain, a leucine zipper motif and a C-terminal helix-loop-helix domain that is required for protein-protein interactions (Fig 1.4).

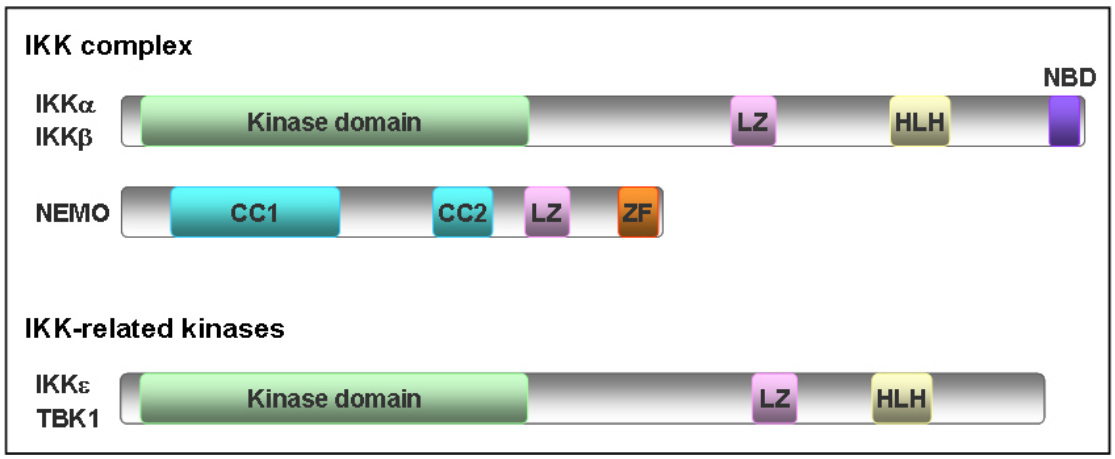

Fig. 1.4 Architecture of IKK complex and IKK-related kinases.

Abbreviations: CC, coiled-coil domains; HLH, helix-loop-helix domain; LZ, leucine zipper domain; NBD, NEMO-binding domain; ZF, zinc finger domain.

IKKε and TBK1 are overall 64% homologous to each other, but show limited homology to the classical IKK kinases, with approximately 30% sequence identity within the kinase domain (Peters and Maniatis, 2001; Pomerantz and Baltimore, 1999; Shimada et al., 1999). Similar to the classical IKKs, dominant-negative versions of IKKε and TBK1 can be generated via mutation of Lys 38 within the ATP-binding pocket (Peters et al., 2000; Pomerantz and Baltimore, 1999). IKKε and TBK1 also possess an activation loop within their kinase domains. While IKKα and IKKβ contain two phosphorylatable serines in the activation loop, IKKε and TBK1 only

contain Ser 172 at the second position, whereas the first serine is replaced by glutamic acid which could mimic the phosphorylated state by its negative charge (Fig 1.5) (Peters et al., 2000; Shimada et al., 1999; Tojima et al., 2000).

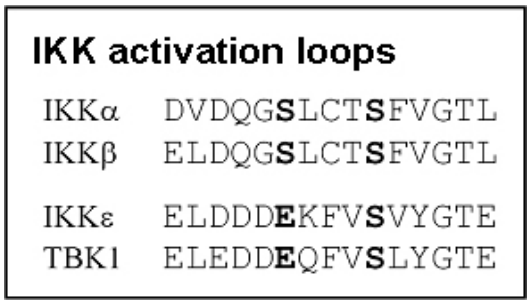

Figure 1.5 The activation loops of IKKs.

The phosphorylatable sites in the activation loops of IKKs are shown in bold type. IKKε and TBK1 have a glutamic acid at the position homologous to the first phosphorylatable serine of IKKα and IKKβ.

Despite their structural homology to IKKα and IKKβ, neither IKKε nor TBK1 is a component of the classical NEMO-containing IKK complex (Peters et al., 2000; Pomerantz and Baltimore, 1999). The enzymatic properties of IKKε and TBK1 are distinct from IKKβ, as well (Kishore et al., 2002), such that, IKKε and TBK1 have much less impact on IκBα phosphorylation than IKKβ. Both kinases can phosphorylate IκBα only at Ser 36, but not at Ser 32, thus failing to create a proper $SCF^{\beta\text{-}TrCP}$ recognition site (Brown et al., 1995; Peters et al., 2000; Tojima et al., 2000).

IKKε is prominently expressed in T cells and peripheral blood cells (Kravchenko et al., 2003; Peters et al., 2000; Shimada et al., 1999). The contribution of IKKε to activation of selective NF-κB target genes has been revealed by gene array experiments: LPS-induced expression of some selective late NF-κB target genes, including IL-1β, IL-6, IP-10, TNF, COX-2, and RANTES is lost in IKKε-deficient cells, suggesting a role for IKKε in the regulation of NF-κB response at a later step (Kravchenko et al., 2003). These effects may be related to the ability of IKKε to phosphorylate p65, as discussed in section 1.3.1. In addition to its ability to phosphorylate p65, IKKε can mediate the phosphorylation of interferon regulatory factor 3 (IRF3) and IRF7 in response to viral infection, thus leading to the induced production of interferon (Fitzgerald et al., 2003; Paz et al., 2006; Sharma et al., 2003). Moreover, IKKε overexpression also contributes to the DNA-binding activity of CCAAA/enhancer-binding protein δ (C/EBPδ), thereby affecting the expression of

target genes which depend on the coordinate binding of NF-κB and C/EBP (Kravchenko et al., 2003).

TBK1 is constitutively expressed in embryonic fibroblasts (Perry et al., 2004). Similar to IKKε, TBK1 can also phosphorylate IRF3 and IRF7, thereby inducing the transcription of type I interferon (IFN) in response to viral infection or stimulation through dsRNA or LPS (Hemmi et al., 2004; McWhirter et al., 2004; Paz et al., 2006; tenOever et al., 2004). Some recent reports have revealed that TBK1 is involved in further physiological processes, such as in angiogenesis (Korherr et al., 2006) and in tumor cell survival through a RalB GTPase pathway (Chien et al., 2006).

1.5 Termination of NF-κB activity

In order to achieve controlled target gene expression and to prevent uncontrolled NF-κB activity, the termination of NF-κB-dependent transcriptional activity is tightly regulated and employs a battery of different control mechanisms (Hinz and Scheidereit, 2007; Natoli and Chiocca, 2008).

As an early NF-κB target gene, IκBα plays an important role in terminating the NF-κB response through a negative feedback loop. After NF-κB activation, the rapidly resynthesized IκBα can migrate into the nucleus as a free, NF-κB-unbound protein, dissociate NF-κB from its cognate DNA, and bring it back to the cytoplasm, thereby rapidly terminating NF-κB activation (Brown et al., 1993; Zabel and Baeuerle, 1990). The NF-κB response can also be terminated in the absence of IκBα (Saccani et al., 2004), which indicates the existence of additional regulatory mechanisms to switch off NF-κB target gene expression. Nuclear export and post-inductive degradation of the DNA-binding subunits are two major steps to limit the duration of the NF-κB response (Hayden and Ghosh, 2008; Maine and Burstein, 2007; Natoli and Chiocca, 2008). The p50 and p65 subunits have been found to be ubiquitinated and degraded by the proteasome in the nucleus, thus contributing to the efficient and

prompt termination of the nuclear NF-κB response (Carmody et al., 2007; Ryo et al., 2003; Saccani et al., 2004).

Ubiquitination is an evolutionarily conserved, post-translational modification that participates in a wide array of cellular processes, including protein degradation, transcriptional regulation, signal transduction, control of the cell cycle, activation of transcription factors and kinases, DNA repair, antigen presentation, endocytosis, and apoptosis (Hershko and Ciechanover, 1998; Liu, 2004; Natoli and Chiocca, 2008). This process involves the covalent attachment of ubiquitin to substrates. Ubiquitination occurs through a well-defined, three-step process and requires three enzymes: a ubiquitin-activating enzyme (E1), a ubiquitin-conjugating enzyme (E2) and a ubiquitin ligase (E3). Among these, E3 ligases regulate the specificity of the reaction, as they selectively bind to target proteins and accelerate ubiquitin attachment in a substrate-specific fashion. In brief, ubiquitin is first activated by E1 in an ATP-dependent manner, and then transferred to E2, forming an E2-ubquitin thioester. Finally, in the presence of E3, ubiquitin is attached to a target protein through an isopeptide bond between the C-terminus of ubiquitin and the ε-amino group of a lysine residue in the substrate. Ubiquitin contains seven lysine residues that can be attached to other ubiquitins in a highly processive reaction. Therefore, a substrate can be tagged with a single ubiquitin molecule, a process known as monoubiquitination, or elongated ubiquitin chains. Lys 48-linked polyubiquitination is mainly recognized by the 26S proteasome and results in proteolysis of the modified protein, while polyubiquitination branching of other lysines has regulatory functions. Ubiquitination is highly dynamic and can be reversed by multiple de-ubiquitinating enzymes (DUBs) (Welchman et al., 2005; Wullaert et al., 2006).

The stability of the DNA-binding subunits p50 and p65 is controlled by the ubiquitin-proteasome system in a tightly regulated manner. Upon LPS stimulation, p50 is subjected to ubiquitination as well as subsequent degradation within the nucleus. This ubiquitin-dependent elimination is inhibited by Bcl3, which allows regulation of the

strength of NF-κB responses and limits inflammation (Carmody et al., 2007). p65 is also inducibly ubiquitinated and degraded via proteasome-mediated proteolysis, that results in the down-regulation of NF-κB-dependent target gene expression and the prevention of excessive inflammatory responses (Lawrence et al., 2005; Maine et al., 2007; Saccani et al., 2004).

1.6 Ubiquitination of p65

During the past couple of years, a steadily growing number of enzymes from the ubiquitination machinery have been identified in NF-κB signaling pathways (Chen, 2005; Krappmann and Scheidereit, 2005; Wullaert et al., 2006). These modifiers control the induction, duration and termination of the NF-κB response. Several ubiquitin-modifying enzymes, such as β-TrCP, the receptor subunit of an SCF-type ubiquitin E3 ligase, control the ubiquitination of IκB and also the p50 precursor p105 (Lang et al., 2003; Yaron et al., 1998). Up to date, three ubiquitin E3 ligases, SOCS1 (suppressor of cytokine signaling 1), PDLIM2 (also known as SLIM or mystique) and COMMD1 (copper metabolism gene MURR1 domain-containing 1), have been found as regulators of p65 ubiquitination (Maine et al., 2007; Ryo et al., 2003; Tanaka et al., 2007).

SOCS1 is a member of a larger family of proteins containing the conserved carboxy-terminal SOCS box domain, through which these factors associate with Cullin-containing multisubunit ubiquitin ligases (Willems et al., 2004). It has been reported that SOCS1 directly associates with p65 and increases LPS-induced p65 ubiquitination and proteolysis (Ryo et al., 2003). Interaction sites of SOCS1 within p65 are very close to those for Pin1 binding, suggesting that both proteins may compete for the association with p65. Therefore, NF-κB function is tightly regulated by both Pin1-mediated prolyl isomerization and SOCS1-promoted ubiquitination (Ryo et al., 2003).

A current study has confirmed the role of SOCS1 in p65 ubiquitination and demonstrated that SOCS1 is contained in a multisubunit ubiquitin ligase complex containing Elongins B and C, Cullin-2 and COMMD1, which promotes ubiquitination and degradation of p65 (Maine et al., 2007). COMMD1 belongs to the COMMD family that contains 10 factors, and functions to repress NF-κB. The COMMD proteins are characterized by a high homology COMM domain in their extreme C-termini. This motif enables COMMD proteins not only to interact with each other, but also with NF-κB subunits. COMMD1 can be recruited to κB-responsive promoters to decrease the duration of p65-chromatin association (Burstein et al., 2005). Loss-of-function experiments show that down-regulation of COMMD1 by shRNA results in NF-κB stabilization and enhanced NF-κB-dependent transcription in TNF-stimulated cells. TNF also augments the binding of COMMD1 and Cullin-2, thereby strengthening the interaction between SOCS1 and p65, which in turn causes p65 ubiquitination and destabilization (Maine et al., 2007).

PDLIM2, a nuclear LIM domain-containing protein, is another ubiquitin E3 ligase that targets the p65 subunit and turns off p65-mediated immune and inflammatory responses (Tanaka et al., 2007; Torrado et al., 2004). In response to LPS stimulation, PDLIM2 interacts with nuclear p65 and sequesters this transcription factor into intranuclear compartments, where the ubiquitinated p65 undergoes proteasomal degradation. In this inducible event, PDLIM2 has two distinct activities that have been ascribed to its PDZ and LIM domains. The PDZ domain serves as a chaperone to promote the translocation of NF-κB to an insoluble compartment that consisted of promyelocytic leukemia (PML) nuclear bodies, whereas the LIM domain promotes the ubiquitination and degradation of p65 (Tanaka et al., 2007).

Taken together, nuclear p65 protein is short-lived and its stability is firmly controlled. Both ubiquitination and degradation of p65 appear to play a critical role in limiting the intensity and duration of transactivation, thus allowing efficient and prompt termination of the pro-inflammatory NF-κB response.

1.7 Aims of this study

The NF-κB p65 subunit undergoes multiple post-translational modifications. It is clear that p65 can be phosphorylated in response to various stimuli, but the involved kinases and the functional consequences of this modification are not completely clear. Based on the identification of p65 Ser 468 as a phosphorylation site in this laboratory, it was planned to:

1) Identify the kinases responsible for p65 Ser 468 phosphorylation triggered by T cell costimulation using *in vivo* analyses as well as *in vitro* kinase assays.
2) Investigate the distribution of Ser 468-phosphorylated p65 in response to T cell costimulation by subcellular fractionation.
3) Establish the function of this p65 phosphorylation event on NF-κB activation using reporter gene assays, gene arrays as well as real-time PCR analyses, and to test the potential impact of p65 phosphorylation on DNA-binding activity.
4) Explore the signaling pathways mediating p65 ubiquitination and degradation.
5) Determine the mechanisms and kinetics of p65 ubiquitination/elimination on individual target genes by chromatin immunoprecipitation (ChIP) assays.

2 Materials

2.1 Eukaryotic cell lines

Name	Organism	Characteristics	Cell type
Hela	Human cervical carcinoma cells		Adherent
Hela tet-on	Human cervical carcinoma cells	Stably transfected with pTet-On regulatory plasmid, doxycycline-inducible	Adherent
HEK 293	Human embryonic kidney cells		Adherent
HEK 293T	Human embryonic kidney cells	Expressing the large T antigen of the SV40 virus	Adherent
Jurkat-Tag	Human leukemia T cells	Expressing the large T antigen of the SV40 virus	Suspension
Jurkat tet-on	Human leukemia T cells	Stably transfected with pTet-On regulatory plasmid, doxycycline-inducible	Suspension
$NEMO^{-/-}$	Human leukemia T cells	Jurkat cells lacking NEMO expression	Suspension
$NEMO^{+}$	Human leukemia T cells	Jurkat cells re-transfected to express NEMO	Suspension
MEFs	Mouse embryonic fibroblasts		Adherent
$p65^{-/-}$	Mouse embryonic fibroblasts	MEFs lacking p65 expression	Adherent
$I\kappa B\alpha^{-/-}$	Mouse embryonic fibroblasts	MEFs lacking IκBα expression	Adherent
U2OS	Human bone osteosarcoma cells		Adherent

2.2 Bacteria *E.coli* strains

Strain	Genotype	Source
TOP10	F^- *mcr*A Δ(*mrr-hsd*RMS-*mcr*BC) ϕ80*lacZ*ΔM15 Δ*lac*X74 *deo*R *rec*A1 *end*A1 *ara*Δ139 Δ(*ara,leu*) 7697 *gal*U *gal*K λ^- *rps*L (Str^R) *nup*G	Invitrogen

GM2163	F$^-$ *ara-14 leuB6 fhuA31 lacY1 tsx78 glnV44 galK2 galT22 mcrA dcm-6 hisG4 rfbD1 rpsL136 dam-13*::Tn*9*(Cam^r) *xylA5 mtl-1 thi-1 mcrB1 hsdR2*	New England Biolabs
SURE	e14$^-$(mcrA$^-$) Δ (mcrCB-hsdSMR-mrr)171 endA1 supE44 thi-1 gyrA96 relA1 lac recB recJ sbcC umuC::Tn5(Kan^r) uvrC [F' proAB, lacI^{q}ΔM15, Tn10(Tet^r)]	Stratagene
BL21	*F$^-$* omp*T* hsd*S* $_{(rB\text{-}mB\text{-})}$ gal dcm	Novagen

2.3 Antibodies

Antibody	**Western blotting Dilution**	**Company**
Rabbit anti-β-actin, polyclonal	1:1000 in TBST	Abcam
Mouse anti-actin (C-2), monoclomal	1: 1000 in TBST	Santa Cruz Biotech
Mouse anti-E-tag, monoclonal	8 μg/ml in TBST	Amersham
Mouse anti-Flag (M2), monoclonal	1: 5000 in TBST	Sigma
Rabbit anti-GFP, polyclonal	1: 400 in TBST	BD Biosciences
Rat anti-HA (3F10), monoclonal	1: 4000 in TBST	Roche
Mouse anti-HDAC1 (H11), monoclonal	1: 1000 in TBST	Santa Cruz Biotech
Mouse anti-IKKα (M-280), polyclonal	1: 1000 in TBST	Santa Cruz Biotech
Mouse anti-IKKε, monoclonal	1: 500 in TBST	Abcam
Rabbit anti-IKKγ (FL-419), polyclonal	1: 1000 in TBST	Santa Cruz Biotech
Rabbit anti-IκBα (C-21), polyclonal	1: 1000 in TBST	Santa Cruz Biotech
Mouse anti-c-Myc (9E10), monoclonal	1: 1000 in TBST	Roche
Rabbit anti-p65 (C-20), polyclonal	1: 1000 in TBST	Santa Cruz Biotech
Mouse anti-p65 (F-6), monoclonal	1: 1000 in TBST	Santa Cruz Biotech
Rabbit anti-p65 (A), polyclonal	1: 1000 in TBST	Santa Cruz Biotech
Mouse anti-p50 (E-10), monoclonal	1: 500 in TBST	Santa Cruz Biotech
Rabbit anti-phospho-GSK-3α/β (Ser21/9), polyclonal	1: 1000 in TBST	Cell Signaling Tech
Mouse anti-phospho-IκBα (Ser32/36) (5A5), monoclonal	1: 2000 in TBST	Cell Signaling Tech
Rabbit anti-phospho-p65 (Ser468), polyclonal	1: 1000 in TBST	Cell Signaling Tech

Rabbit anti-phospho-p65 (Ser536), polyclonal	1: 1000 in TBST	Cell Signaling Tech
Rabbit anti-phospho-p65 (Ser536) (93H1), monoclonal	1: 1000 in TBST	Cell Signaling Tech
Rabbit anti-Pol II (N-20), polyclonal	1: 1000 in TBST	Santa Cruz Biotech
Mouse anti-tubulin, monoclonal	1: 1000 in TBST	Sigma
Mouse anti-ubiquitin (P4D1), monoclonal	1: 1000 in TBST	Cell Signaling Tech
Secondary antibody		
Peroxidase-conjugated AffiniPure Goat anti-mouse-IgG	1: 5000 in TBST	Dianova
Peroxidase-conjugated AffiniPure Goat anti-rabbit-IgG	1: 5000 in TBST	Dianova
Peroxidase-conjugated AffiniPure Goat anti-rat-IgG	1: 25000 in TBST	Dianova

2.4 Plasmids

cDNA	Vector	Epitope tag	Source
p65	pEFpuro	HA	I. Mattioli, Bern
p65 S468A	pEFpuro	HA	This study
p65 S468E	pEFpuro	HA	This study
p65 S536A	pEFpuro	HA	This study
p65 S536E	pEFpuro	HA	This study
p65 SS468/536AA	pEFpuro	HA	This study
p65 SS468/536EE	pEFpuro	HA	This study
p65 S468N	pEFpuro	HA	This study
p65 E39I	pEFpuro	HA	This study
p65 S468A/E39I	pEFpuro	HA	This study
p65	pEGFP	GFP	M. Kracht, Hannover
p65 S468A	pEGFP	GFP	I. Mattioli, Bern
p65	pAB	Gal4	M. L. Schmitz, Bern
p65 (354-551)	pGEX-4T1	GST	I. Saiki, Japan

p50	pcDNA3.1	Flag	D. Krappmann, Munich
IKKα	pcDNA3.1	Flag	T. Maniatis, USA
IKKβ	pcDNA3.1	Flag	T. Maniatis, USA
IKKε	pEFpuro	Flag	T. Maniatis, USA
IKKε K/A	pEFpuro	Flag	T. Maniatis, USA
GSK3β	pcDNA3.1	HA	J. R. Woodgett, Canada
$(\kappa B)_3$_Luc	pGL3	none	G. Haegeman, Gent
A20	PCAGGS	E	R. Beyaert, Belgium
ABIN1	PCAGGS	E	R. Beyaert, Belgium
ABIN2	PCAGGS	E	R. Beyaert, Belgium
COMMD1	pEBB	Flag	E. Burstein, USA
Cul2	pEBB	Flag	E. Burstein, USA
CYLD	pcDNA3	Flag	M. Kracht, Hannover
Itch	pEF4	Flag	D. Krappmann, Munich
Nedd4	pEF4	Flag	D. Krappmann, Munich
PDLIM2	pCMV	Myc	T. Kaisho, Japan
SOCS1	pEF	Flag	T. Willson, Australia
TRAF2	pcDNA3	Flag	D. Krappmann, Munich
TRAF6	pcDNA3.1	None	M. Kracht, Hannover
βTrCP	pCMV	Flag	Y. Nen-Neriah, Jerusalem
hCOMMD1 small hairpin	pSUPER-Puro	None	This study
mCOMMD1 small hairpin	pSUPER-Puro	None	This study
mIκbα small hairpin	pSUPER-Puro	None	This study

2.5 DNA Oligonucleotides

All oligonucleotides were obtained from Microsynth (Switzerland) or MWG (Germany).

Oligo	**Sequence (5'→3')** (restriction digestion sites, point mutation sites or target gene sequences are presented in bold type)	**Relevant features**
pEF-HA p65 fwd	TATTT**GGATCC**ATGGACGAACTGTT CCCCCTC	p65 cloning, contains *BamHI* digestion site
p65-new_rev	**TCTAGA**GGAGCTGATCTGACTCAGC AG	p65 cloning, contains *XbaI* digestion site
p65-S468A_for	TTCACAGACCTGGCA**GCC**GTCGACA	p65 point mutation, S to A at 468
p65-S468A_rev	CTCGGAGTTGTCGAC**GGC**TGCCAGG	p65 point mutation, S to A at 468
p65_S468E_for	TTCACAGACCTGGCA**GAA**GTCGACA	p65 point mutation, S to E at 468
p65_S468E_rev	CTCGGAGTTGTCGAC**TTC**TGCCAGG	p65 point mutation, S to E at 468
S/A-sense	GAGATGAAGACTTCTCC**GCC**ATTGC G	p65 point mutation, S to A at 536
S/A-antisense	GTCCATGTCCGCAAT**GGC**GGAGAAG T	p65 point mutation, S to A at 536
S/E-sense	GGAGATGAAGACTTCTCC**GAA**ATTG CGGACA	p65 point mutation, S to E at 536
S/E-antisense	TGAGAAGTCCATGTCCGCAAT**TTC**G GAGAAGTCT	p65 point mutation, S to E at 536
S468N_for	GCTGTGTTCACAGACCTGGCA**AAC**G TCGACAACTCC	p65 point mutation, S to N at 468
S468N_rev	CTCGGAGTTGTCGAC**GTT**TGCCAGG TCTGTGAACAC	p65 point mutation, S to N at 468
p65E39I-for	GCGCTTCCGCTACAAGTGC**ATC**GGG CGCTCCGC	p65 point mutation, E to I at 39
p65E39I-rev	CCGCGGAGCGCCC**GAT**GCACTTGTA GCGGAAGC	p65 point mutation, E to I at 39
RT-ICAM1_for	GGAGACGCAGAGGACCTTAAC	Real-time PCR primer for mouse ICAM-1
RT-ICAM1_rev	CGCTCAGAAGAACCACCTTC	Real-time PCR primer for mouse ICAM-1
RT-MIP2_for	AGTGAACTGCGCTGTCAATG	Real-time PCR primer for mouse MIP-2
RT-MIP2_rev	CTTCAGGGTCAAGGCAAACT	Real-time PCR primer for mouse MIP-2
RT-β-actin_for	GAGATTACTGCTCTGGCTCCTA	Real-time PCR primer for mouse β-actin
RT-β-actin_rev	TCATCGTACTCCTGCTTGCT	Real-time PCR primer for mouse β-actin

ChIP-ICAM1_ for2	AGGGGACTAGGCAGTAGTCAATCAG	ChIP primer for mouse ICAM-1
ChIP-ICAM1_ rev2	GAACGAGGGCTTCGGTATTT	ChIP primer for mouse ICAM-1
ChIP-MIP2_ for2	AGGGCAGGGCAGTAGAATGA	ChIP primer for mouse MIP-2
ChIP-MIP2_ rev2	TGTGGCTGGAGTCTGGAGTG	ChIP primer for mouse MIP-2
ChIP-GAPDH_ For	GCCCTTGAGCTAGGACTGGATA	ChIP primer for mouse GAPDH
ChIP-GAPDH_ Rev	ACCTGGCACTGCACAAGAAGAT	ChIP primer for mouse GAPDH
COMMD1-siRNA_for	GATCCCC**GTCTATTGCGTCTGCAGAC**ttcaagaga**GTCTGCAGACGCAATAGAC**TTTTTGGAAA	Knock-down of human COMMD1
COMMD1-siRNA_rev	AGCTTTTCCAAAAA**GTCTATTGCGTCTGCAGAC**tctcttgaa**GTCTGCAGACGCAATAGAC**GGG	Knock-down of human COMMD1
siCOMMD1-m1_ for	GATCCCC**GTCTATTGCATCTGCAGAC**ttcaagaga**GTCTGCAGATGCAATAGAC**TTTTTGGAAA	Knock-down of mouse COMMD1
siCOMMD1-m1_ rev	AGCTTTTCCAAAAA**GTCTATTGCATCTGCAGAC**tctcttgaa**GTCTGCAGATGCAATAGAC**GGG	Knock-down of mouse COMMD1
mIκBα-AB_for	GATCCCC**GGACGAGGAGTACGAGCAA**ttcaagaga**TTGCTCGTACTCCTCGTCCT**TTTTGGAAA	Knock-down of mouse IκBα
mIκBα-AB_rev	AGCTTTTCCAAAAA**GGACGAGGAGTACGAGCAA**tctcttgaa**TTGCTCGTACTCCTCGTCC**GGG	Knock-down of mouse IκBα

2.6 Antibiotics

All antibiotics were sterilized by 0.22 μm filter.

Antibiotic	**Source**	**Solvent**	**Stock concentration**	**Final concentration**
Ampicillin	Sigma	H_2O	100 mg/ml	100 μg/ml
Kanamycin	Sigma	H_2O	50 mg/ml	50 μg/ml
Doxycycline	Sigma	H_2O	2 mg/ml	1-2 μg/ml
Puromycin	Invivogen	H_2O	10 mg/ml	1-5 μg/ml

Plasmocin	Invivogen	H_2O	25 mg/ml	25 μg/ml
Geneticin (G418)	Sigma	H_2O	50 mg/ml	200-400 μg/ml
Actinomycin D	Sigma	DMSO	1 mg/ml	1 μg/ml

2.7 Specific inhibitors for signaling pathways

Inhibitor	**Source**	**Solvent**	**Stock concentration**	**Final concentration**	**Inhibited pathway**
AS602868	Serono inter-national SA	DMSO	12 mg/ml	12 μg/ml	IKKβ
Cycloheximide	Sigma	Ethanol	10 mg/ml Freshly made	10 μg/ml	Protein synthesis
LiCl	Merck	H_2O	5 M	25 mM	GSK3
MG132	Alexis	DMSO	10 mM	10 μM	Proteasome
PD332991	Pfizer	50% DMSO	2.5 mM	10 μM	CDK 4/6
PD98059	Alexis	DMSO	10 mM	50 μM	ERK
SB203580	Alexis	DMSO	10 mM	20 μM	p38 MAPK
SP600125	Calbiochem	DMSO	5 mM	20 μM	JNK
Wortmannin	Sigma	DMSO	1 mM	2 μM	PI3K

2.8 Enzymes and enzyme inhibitors

All restriction enzymes were purchased from Fermentas or New England Biolabs.

Other enzymes and enzyme inhibitors:

Enzyme or enzyme inhibitor	**Firm**
DNase I (RNase-free)	Fermentas
DNA polymerase (Klenow fragment)	Fermentas
Proteinase K	Sigma
RNase A	Sigma
Shrimp alkaline phosphatase (SAP)	Roche
SuperScript™ II reverse transcriptase	Invitrogen
T4 DNA ligase	Fermentas
T4 DNA polymerase	Fermentas

T4 polynucleotide kinase (T4 PNK)	Fermentas
Taq DNA polymerase	Fermentas
Ribolock RNase inhibitor	Fermentas

2.9 Kits

Kits	**Firm**
ABsolute^{TM} QPCR SYBR Green Mixes	Thermo (ABgene)
Endofree® Plasmid Maxi	Qiagen
Expand High Fidelity^{PLUS} PCR System	Roche
Gel Extraction Spin	JETquick
Plasmid Midi and Maxi	Qiagen or JETstar
QuikChange Site-Directed Mutagenesis	Stratagene
RNeasy Mini	Qiagen
RNase-Free DNase Set	Qiagen

2.10 Chemicals and reagents

Product	**Manufacturer**
[γ-^{32}P]ATP	Amersham
[^{35}S]-Methionine	Amersham
[^{35}S]-Cysteine	Amersham
Acetic acid	Roth
Agarose	Invitrogen
Ammonium persulfate (APS)	Bio-Rad
Aphidicolin	Sigma
Aprotinin	Sigma
Bacto^{TM} agar	BD Bioscience
Boric acid	Fluka
Bovine serum albumin (BSA)	Sigma
Bradford reagent	Sigma
Bromophenol blue	Merck
Calcium chloride ($CaCl_2$)	Sigma
L-Cysteine	Sigma
Dimethyl sulfoxide (DMSO)	Fluka
1,4-Dithiothreitol (DTT)	Biocheringer
EGTA	Fluka
Ethanol	Merck
Ethidium bromide (EB)	Roth

Ethylendiaminetetraacetic acid (EDTA)	Fluka
Ficoll 400	Serva
Formaldehyde	Roth
X-gal	AppliChem
Glass beads	Roth
Glucose	Fluka
Glycerol	Acros Organics
β-Glycerophosphate	Acros Organics
Glycine	Roth
Guanidine-HCl	Roth
HEPES	Sigma
Hydrochloric acid 30% (HCl)	Merck
Imidazole	Fluka
IPTG	AppliChem
Isopropanol	Merck
Leupeptin	Sigma
Lithium chloride (LiCl)	Merck
Magnesium chloride ($MgCl_2$)	Merck
Magnesium sulfate ($MgSO_4$)	Merck
β-Mercaptoethanol	Fluka
Methanol	Merck
L-Methionine	Sigma
Nonidet P40	Roche
Phenylmethanesulfonyl fluoride (PMSF)	Fluka
Potassium chloride (KCl)	Fluka
Potassium dihydrogen phosphate (KH_2PO_4)	Fluka
di-Potassium hydrogen phosphate (K_2HPO_4)	Fluka
Potassium hydroxide (KOH)	Merck
Skim milk powder	Merck
Sodium azide (NaN_3)	Fluka
Sodium chloride (NaCl)	Roth
Sodium dodecyl sulfate (SDS)	Bio-Rad
Sodium fluoride (NaF)	Roth
Sodium dihydrogen phophate (NaH_2PO_4)	Acros organics
di-Sodium hydrogen phosphate (Na_2HPO_4)	Merck
Sodium hydroxide (NaOH)	Fluka
Sodium orthovanadate (Na_3VO_4)	Sigma
N,N,N',N'-Tetra-methyl-ethylenediamine (TEMED)	Bio-Rad
Thymidine	Sigma
Tris-base	Acros organics
Triton X-100	Sigma
Tryptone/peptone	Roth
Tween 20	Gerbu

Urea	Roth
Yeast extract	Roth
Other reagent	
Control IgG mouse	Santa Cruz Biotech
Control IgG rabbit	Santa Cruz Biotech
Control IgG rat	Santa Cruz Biotech
Dialyzed FBS	Gibro (Invitrogen)
DMEM high glucose medium	Cell concepts
DMEM (L-methionine and L-cysteine-free) medium	Gibro (Invitrogen)
Fetal calf serum (FCS)	Cell concepts
Glutathione Sepharose™ 4B	GE Healthcare
L-Glutamine 200 mM	Amimed (BioConcept)
Ionomycin	Sigma
O' GeneRuler™ 100 bp DNA ladder	Fermemtas
O' GeneRuler™ 1 kb DNA ladder	Fermentas
PMA	Sigma
Penicillin-Streptomycin	Amimed (BioConcept)
Precision Plus Protein™ all blue standards	Bio-Rad
Protein A/G PLUS-agarose	Santa Cruz Biotech
Ni-NTA agarose	Qiagen
Rabbit gamma globulin	Rockland
Recombinant TNF	Knoll AG
Roti-Fect®	Roth
RPMI 1640 medium	Cell concepts
Sodium pyruvate 100 mM	Gibro (Invitrogen)
Trypsin/EDTA	PAN™ (Biotech)

3 Methods

3.1 Molecular biology methods

3.1.1 Polymerase chain reaction (PCR)

PCR is used to produce high yields of specific target DNA fragments *in vitro*. The reaction uses two specific oligonucleotides (primers), which hybridize to sense and antisense strands of the template DNA fragment, four deoxyribonucleotide triphosphates (dNTPs) and a heat-stable DNA polymerase.

A typical 50 µl PCR reaction mixture consists of:

Template DNA	20 ng
Forward primer	20 pmol
Reverse primer	20 pmol
10 mM dNTP mix	1 µl
10 x PCR buffer	5 µl
DNA polymerase	1.0 U
H_2O	to 50 µl

The reaction is performed in a thermocycler apparatus. Usually, there is a preheating step of 5 min at 95°C during which template DNA is denatured. This is followed by 30-32 cycles of:

Denaturation	30-60 sec	95°C
Annealing	30-60 sec	55-65°C
Extension	1 min/kb	72°C

The last cycle is followed by an extra elongation step of 7-10 min at 72°C. The annealing temperature is dependent on the composition of the primers, i.e., on their melting temperature (Tm). The primers may have modifications, such as extensions with 1-5 extra nucleotides at their 5'-end, adjacent to the recognition site for desired restriction enzymes.

PCR can also be performed directly from bacterial colonies. For this purpose, bacterial colonies were picked with a pipette tip from agar plates, dissolved in 50 µl of 1 x PCR buffer and boiled at 95°C for 5 min, after which 5 µl of the mixture were used as template for the PCR reaction.

PCR products were analyzed by agarose gel electrophoresis and then purified with a PCR purification kit, according to the manufacturer's instructions. Modified PCR products were digested with specific restriction enzymes and ligated into the corresponding linearized vector DNA.

3.1.2 Agarose gel electrophoresis

The DNA sample was mixed with 6 x loading buffer and loaded onto a 0.8-2% ethidium bromide agarose gel in 1 x TAE buffer. The voltage of electrophoresis was set to ~10V/cm gel length. DNA was visualized with a UV light source and photographed directly. For subcloning, DNA was visualized at 320 nm wavelength. The desired bands were excised with a clean scalpel and purified using gel extraction kit, according to the manufacturer's instructions.

50 x TAE	2 M	Tris base
	1M	Acetic acid (adjust to pH 8.3)
	0.05 M	EDTA
6 x DNA loading buffer	60%	Glycerol
	60 mM	EDTA pH 8.0
	0.09%	Bromophenol blue

3.1.3 Restriction endonuclease digestion

Digestion with restriction endonucleases was carried out according to the manufacturer's instructions. Briefly, plasmid DNA or PCR product, optimal 10 x reaction buffer, restriction endonucleases and H_2O were mixed to a total volume

of 10-50 µl. The reaction mixture was incubated at the recommended temperature for 1-3 h. When appropriate, restriction endonucleases were inactivated by heating.

3.1.4 Ligation

The purified DNA fragments were ligated into the linearized plasmids with T4 DNA ligase. A ligation reaction mixture consists of 1 µl T4 DNA ligase, 2 µl of 10 x ligation buffer, an appropriate molar ratio of linearized vector DNA and purified insert DNA fragment (1:5 for blunt ends and 1:3 for sticky ends) to a total volume of 20 µl. The reaction mixture was incubated at 4°C overnight or at room temperature for 2 h and then transformed into competent *E.coli* cells.

3.1.5 Preparation of chemically competent *E.coli* cells

Competent *E.coli* cells were prepared by the $CaCl_2$ method. Glycerol stock *E.coli* cells were grown in 20 ml of antibiotic-free LB medium at 37°C overnight. This bacterial culture was then diluted with 120 ml of pre-warmed LB medium and cultured until an OD_{600nm} of 0.5-0.7 was achieved. All the following steps were performed on ice or at 4°C. The cells were cooled on ice during 15 min and then harvested by centrifugation at 4000 g for 15 min. The cell pellet was carefully resuspended in 100 ml of sterilized cold 0.1 M $CaCl_2$ and incubated for 30 min. The suspension was pelleted at 4000 g for 15 min, and the cells were gently resuspended in 10 ml of a 10% glycerol/0.1 M $CaCl_2$ solution; 100 µl aliquots of the bacteria suspension were transferred to pre-chilled tubes and immediately frozen in liquid nitrogen. The competent cells were stored at -80°C until further use.

LB (Luria-Bertani) medium	10 g/L	Tryptone
	5 g/L	Yeast extract
	10 g/L	NaCl

3.1.6 Transformation of competent cells

Frozen competent cells were thawed on ice just before use. Plasmid DNA (1 ng-1 µg) or 20 µl of the ligation mixture was gently mixed with 100 µl of competent bacteria and then incubated on ice for 30 min. Competent cells were heat shocked at 42°C for 90 sec, and then placed on ice for 2 min. For each transformation, 800 µl LB or SOC medium without antibiotics was added. Following incubation at 37°C for 1 h, the mixture was centrifuged at 3000 rpm for 3 min. After discarding the supernatant, the pellet was resuspended in about 80 µl of transformation mixture and spread over a pre-warmed selective LB-agar plate. The plate was incubated overnight at 37°C. The clones were then screened for positive ones using PCR, restriction analysis or DNA sequencing.

SOC medium	2 % (w/v)	Tryptone
	0.5% (w/v)	Yeast extract
	10 mM	NaCl
	2.5 mM	KCl
	10 mM	$MgCl_2$
	10 mM	$MgSO_4$
	20 mM	Glucose
LB Agar	10 g/L	Trypone
	5 g/L	Yeast extract
	10 g/L	NaCl
	14 g/L	Agar
	antibiotics (see section 2.6)	

3.1.7 Plasmid DNA purification

Small-, medium- and large-scale plasmid extractions were performed using plasmid mini-, midi- and maxi-prep kits from QIAGEN or JETstar, according to the manufacturer's recommendations, respectively.

3.1.8 Measurement of DNA concentration

The DNA concentration was calculated based on the value of OD_{260nm} measured with a spectrophotometer. The OD_{260nm}/OD_{280nm} ratio yielded a determination of DNA purity. For pure DNA, this ratio was approximately 1.8. The concentration of DNA was calculated with the following formula:

dsDNA concentration (μg/ml) = OD_{260nm} × 50 × dilution factor.

3.1.9 *In vitro* mutagenesis

The QuikChange site-directed mutagenesis kit from Stratagene was used to create point mutations. The general procedure utilizes a supercoiled double-stranded DNA vector with the insert of interest and two synthetic primers containing the desired mutation. The oligonucleotide primers, each complementary to opposite strands of the vector, are extended by *PfuUltra* DNA polymerase during thermal cycling. Incorporation of the primers generates a mutated plasmid containing staggered nicks. Following temperature cycling, the product is treated with *DpnI*, which is used to digest the methylated parental DNA template. After incubation, the nicked vector DNA containing the desired mutations is then transformed into competent cells.

A typical 50 μl reaction mixture consists of:

5 μl of 10 x reaction buffer
X μl (10 ng) of dsDNA template
X μl (125 ng) of oligonucleotide primer 1
X μl (125 ng) of oligonucleotide primer 2
1 μl of dNTP mix
H_2O to a final volume of 50 μl
1 μl of *PfuUltra* DNA polymerase (2.5 U/μl)

Table 3.1 Cycling parameters for the QuikChange site-directed mutagenesis method

Segment	Cycles	Temperature	Time
1	1	95°C	30 sec
2	12-18	95°C (denaturing)	30 sec
		55°C (annealing)	1 min
		68°C (elongation)	1 min/kb of plasmid length

3.1.10 Cloning of short interfering RNA

The pSUPER plasmid allows the expression of short hairpin RNA. The vector uses the RNA polymerase III H1-RNA gene promoter, as it produces a small RNA transcript lacking a polyadenosine tail and has a well-defined start of transcription and a termination signal consisting of five consecutive thymidines. The cleavage of the transcript at the termination site is after the second uridine, yielding a transcript resembling the ends of synthetic siRNAs, which also contain two 3' overhanging T or U nucleotides.

The pSUPER vector contains a multiple cloning site, which allows the convenient insertion of the dsDNA inserts. After digestion of the vector with *BglII* and *HindIII,* a compatible insert is ligated into the vector. This leads to the destruction of the *BglII* site, but allows for checking positive clones after digestion with *EcoRI* and *HindIII*. While an empty vector yields a band of about 300 bps, positive clones yield bands of around 360 bps.

Ideally, the 19 nt target sequence should be flanked in the mRNA with AA at the 5' end and TT at the 3' end. Good results may also be obtained in sequences with flanking 5' AA only. Regions in the mRNA to select the 19 nt target sequence should be in the coding zone. The GC content of this 19 nt targeting sequence should be preferably more than 30%. A stretch of four or more adenines or thymidines in the selected 19 nts should be avoided, as this will result in premature termination of the transcript.

An example for the design of synthetic oligos

Forward primer:

Sense of the19 nts

Antisense of the 19 nts

GATCCCC**GACTCCAGTGGTAATCTAC**ttcaagaga**GTAGATTACCACTGGAG**
TCTTTTTGGAAA

Reverse primer:

Sense of the 19 nts

Antisense of the 19 nts

AGCTTTTCCAAAAA**GACTCCAGTGGTAATCTAC**tctcttgaa**GTAGATTACCA CTGGAGTC**GGG

Each oligo consists of 64 nts. The selected 19 nt sequence of the target gene should be replaced with the sequences in bold type.

The forward and reverse oligos (64 nt) were dissolved in H_2O to achieve a final concentration of 3 mg/ml. 1 µl of each oligo was taken out and mixed with 48 µl annealing buffer. This mixture was incubated at 95°C for 4 min, followed by incubation at 70°C for 10 min, and then slowly cooled to 4°C. 2 µl of these annealed oligos were phosphorylated by T4 polynucleotide kinase and then ligated into the linearized pSUPER vector opened with *BglII/BamHIII*.

Annealing buffer	100 mM	Potassium acetate
	30 mM	HEPES-KOH pH 7.4
	2 mM	Magnesium acetate

3.2 Cell biology methods

3.2.1 Cell culture

Adherent cells were grown in DMEM medium supplemented with 10% (v/v) fetal calf serum, 2 mM L-glutamine, and 1% (v/v) penicillin/streptomycin at 37°C in a humidified atmosphere containing 5% CO_2. Adherent cells were passaged by trypsinization. Cells were washed once with pre-warmed PBS, and then treated with trypsin/EDTA solution. After incubation at 37°C for 3-5 min, the detached cells were diluted with warm DMEM culture medium and split into new flasks.

Suspension cells were cultured in complete RPMI 1640 medium, containing 10% (v/v) fetal calf serum, 2 mM L-glutamine, 1% (v/v) penicillin/streptomycin, and 10 mM

HEPES at 37°C, 5% CO_2 and 100% humidity. For passaging, these cells were diluted with fresh medium.

PBS	137 mM	NaCl
	2.7 mM	KCl
	8.1 mM	Na_2HPO_4
	1.5 mM	KH_2PO_4
	pH 7.4	

3.2.2 Transfection of DNA into mammalian cells

One day prior to transfection, adherent cells were seeded into culture dishes, so that a density of 40-70% confluence was reached by the time of transfection. Plasmid DNA and Roti-Fect® transfection reagent were mixed and added to the cells, according to the manufacturer's instructions (Roth).

Suspension cells were collected and washed with warm, serum-free RPMI medium. Then the pellet was resuspended in 350 µl serum-free medium and mixed with 5-20 µg plasmid DNA. The cell/DNA suspension was transfected by electroporation using a gene pulser (Bio-Rad), at 250V/950 µF. After allowing the cells to recover for 5 min, they were transferred into a small tissue culture flask with fresh complete medium.

3.2.3 Luciferase reporter assay

The luciferase assay is based on enzyme-catalyzed chemiluminescence. Luciferin present in the luciferase assay reagent is oxidized by luciferase in the presence of ATP, atmospheric oxygen and magnesium ions. This reaction produces light with a wavelength of 562 nm that can be measured by a luminometer. This method is used to quantify the expression of the luciferase reporter protein.

Cells were transfected with reporter vectors containing the firefly luciferase gene. 24-30 h later, after washing two times with PBS, the cells were lyzed in 80-100 µl

1 x lysis buffer for 15 min at room temperature. For the measurement, 10 µl of cell lysate was mixed with 10 µl luciferase assay reagent and light emission was determined in a luminometer.

5 x Lysis buffer	125 mM	Tris-phosphate pH 7.8
	10 mM	EDTA
	10 mM	DTT
	50%	Glycerol
	5%	Triton X-100
Luciferase assay reagent	20 mM	Tricine
	1.07 mM	$(MgCO_3)_4Mg(OH)_2 \cdot 5H_2O$
	2.67 mM	$MgSO_4$
	0.1 mM	EDTA
	33.3 mM	DTT
	270 µM	Coenzyme A
	470 µM	Luciferin
	530 µM	ATP

3.2.4 Protein extractions

3.2.4.1 Total cell lysis in 1 x SDS sample buffer

After washing in ice-cold PBS, cells were collected by centrifugation. The pellet was resuspended in 150-200 µl of 1 x SDS sample buffer, followed by sonification (2 x 15 sec, Sonifier 250, Branson). The cell extract was boiled at 95°C for 5 min and further analyzed by Western blotting.

5 x SDS sample buffer	312.5 mM	Tris/HCl pH 6.8
	10% (w/v)	SDS
	50% (v/v)	Glycerol
	25% (v/v)	β-Mercaptoethanol
	0.01% (w/v)	Bromophenol blue

3.2.4.2 Total cell extraction in NP-40 lysis buffer

Cell pellet was resuspended in 80-120 µl of NP-40 lysis buffer (freshly added phosphatase and protease inhibitors) and incubated on ice for 20 min. Cell debris was

removed by a 13,200 rpm centrifugation at 4°C for 15 min. The supernatant containing total cell extract was collected for further use.

NP-40 lysis buffer	20 mM	Tris/HCl pH 7.5
	150 mM	NaCl
	1% (v/v)	Nonidet P-40
Phosphatase and protease inhibitors	10 mM	NaF
	0.5 mM	Sodium vanadate
	10 µg/ml	Leupeptin
	10 µg/ml	Aprotinin
	1 mM	Phenylmethylsulfonylfluoride (PMSF)

3.2.4.3 Subcellular fractionation (nuclear and cytosolic extractions)

After washing with ice-cold PBS, cells were collected by centrifugation. Nuclear and cytosolic proteins were separated upon resuspending pelleted cells in 400 µl cold low salt buffer A (freshly added phosphatase and protease inhibitors) by gentle pipetting. After incubation for 10 min on ice, 10 µl of 10% NP-40 was added and cells were lyzed by vortexing gently. The homogenate was centrifuged for 10 sec at 13,200 rpm. The supernatant representing the cytosolic fraction was collected. After washing 4 times in buffer A, the pellet containing the cell nuclei was dissolved in 100 µl high salt buffer C (including phosphatase and protease inhibitors). The cell suspension was either incubated for 15 min on ice or sonified for 10 sec, and spun down for 10 min at 13,200 rpm. The supernatant representing the nuclear fraction was then collected.

Buffer A	10 mM	HEPES/KOH pH 7.9
	10 mM	KCl
	0.1 mM	EDTA
	0.1 mM	EGTA
	1 mM	β-Mercaptoethanol
Buffer C	20 mM	HEPES/KOH pH 7.9
	400 mM	NaCl
	1 mM	EDTA
	1 mM	EGTA
	1 mM	β-Mercaptoethanol

3.2.4.4 Measurement of protein concentration

Protein concentrations were determined according to the Bradford method. This test employs the protein-specific dye coomassie brilliant blue G-250 that undergoes an absorbance shift from 465nm to 595nm upon binding to protein. Therefore, the OD_{600nm} value of this dye depends, in a linear fashion, on the concentration of most soluble proteins. NP-40 lysis buffers are not suitable for measurement, as NP-40 by itself tends to absorb light at OD_{600nm}. For routine use, 10 µl of protein solution was first diluted with 90 µl of 1 M NaCl and 10 µl of this diluted solution was mixed with 90 µl of 1 x Bradford solution. The OD_{600nm} of this sample was measured and plotted against a reference curve obtained with known concentrations of BSA.

3.2.5 RNA isolation and gene expression analysis

3.2.5.1 Isolation of total RNA from mammalian cells

To prevent contamination with RNases, gloves were worn and RNase-free tubes, filter pipette tips, glassware and solutions were used. Total RNA was extracted using the RNeasy Mini kit, according to the manufacturer's instructions (Qiagen). During RNA purification, the RNase-Free DNase Set (Qiagen) was used to completely remove DNA from the samples.

3.2.5.2 Measurement of RNA concentration

The RNA concentration of a given sample was calculated depending on the value of OD_{260nm} measured with a spectrophotometer. The OD_{260nm}/OD_{280nm} of pure RNA should be approximately 2.0. The concentration of RNA was calculated with the following formula:

RNA concentration (µg/ml) = $OD_{260nm} \times 40 \times$ dilution factor.

The quality of the obtained RNA was evaluated by running samples on a 1.5% agarose gel and visualization of the rRNA bands.

3.2.5.3 Synthesis of cDNA

Reverse transcription was employed to convert mRNAs into cDNAs by using Oligo(dT) primers and reverse transcriptase (Invitrogen). Briefly, 1 μg of total RNA was mixed with 10 mM dNTPs (final concentration), 0.5 μg $Oligo(dT)_{12-18}$ and H_2O to 12 μl. This mixture was heated at 65°C for 5 min, and quickly chilled on ice. Then, 4 μl of 5 x first-strand buffer and 2 μl of 0.1 M DTT were added to the sample and incubated at 42°C for 2 min. Finally, 1 μl of SuperScript™ II RT (200 U) was added to the mixture, followed by incubating at 42°C for 50 min and heating at 70°C for 15 min.

3.2.5.4 Real-time PCR analysis

Real-time PCR was used to amplify a segment of a known sequence from cDNA with gene-specific primers.

A typical 25 μl reaction mixture consists of:

12.5 μl	Absolute QPCR SYBR Green MIX (2 x)
X μl (20 ng)	cDNA template
X μl (70 nM)	Forward primer
X μl (70 nM)	Reverse primer
RNase-free H_2O to a final volume of 25 μl	

Quantitative real-time PCR was performed on an ABI 7300 real-time PCR cycler (Applied Biosystems) using the following programs:

Table 3.2 QPCR thermal cycling program

	Temp.	**Time**	**Number of cycles**
Enzyme activation	95°C	15 min	1 cycle
Denaturation	95°C	15 sec	40 cycles
Annealing	50-60°C	30 sec	
Extension	72°C	30 sec-1 min	

After amplification, a melting curve was performed to confirm the specificity of the reaction.

Table 3.3 Melting curve program

	Temp.	Time	Number of cycles
Denaturation	95°C	30 sec	1 cycle
Starting temp.	60°C	30 sec	1 cycle
Melting step	60°C	10 sec	80 cycles

The threshold value ct for each individual PCR product was calculated by the instrument's software and ct values obtained for the target gene were normalized by subtracting the ct values obtained with the reference gene. The resulting Δct values were then used to calculate relative changes of mRNA expression as the ratio (R) of mRNA expression of stimulated/unstimulated cells according to the equation:

$R=2^{(\Delta ct(stimulated)-\Delta ct(unstimulated))}$

3.2.6 Cell-cycle synchronization

Cells were synchronized with a double thymidine and aphidicolin block. In brief, cells were first blocked with thymidine (2 mM) for 14 h, followed by extensive washing and release for 11 h, and subsequent block for 14 h with aphidicolin (1 μg/mL). After washing, cells were released to proceed in the cell cycle using normal medium and harvested at different time points.

3.2.7 ^{35}S-Methionine/cysteine pulse-chase labeling

Cells were washed twice in warm PBS and incubated in methionine/cysteine-free DMEM containing 5% dialyzed FBS and 2 mM glutamine for 30 min. Then, they were pulsed with approximately 500 μCi ^{35}S-methionine/cysteine for 1 h, washed with warm PBS and incubated further with regular DMEM supplemented with 10% FBS, excess unlabeled methionine and cysteine (2 mM each) for the indicated periods. Upon harvesting, cells were washed in ice-cold PBS, pelleted and stored at -80°C until immunoprecipitation was performed. Harvested cells were analyzed further following denaturing lysis in TSD buffer and boiling for 10 min at 95°C. This

buffer was then supplemented with TNN buffer to decrease the SDS concentration to 0.2%. Afterwards, the samples were pre-cleared with protein A/G agarose beads for 1 h at 4°C, and the supernatant obtained after centrifugation was subjected to immunoprecipitation.

TSD buffer	50 mM	Tris/HCl pH7.5
	1%	SDS
	5 mM	DTT
TNN buffer	50 mM	Tris/HCl pH7.5
	250 mM	NaCl
	5 mM	EDTA
	0.5%	NP-40

3.3 Biochemistry methods

3.3.1 SDS-polyacrylamide gel electrophoresis (SDS-PAGE)

SDS-PAGE is used to separate proteins on the basis of their molecular size. The system contains two gels: a "stacking gel" with a low level of crosslinkage and of low pH, allowing proteins to enter the gel and compact without smearing; and a "seperation gel" of higher pH, where the proteins are separated according to molecular size. For an 8×10×0.1 cm gel, the following volumes were used:

Table 3.4 compositions of separation gel and stacking gel

Seperation gel	**15%**	**12%**	**10%**	**8%**	**Stacking gel**	
4 x lower buffer	1.25 ml	1.25 ml	1.25 ml	1.25 ml	4 x upper buffer	0.5 ml
AA (30%)	2.5 ml	2 ml	1.66 ml	1.33 ml	AA (30%)	0.25 ml
H_2O	1.25 ml	1.75 ml	2.09 ml	2.42 ml	H_2O	1.25 ml
APS (10%)	25 µl	25 µl	25 µl	25 µl	APS (10%)	20 µl
TEMED	4 µl	4 µl	4 µl	4 µl	TEMED	2 µl

4 x Lower buffer	1.5 M	Tris/HCl pH8.8
	0.4%	SDS
4 x Upper buffer	0.5 M	Tris/HCl pH6.8
	0.4%	SDS

Protein samples derived from cell extracts were denatured by heating at 95°C for 5 min in 1 x SDS sample buffer, and then cooled immediately on ice. The samples were collected by brief centrifugation and then equal amounts of protein were loaded on a SDS gel. The electrophoresis was performed with a vertical gel chamber in 1 x SDS running buffer. After electrophoresis, the gel could be used for Western blotting analysis, or fixed and stained with coomassie brilliant blue. For the analysis of radiolabeled proteins, the gel was fixed in destain buffer for 30 min with gentle agitation. Afterwards, the gel was dried and autoradiographed.

10 x SDS running buffer	250 mM	Tris
	2 M	Glycine
	1%	SDS
	pH 8.3	
Destain buffer	10%	Acetic acid
	20%	Methanol

3.3.2 Western blotting

The separated proteins were electrically transferred from the gel to a polyvinylidene difluoride (PVDF) membrane (Millipore) by semi-dry blotting (Bio-Rad), according to the manufacturer's instructions. After blocking in 1 x TBS containing 0.1% Tween 20 and 5% non-fat milk powder or BSA for 1 h at room temperature, the membrane was incubated overnight with the appropriate primary antibodies at 4°C. Followed by 4-5 washes in TBST (1 x TBS with 0.1% Tween 20), the membrane was incubated with horseradish peroxidase-conjugated secondary antibodies for 2 h at 4°C. After another 4-5 washes in TBST, the bound proteins were then detected using the Pharmacia-Amersham enhanced chemiluminescence system (ECL).

Transfer buffer	50 mM	Tris
	40 mM	Glycine
	0.04% (w/v)	SDS
	20%	Methanol

10 x TBS	250 mM	Tris/HCl pH 7.6
	1.37 M	NaCl
	50 mM	KCl
	7 mM	$CaC1_2 \cdot 2H_2O$
	1 mM	$MgCl_2 \cdot 6H_2O$

3.3.3 Immunoprecipitation (IP)

36 h after transfection, cells were lyzed in NP-40 lysis buffer supplemented with phosphatase and protease inhibitors. One aliquot was used to confirm correct expression of the proteins. Equal amounts of protein contained in the remaining supernatants were incubated, either with specific or control antibodies, on a spinning wheel for 4 h at 4°C. 25 µl of protein A/G-sepharose beads were added and the samples were rotated at 4°C overnight. The immunoprecipitates were washed five times in NP-40 lysis buffer and then boiled in 1 x SDS sample buffer prior to SDS-PAGE and further analyzed by Western blotting.

3.3.4 Nickel-affinity purification

His-tagged fusion proteins can be purified on Ni-NTA metal affinity chromatography matrices. 36 h after transfection, cells were dissolved in lysis buffer and cleared by sonification (2 x 20 sec). After centrifugation, 50 µl of prewashed Ni-NTA agarose was added to the supernatant and the mixture was rotated at 4°C overnight. Then, the beads were successively washed with lysis buffer, wash buffer-1, wash buffer-2 and wash buffer-3. Afterwards, the bound proteins were eluted with 250 mM imidazole in 2 x SDS sample buffer and analyzed further by Western blotting.

Lysis buffer	6 M	Guanidine-HCl
	0.1 M	Na_2HPO_4/NaH_2PO_4
	10 mM	Tris/HCl pH 8.0
	10 mM	Imidazole
	10 mM	β-Mercaptoethanol

Wash buffer-1	8 M	Urea
	0.1 M	Na_2HPO_4/NaH_2PO_4
	10 mM	Tris/HCl pH 8.0
	25 mM	Imidazole
	10 mM	β-Mercaptoethanol
Wash buffer-2	8 M	Urea
	0.1 M	Na_2HPO_4/NaH_2PO_4
	10 mM	Tris/HCl pH 6.3
	25 mM	Imidazole
	10 mM	β-Mercaptoethanol
	0.2%	Triton X-100
Wash buffer-3	8 M	Urea
	0.1 M	Na_2HPO_4/NaH_2PO_4
	10 mM	Tris/HCl pH 6.3
	25 mM	Imidazole
	10 mM	β-Mercaptoethanol
	0.1%	Triton X-100

3.3.5 Electrophoretic mobility shift assay (EMSA)

EMSA is used to detect the DNA-binding activity of proteins. This method is based on the fact that protein-free DNA-fragments migrate faster in a polyacrylamide gel than protein-DNA complexes. Cells were lyzed in TOTEX buffer supplemented with phosphatase and protease inhibitors, and incubated on ice for 30 min. The samples were carefully vortexed every 10 min and the cell debris was pelleted upon centrifugation. Equal amounts of supernatants were tested for DNA-binding activity. Briefly, 10 µl of cell extract was mixed with 2 µg of poly (dI-dC), 2 µg BSA, 10,000 c.p.m. of a ^{32}P-labeled oligonucleotide and 5 x binding buffer in a final volume of 20 µl. After incubating on ice for 15 min, the samples were immediately loaded onto a 4% native polyacrylamide gel. The free and complexed oligonucleotides were separated on electrophoresis in 0.5 x TBE buffer. Afterwards, the gel was dried and exposed to an X-ray film.

The ^{32}P-radiolabeled oligonucleotide used here were (NF-κB binding site underlined):

5'-AGTTGAGGGGACTTTCCCAGGC-3'
3'-TCAACTCCCCTGAAAGGGTCCG-5'

TOTEX buffer	20 mM	HEPES/KOH pH 7.9
	0.35 M	NaCl
	1 mM	$MgCl_2$
	0.5 mM	EDTA
	0.1 mM	EGTA
	20% (v/v)	Glycerol
	1% (v/v)	NP-40
5 x Binding buffer	20% (w/v)	Ficoll 400
	100 mM	HEPES/KOH pH 7.9
	1 mM	DTT
	300 mM	KCl
5 x TBE	445 mM	Tris base
	445 mM	Boric acid
	10 mM	EDTA

3.3.6 Chromatin immunoprecipitation (ChIP)

Six 10 cm dishes of confluent MEFs were used for each condition. Cells were fixed *in vivo* with 1% formaldehyde in warm PBS for 5 min after stimulation. This solution was then replaced by cold PBS containing 0.125 M glycine to stop cross-linking. The supernatant was removed, and the cells were washed two times with cold PBS and scraped off the dishes. After centrifugation and removal of the supernatant, the pellets were lyzed in ChIP-RIPA buffer (freshly added phosphatase and protease inhibitors) for 10 min on ice. Chromatin was sheared by sonification (7 x 30 sec, on ice) and centrifuged at 13,200 rpm for 20 min at 4°C. The supernatants were then collected and stored as aliquots at -80°C for subsequent ChIP assay.

In order to obtain the concentration of chromatin contained in the initial lysates, the protein-DNA cross-link was reversed. Briefly, 50 µl of these lysates (input samples) were diluted to a final volume of 200 µl with TE buffer containing 1% SDS and

50 µg/ml RNAse A, and incubated at 37°C for 30 min to remove RNA. Followed by proteinase K (0.5 mg/ml) digestion for at least 6 h at 37°C, the mixture was heated for an additional 6 h at 65°C. Afterwards, the samples were diluted to a final volume of 600 µl with loading buffer H1 (JETquick). Chromatin was purified with spin columns (JETquick), according to the manufacturer's instructions and its concentration was measured with a spectrophotometer.

Equal amounts of chromatin (ranging from 20-40 µg) were used for immunoprecipitation and the volume of each sample was adjusted to 500 µl with ChIP-RIPA buffer. 2 µg of specific and control antibodies were added to these 500 µl solutions and the mixtures were rotated at 4°C overnight. 40 µl of protein A/G sepharose beads pre-equilibrated in ChIP-RIPA buffer were added to the samples and the incubation continued for another 2 h at 4°C. Beads were collected by centrifugation, washed subsequently with the following buffers: twice in ChIP-RIPA buffer at 4°C, once in high-salt buffer at 4°C, once in ChIP-RIPA buffer at 4°C, and finally once in TE buffer at room temperature. The extensively washed beads were resuspended in 55 µl of elution buffer, vigorously mixed for 15 min at 25°C and then cleared by centrifugation. 50 µl of each supernatant was diluted to 200 µl with TE buffer and treated as the input samples to reverse the protein-DNA cross-link. After purification, the chromatin was stored at -20°C until further PCR analysis.

ChIP-RIPA buffer	10 mM	Tris/HCl pH 7.5
	150 mM	NaCl
	1%	NP-40
	1%	Deoxycholate
	0.1%	SDS
	1 mM	EDTA
ChIP high-salt buffer	10 mM	Tris/HCl pH 7.5
	2 M	NaCl
	1%	NP-40
	0.5%	Deoxycholate
	1 mM	EDTA

TE buffer	10 mM	Tris/HCl pH 7.5
	1 mM	EDTA
ChIP elution buffer	10 mM	Tris/HCl pH 7.5
	1 mM	EDTA
	1%	SDS

4 Results

4.1 IKKε mediates the T cell costimulation-induced phosphorylation of NF-κB p65 at Ser 468

It has been shown that phorbol ester leads to p65 phosphorylation in TAD2 (Schmitz et al., 1995), which contains Ser 468 as a T cell costimulation-induced phosphorylation site (Mattioli et al., 2004a). Therefore, it was interesting to find the responsible kinase. Basal phosphorylation at Ser 468 is mediated by GSK3β (Buss et al., 2004a), while TNF-α- and IL-1-induced phosphorylation of this site is triggered by IKKβ (Schwabe and Sakurai, 2005). However, the kinase mediating inducible phosphorylation in response to T cell costimulation was still unknown. The amino acid motifs surrounding Ser 536 and Ser 468 share some homology (Fig. 4.1), raising the possibility that both sites may employ the same kinase.

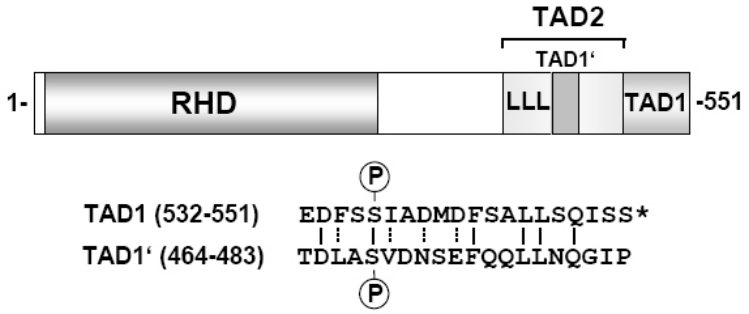

Figure 4.1 Schematic representation of the p65 protein.

N-terminal RHD and TADs are indicated. The homology region within TAD2 is designated TAD1' and is preceded by a potential leucine zipper that is indicated by three repeats of L. The two sequences are aligned in the lower part of the figure. Identical amino acids are marked by solid bars, homologous and related amino acids are indicated by dashed lines. The phosphorylated amino acids 468 and 536 are shown and the asterisk marks the C-terminal end of the p65 protein.

4.1.1 IKKε phosphorylates p65 at Ser 468

From all the kinases known to mediate Ser 536 phosphorylation, only IKKα, IKKβ and IKKε can be induced by T cell costimulation or by PMA and Ionomycin, which mimic T cell costimulation and activate NF-κB via PKC activation and calcium

elevation, respectively (Tanahashi et al., 2001). To examine the relative roles of IKKα, IKKβ and IKKε for p65 phosphorylation, Jurkat T cells were transfected with expression vectors encoding these three kinases together with very low amounts GFP-tagged p65 plasmid to express this fusion protein at physiological levels. This experimental approach was taken, as the low transfection efficiency of Jurkat T cells hampers to analyse the impact of transfected kinases on the endogenous p65 protein, thus enabling the detection of the slower migrating GFP-p65 fusion protein which is fully regulated and functional (Schmid et al., 2000). The expression of IKKα only slightly induced GFP-p65 phosphorylation at Ser 536, whereas IKKβ strongly triggered Ser 536 phosphorylation of GFP-p65 and the endogenous p65 protein. IKKβ also caused a slight induction of Ser 468 phosphorylation. In contrast, even faint amounts of IKKε potently stimulated GFP-p65 phosphorylation at Ser 536 and Ser 468. However, the overexpressed IKKε failed to cause the phosphorylation of the endogenous p65 which is in complex with the IκB proteins (Fig. 4.2). These results identify IKKε as a kinase with the ability to mediate p65 phosporylation at Ser 468 as well as Ser 536 in T cells.

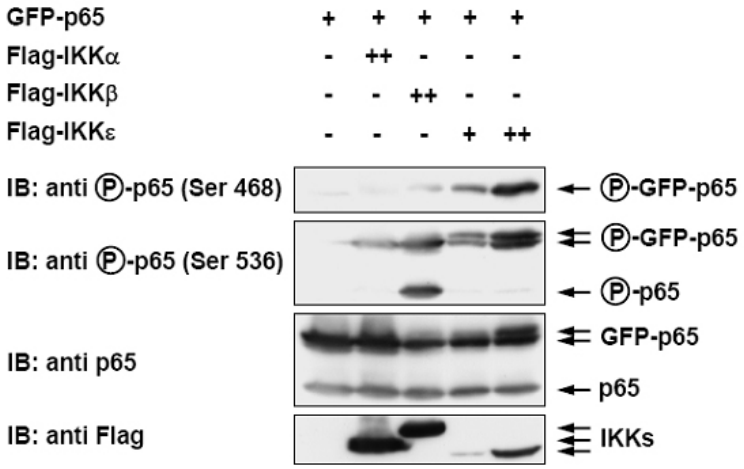

Figure 4.2 IKKε phosphorylates NF-κB p65 at Ser 468 and Ser 536.

Jurkat human T cells were transiently transfected to express GFP-p65 along with Flag-tagged IKKα, IKKβ and increasing amounts of IKKε as indicated. After 36 h, cells were lyzed and equal amounts of protein contained in the total cell extracts were analyzed by immunoblotting (IB) to detect the phosphorylation of p65 at Ser 468 and Ser 536, respectively. Phosphorylated p65 displays an upshifted band, as indicated by the double arrows. Control blots ensured the proper expression of GFP-p65 and the IKK proteins.

4.1.2 p65 phosphorylation at Ser 468 is predominantly located in the nucleus

Ser 536-phosphorylated p65 is mainly found in the cytosol (Mattioli et al., 2004b), thus raising the question whether the same holds true for Ser 468-phosphorylated p65. Jurkat cells were stimulated for various time periods with PMA/Ionomycin, followed by subcellular fractionation into cytosolic and nuclear extracts (Fig. 4.3A). The Ser 468-phosphorylated p65 was found predominantly in the nucleus, while the Ser 536-phosphorylated form of this transcription factor was mainly present in the cytosol. Moreover, Ser 468 was phosphorylated with slower kinetics and remained longer in the phosphorylated state when compared to Ser 536.

To test whether the same intracellular distribution occurs when p65 phosphorylation is triggered by IKKε, Jurkat cells were transfected to express GFP-p65 in the absence or presence of cotransfected IKKε. IKKε-mediated p65 Ser 468 phosphorylation was found mainly in the nucleus, while Ser 536-phosphorylated p65 was equally distributed in the cytosol and the nucleus (Fig. 4.3B). Overexpressed IKKε was found not only in the nucleus, but also in the cytosol, which reflected the distribution of the endogenous kinase that was also found in both fractions (Fig. 4.3A).

Another experiment confirmed that IKKε-mediated p65 phosphorylation at Ser 468 can take place in the nucleus. Jurkat cells were transfected to express the constitutively nuclear Gal4-p65 protein (Schmitz and Baeuerle, 1991) along with IKKε wildtype or its kinase inactive mutant at the indicated combinations. 36 h post-transfection, cells were stimulated with PMA/Ionomycin for 20 min or left untreated (Fig. 4.3C). Western blotting experiments from nuclear extracts revealed that IKKε could mediate Gal4-p65 phosphorylation at Ser 468, and this event was further augmented by PMA/Ionomycin treatment. In contrast, coexpression of the IKKε point mutant completely inhibited this inducible phosphorylation, pointing out the relevance of IKKε in this pathway.

Altogether, these data reveal that the phosphorylation of p65 at Ser 468 occurs predominantly in the nucleus.

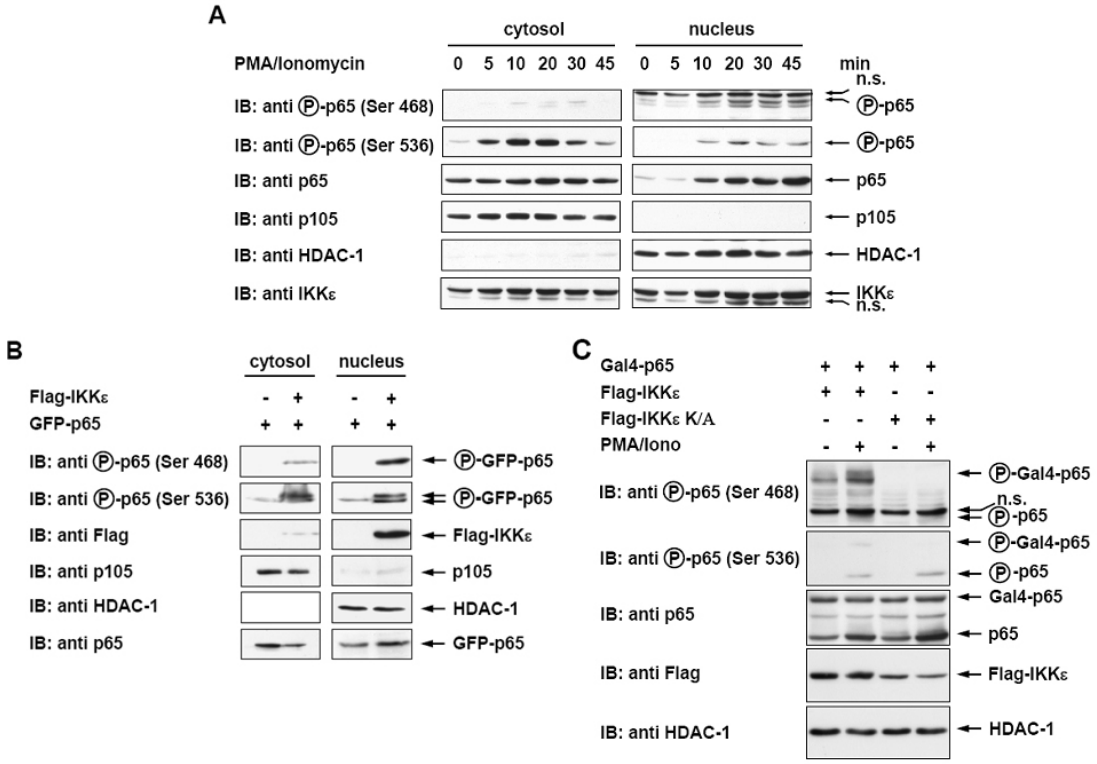

Figure 4.3 Different localization of Ser 468- and Ser 536-phosphorylated p65.

(A) Jurkat cells were stimulated for the indicated periods with PMA/Ionomycin. Cytosolic and nuclear fractions were further analyzed by immunoblotting using the indicated antibodies. The purity of the fractions was controlled with antibodies recognizing the nuclear HDAC-1 and the cytoplasmic p105 protein. (n.s. = non specific) (B) Jurkat T cells expressing the indicated combinations of GFP-p65 and IKKε were fractionated into nuclear and cytosolic extracts and analyzed by immunoblotting for the occurrence of p65 phosphorylations and the distribution of IKKε as shown. (C) Jurkat cells were transfected to express the constitutively nuclear Gal4-p65 protein along with Flag-tagged IKKε wildtype or kinase inactive mutant. After 36 h, cells were stimulated for 20 min with PMA/Ionomycin as shown and nuclear extracts were analyzed for the phosphorylation of p65 and the expression of control proteins.

4.1.3 IKKε is activated in response to T cell costimulation

To study the role of IKK proteins for p65 Ser 468 phophorylation, Jurkat cells lacking NEMO were stimulated with PMA/Ionomycin for various periods. Endogenous IKKε was immunoprecipitated and tested by immune complex kinase assays for its ability to phosphorylate p65. These experiments showed that the endogenous IKKε protein was activated upon T cell costimulation and could induce the phosphorylation of the

GST-p65 (354-551) substrate protein at 20 and 45 min post-stimulation (Fig. 4.4A). These data suggest that induction of IKKε kinase activity parallels p65 Ser 468 phosphorylation and that NEMO is not important for primary IKKε activation at the analyzed time points. Therefore, endogenous IKKε can phosphorylate p65 Ser 468 *in vitro* and this inducible phosphorylation is independent from the functional IKK complex. Furthermore, the amount of IKKε was stable in response to T cell costimulation (Fig. 4.4B).

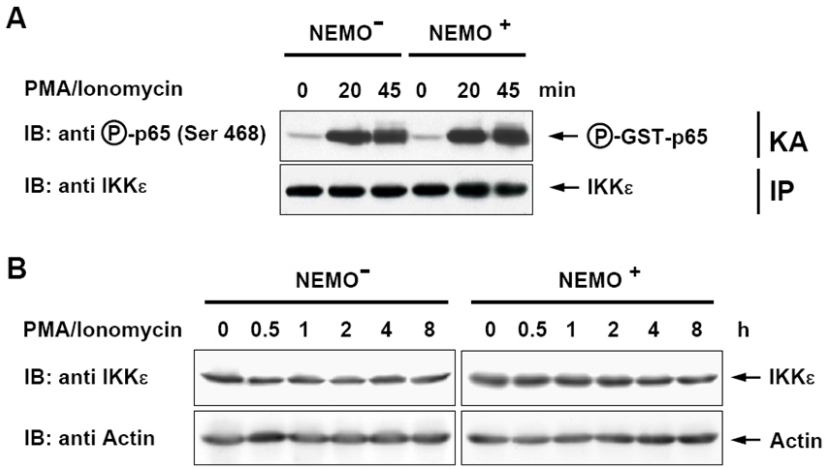

Figure 4.4 IKKε kinase activity is triggered by T cell costimulation.

(A) Jurkat cells either lacking or containing NEMO were left untreated or stimulated with PMA/Ionomycin for 20 and 45 min as shown, followed by immunoprecipitation (IP) of IKKε and kinase assays (KA) using the GST-p65 (354-551) protein as a substrate. Phosphorylation of p65 Ser 468 was revealed by immunoblotting. (B) The indicated cells were treated with PMA/Ionomycin for the given periods. The relative amounts of IKKε and the control protein were analyzed by immunoblotting using specific antibodies.

4.1.4 Phosphorylation of p65 at Ser 468 requires its release from IκBα

In unstimulated cells, NF-κB exists as an IκB bound p50/p65 heterodimer in the cytoplasm. Therefore it was interesting to test if p65 phosphorylation depends on its release from the IκB complex. Jurkat cells lacking the NEMO protein and thus being unable to phosphorylate IκBα and to release the p65 protein from the cytosol (Yamaoka et al., 1998), were stimulated for various periods with PMA/Ionomycin. NEMO deficient cells failed to induce p65 phosphorylation at Ser 468 and Ser 536,

while NEMO retransfected control cells showed full phosphorylation ability at both sites (Fig. 4.5A), suggesting that only free and untrapped p65 can be phosphorylated.

To substantiate this finding by an independent experimental approach, NF-κB activation was blocked by the proteasome inhibitor MG132. Jurkat cells were preincubated with MG132 for 1 h, and then stimulated with PMA/Ionomycin for 20 min. Western blotting experiments revealed that the stabilization of the NF-κB·IκB complex by this inhibitor enhanced PMA/Ionomycin-induced phosphorylation of IκBα and IKKβ-mediated phosphorylation of p65 at Ser 536 within this complex (Fig. 4.5B). In contrast, T cell costimulation-induced p65 phosphorylation at Ser 468 was diminished in the presence of MG132, revealing that this phosphorylation does not take place within the NF-κB·IκB complex.

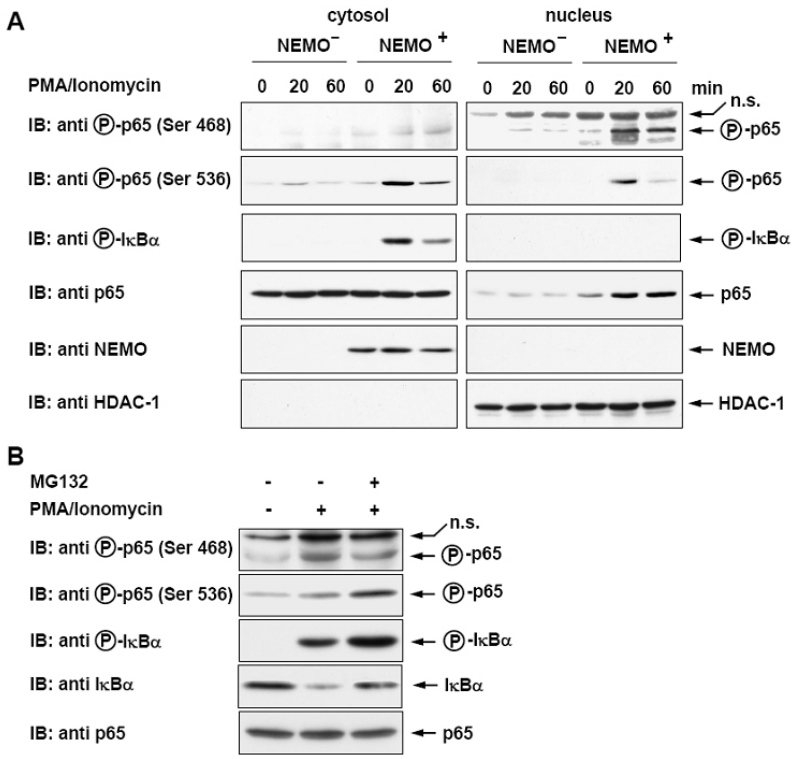

Figure 4.5 Induced p65 Ser 468 phosphorylation occurs in untrapped form of p65.

(A) Jurkat cells lacking NEMO and control cells retransfected to express NEMO were stimulated for the indicated periods as shown. Cytoplasmic and nuclear extracts were analyzed by immunoblotting for the phosphorylation of p65 and the occurrence of control proteins. (B) Jurkat T cells were left untreated or stimulated for 20 min with PMA/Ionomycin in the absence or presence of MG132. Total cell extracts were analyzed by immunoblotting for p65 phosphorylation and also for the occurrence of phosphorylation and degradation of IκBα as shown.

Taken together, all these experiments indicate that IKKε-mediated Ser 468 phosphorylation does not occur when the release of IκB bound p65 is inhibited. Accordingly, co-immunoprecipitation experiments showed no influence of the p65 Ser 468 phosphorylation status on its ability to associate with IκBα (Fig. 4.6).

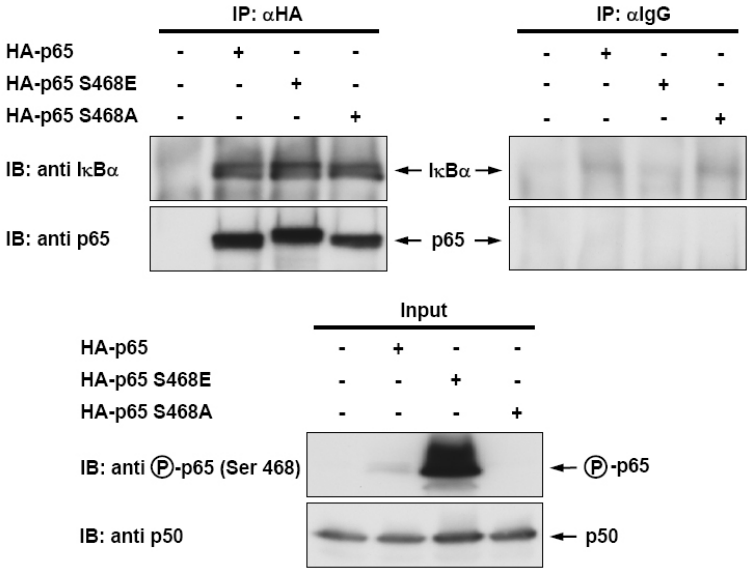

Figure 4.6 Ser 468 phosphorylation of p65 does not affect the binding with IκBα.

Human 293T cells were transiently transfected to express HA-tagged wildtype or point mutated p65 as shown. After 36 h, cells were lyzed and an aliquot of the lysate was used to immunoprecipitate p65 proteins with HA (left) or control (right) antibodies. The co-precipitated endogenous IκBα proteins were detected by immunoblotting using specific antibody. A small aliquot of the whole cell extract was analyzed by immunoblotting to detect the phosphorylation of p65 proteins and the occurence of p50 as a loading control.

4.1.5 GSK3β is not responsible for the inducible phosphorylation of p65 at Ser 468 in response to T cell costimulation

GSK3β mediates basal p65 Ser 468 phosphorylation in unstimulated cells (Buss et al., 2004a), thus raising the possibility that GSK3β and IKKε might synergize for the induced p65 phosphorylation at this serine site. Co-expression experiments showed that only IKKε but not GSK3β phosphorylated GFP-p65 at Ser 468, and this strong, IKKε-triggered phosphorylation could not be further enhanced in the presence of GSK3β (Fig. 4.7A). Therefore, GSK3β has no effect on the IKKε-mediated p65 Ser 468 phosphorylation.

Next, a possible contribution of endogenous GSK3β for PMA/Ionomycin-induced Ser 468 phosphorylation was tested. Jurkat cells were left untreated or stimulated in the absence or presence of the GSK3 inhibitor LiCl (Cohen and Goedert, 2004). As revealed by Western blotting experiments, LiCl dramatically induced the phosphorylation of GSK3α and GSK3β, which keeps these two kinases inactivated. In contrast, nuclear p65 Ser 468 phosphorylation showed no significant changes in the presence of this inhibitor (Fig. 4.7B), thus excluding the role of GSK3β for Ser 468 phosphorylation induced by T cell costimulation.

Additionally, the relevance of some other kinases in this induced phosphorylation process was also investigated. Jurkat cells were pretreated with pharmacological inhibitors of p38 MAPK (SB203580), PI3K (Wortmannin), JNK (SP600125) and ERK (PD98059). At the concentrations used, these inhibitors specifically inhibit their target kinases. Blockage of the kinase signaling pathways did not influence Ser 468 phosphorylation after T cell costimulation (Fig. 4.7C), indicating that none of these kinases is involved in the inducible phosphorylation at Ser 468 in T cells.

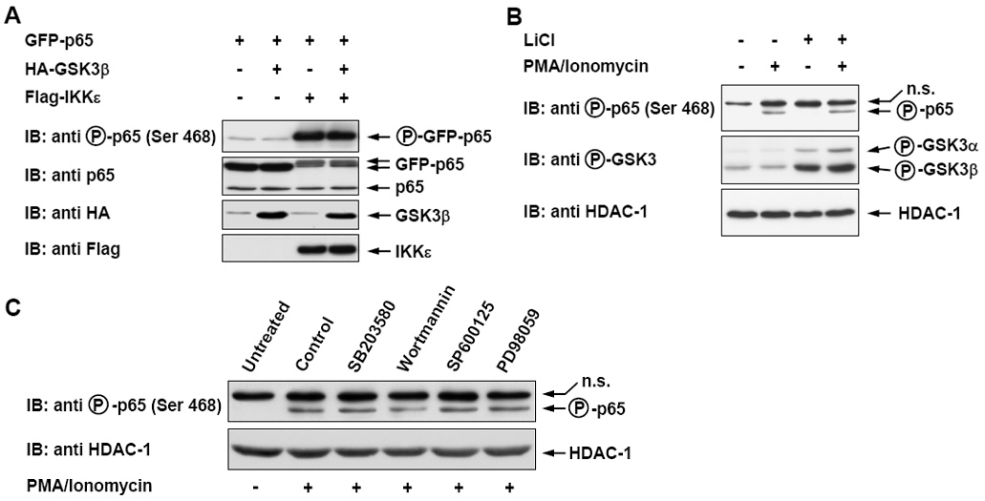

Figure 4.7 GSK3β is not required for costimulation-induced Ser 468 phosphorylation.

(A) Jurkat cells were transiently transfected to express GFP-p65 along with different combination of HA-tagged GSK3β and Flag-tagged IKKε as indicated. Total cell extracts were analyzed by immunoblotting using specific antibodies. (B) Jurkat cells were preincubated for 1 h with LiCl (25 mM) and stimulated for 20 min with PMA/Ionomycin as shown. Nuclear extracts were analyzed by immunoblotting. (C) The experiments were performed as in (B) with the exception that cells were pretreated for 1 h with the following inhibitors: SB203580 (20 μM), Wortmannin (2 μM), SP600125 (20 μM), PD98059 (50 μM) as shown.

4.1.6 Phosphorylation of p65 at Ser 468 and Ser 536 enhances transcriptional activity of a NF-κB reporter gene

The GSK3β-mediated phosphorylation of p65 at Ser 468 has a negative effect on basal transcription (Buss et al., 2004a). However, the function of T cell costimulation-induced p65 Ser 468 phosphorylation was unknown. Reporter gene assays were used to examine the impact of this inducible Ser 468 and Ser 536 phosphorylations on gene expression. p65 deficient MEFs were cotransfected with a NF-κB-dependent luciferase gene and increasing amounts of either wildtype p65 or various phosphoacceptor site point mutants. The phosphomimetic p65 S468E mutant where the serine was changed to glutamic acid activated NF-κB-dependent gene expression slightly stronger when compared to the wildtype protein (Fig. 4.8A), indicating that phosphorylation of Ser 468 serves to enhance p65-dependent transcription. Increased transcription was also observed for p65 S536E and the double mutant where both serines were changed to glutamic acids. While mutation of Ser 536 to alanine did not significantly impair the transcriptional activity of the mutant protein, the Ser 468 to alanine mutant showed a markedly decreased ability to trigger gene expression. Accordingly, a p65 mutant where both serines were changed to alanine showed a significantly reduced ability to trigger transcription. The appropriate expression of various transfected p65 proteins was ensured by Western blotting experiments (Fig. 4.8B). These data suggest that p65 phosphorylation serves to activate expression of a NF-κB reporter gene.

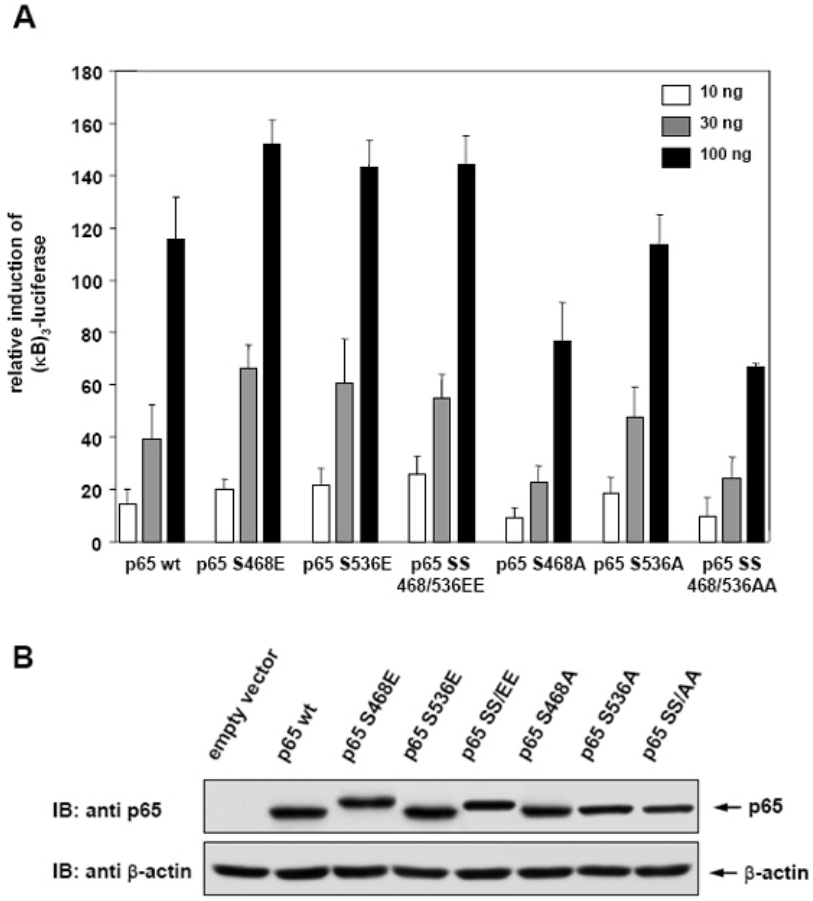

Figure 4.8 Functional analysis of p65 phosphorylation.

(A) p65 deficient MEFs were transiently transfected with a luciferase reporter gene controlled by three NF-κB sites along with the indicated amounts of expression vectors encoding wildtype and point mutated p65 proteins. 30 h post-transfection, cells were harvested and tested for luciferase activity. Fold induction of gene expression is shown and bars indicate standard deviations from at least 3 independent experiments. (B) p65 deficient MEFs were transfected with the same amounts of expression vectors encoding various p65 proteins. 30 h later, cells were harvested and whole cell extracts were analyzed by immunoblotting for the occurrence of various p65 proteins and β-actin using specific antibodies.

4.2 p65 Ser 468 phosphorylation controls its proteasome-dependent ubiquitination, degradation and elimination from specific promoters

The most abundant form of NF-κB is the heterodimer between p65 and p50. Both DNA-binding subunits were found to be ubiquitinated and degraded in the nucleus, thus allowing termination of the nuclear NF-κB response (Carmody et al., 2007; Ryo et al., 2003; Saccani et al., 2004; Tanaka et al., 2007). However, the mechanisms by

which these processes are regulated are not clear. Therefore, it was tempting to find a molecular mechanism that ensures the proper and regulated elimination of p65.

4.2.1 TNF can induce p65 degradation

To find a signaling pathway suitable for the study of p65 degradation, the NF-κB inducing stimuli TNF and LPS were compared for their ability to mediate elimination of the p65 subunit. As only a fraction of p65 undergoes proteasomal degradation, NF-κB induction was followed by cycloheximide (CHX) treatment to prevent resynthesis of the eliminated proteins and to enable the convenient detection of p65 diminishment. MEFs and Hela cells were stimulated with either TNF for 15 min or LPS for 30 min or left untreated, and then blocked by CHX for the indicated periods. Immunoblotting experiments showed that in both cell lines, only TNF but not LPS strongly reduced p65 stability (Fig. 4.9A, C), although both inducers comparably triggered IκBα phosphorylation (Fig. 4.9B, D). These results reveal that TNF is able to mediate p65 degradation and the combination of a TNF pulse with a block of protein synthesis allows the convenient detection of p65 decay.

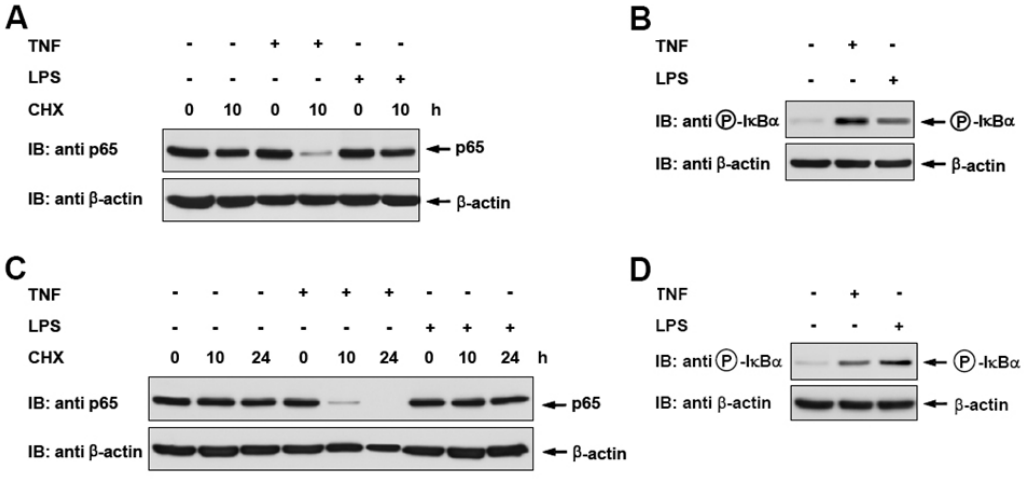

Figure 4.9 p65 degradation is triggered by TNF.

(A) MEFs were stimulated with either TNF (15 min) or LPS (30 min) as shown. After wash-out of the stimuli, protein synthesis was blocked by cycloheximide (10 μg/ml) for the indicated periods. Equal amounts of protein contained in the total cell extracts were analyzed by immunoblotting (IB) for the occurrence of p65 and β-actin using specific antibodies. (B) MEFs were treated with TNF or LPS, and analyzed by immunoblotting for IκBα phosphorylation and β-actin as shown. (C and D) The experiment was done as in (A, B) with the exception that Hela cells were used.

4.2.2 Ser 468 phosphorylation controls TNF-triggered p65 degradation

It has been demonstrated that phosphorylation of Thr 254 is necessary for the nuclear localization as well as protein stability of p65 (Ryo et al., 2003), and that a Ser 536 to alanine mutation abrogates LPS-induced p65 turnover in IKKα deficient cells (Lawrence et al., 2005). Given the relative conservation of the sequences surrounding Ser 536 and Ser 468 (Fig 4.1), it was tempting to explore the possibility that phosphorylation at Ser 468 may also regulate p65 stability. To test this possibility, p65 deficient MEFs were retransfected to express either HA-tagged p65 wildtype or the S468A point mutant, followed by a 15 min pulse of TNF, and CHX blockage for different periods. While TNF-induced p65 degradation was detected after 6 h, the mutated p65 protein remained largely stable (Fig. 4.10A). These data suggest that phosphorylation of p65 at Ser 468 plays a central role for the control of its TNF-triggered degradation.

The basal half life of both p65 proteins was examined by a pulse-chase experiment. 293T cells were transfected to express HA-tagged p65 or the S468A mutant, followed by metabolic labeling with ^{35}S-methionine and ^{35}S-cysteine. At various time points after the addition of unlabeled amino acids, cell lysates were prepared and the transfected p65 was purified by immunoprecipitation with HA antibody. SDS-PAGE and protein detection by autoradiography revealed a comparable half life of wildtype and the mutated p65 in unstimulated cells (Fig. 4.10B).

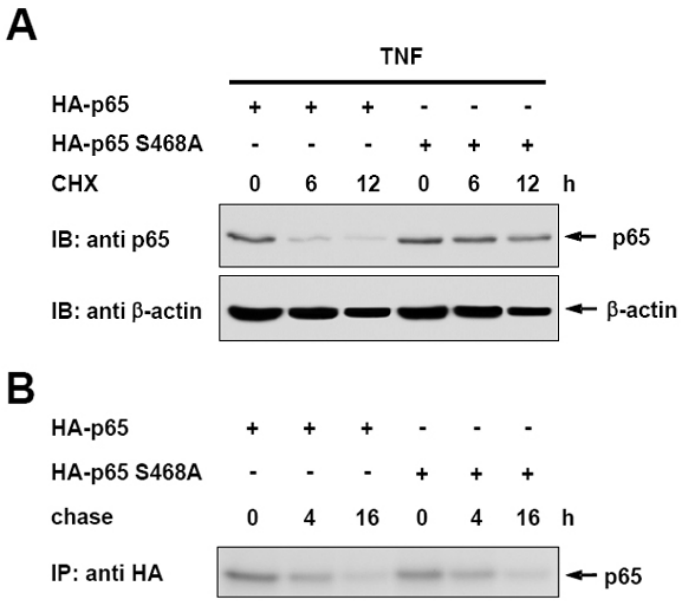

Figure 4.10 TNF-induced p65 degradation is controlled by p65 Ser 468 phosphorylation.

(A) $p65^{-/-}$ MEFs were transiently transfected to express HA-tagged p65 or the S468A mutant as shown. 36 h later, cells were stimulated with a 15 min pulse of TNF, followed by the addition of CHX for the indicated periods. Total cell extracts were tested by immunoblotting for p65 and β-actin protein levels. (B) 293T cells were transiently transfected to express equal amounts of p65 wildtype and mutated proteins. The next day, cells were metabolically labeled with ^{35}S-methionine/cysteine. After replacement of the medium by normal growth medium supplemented with excess unlabeled methionine and cysteine (2 mM each) for the indicated periods, the p65 proteins were immunoprecipitated with HA antibody and analyzed by SDS-PAGE as well as autoradiography.

It was previously shown that p65 degradation is more prominent in IκBα$^{-/-}$ cells where the IκBα-dependent removal of NF-κB from its target genes is absent (Saccani et al., 2004). Therefore, it was very interesting to check the inducible diminishment of p65 in this type of cells, as well. The analysis of p65 stability with different combinations of pulsed TNF or LPS stimulation followed by CHX blockage revealed that diminishment of endogenous p65 also occurred in the absence of IκBα-mediated removal of p65 from its target genes (Fig. 4.11A). Afterwards, the stabilities between the p65 wildtype and the phosphorylation mutant were compared in IκBα deficient cells, and this experimental setting also identified the relevance of Ser 468 for the control of p65 stability (Fig. 4.11B). Moreover, the endogenous p65 protein disappeared much faster when compared to the transfected p65. The increased stability of S468A mutant was also detected after immunoprecipitation of the p65

proteins (Fig. 4.11C). Altogether, these results indicate that Ser 468 is essential for TNF-triggered p65 degradation.

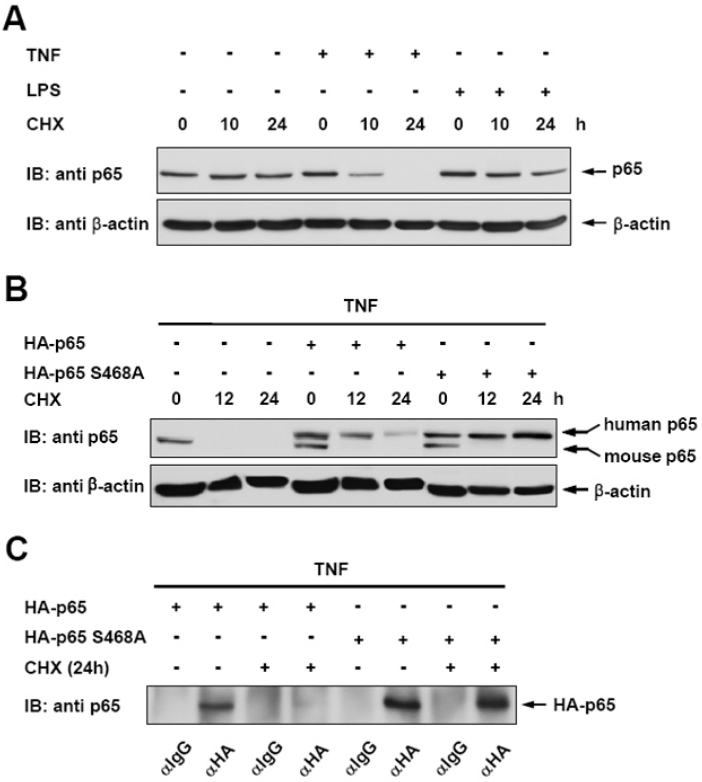

Figure 4.11 Ser 468 is important for TNF-triggered p65 degradation in IκBα$^{-/-}$ MEFs.

(A) IκBα$^{-/-}$ MEFs were stimulated with either TNF or LPS, followed by blockage with CHX for the indicated periods. Equal amounts of protein contained in the total cell extracts were analyzed by immunoblotting for p65 and β-actin using specific antibodies. (B) IκBα$^{-/-}$ MEFs were transfected with empty vector or the indicated p65 expression vectors as shown, followed by analysis of p65 stability with combination of a 15 min TNF pulse and CHX blockage for the indicated periods. Total cell extracts were then tested by immunoblotting. (C) Cells was treated the same as in (B), but cell lysates were subjected to immunoprecipitation with either HA or control antibodies, and then analyzed by immunoblotting for p65 occurrence.

To investigate whether p65 degradation depends on sequence-specific DNA binding and involves p65-dependent gene expression, a p65 DNA-binding defective mutant was generated, in which the critical glutamic acid at position 39 was changed to an isoleucine (Toledano et al., 1993). Another p65 mutant was also produced to have a p65 form that is deficient in both DNA-binding and phosphorylation. The p65 E39I and S468A/E39I mutants were virtually unable to bind canonical κB sites, as revealed by EMSA experiments (Fig. 4.12A), whereas they both showed full activity to enter the nucleus after TNF stimulation (Fig. 4.12B). Moreover, p65 wildtype and S468A

mutant showed similar DNA-binding affinity and nuclear translocation activity (Fig. 4.12A, B).

Then, the TNF-induced destabilization was compared between the wildtype p65 and these two DNA-binding defective mutants. IκBα$^{-/-}$ MEFs were transiently transfected with wildtype, E39I or S468A/E39I p65 plasmids, followed by stability analysis with TNF/CHX treatment. As detected by Western blotting experiments, all p65 forms showed comparable TNF-mediated degradation, and disappeared with similar kinetics (Fig. 4.12C). These results demonstrate that DNA binding ability is not essential for p65 degradation. The double mutant is no longer stabilized, suggesting that DNA-unbound p65 undergoes elimination.

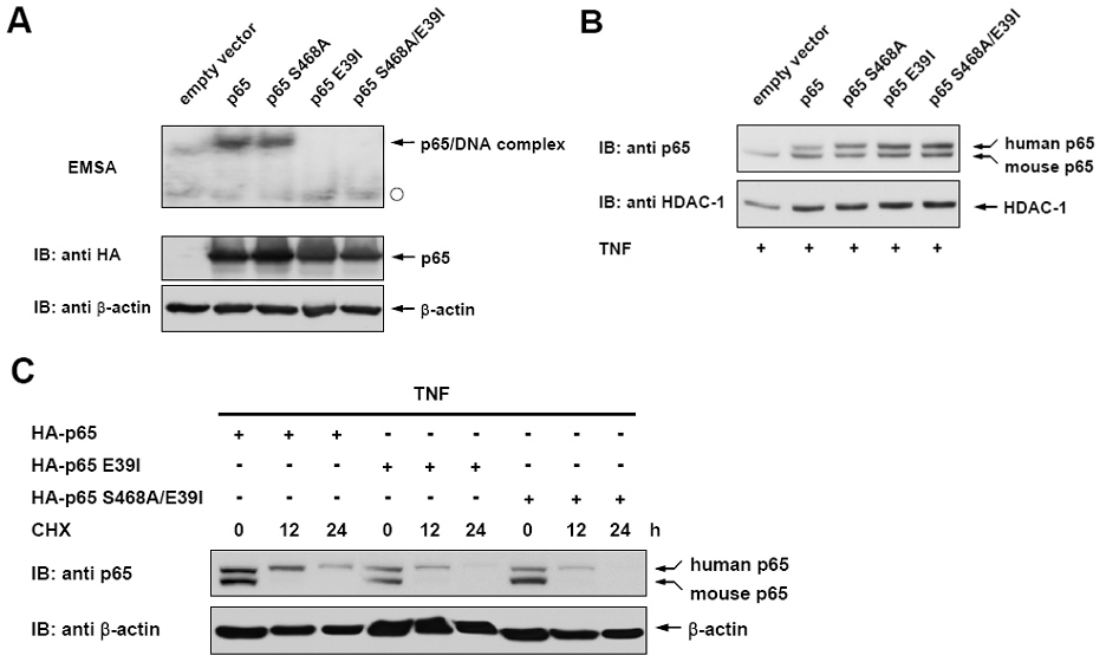

Figure 4.12 p65 degradation is independent from DNA binding.

(A) The indicated p65 proteins were overexpressed in 293T cells. Cell extracts were prepared and tested for NF-κB DNA-binding by EMSA, the positions of a constitutively DNA-binding protein (open circle) and of the NF-κB/DNA complexes (arrow) are shown (upper). An aliquot of the extract was assayed by immunoblotting for the expression of HA-tagged p65 proteins and equal loading (lower). (B) IκBα$^{-/-}$ cells were transfected to express p65 or the various point mutants. 36 h post-transfection, cells were stimulated with TNF for 30 min. Nuclear fractions were further analyzed by immunoblotting for the occurrence of p65 and HDAC-1. (C) IκBα$^{-/-}$ MEFs were transfected to express p65 wildtype or the DNA-binding mutants. 36 h later, cells were stimulated with a 15 min pulse of TNF and CHX blockage as shown. Total cell extracts were further analyzed by immunoblotting using the indicated antibodies.

4.2.3 p65 stability is enhanced in the complex with p50

As the p50/p65 heterodimer is the most frequently detected form of NF-κB, it was intriguing to examine the stability of p65 within this NF-κB complex. Wildtype p65 or the S468A mutant was expressed either alone or together with epitope-tagged p50 in IκBα$^{-/-}$ MEFs, followed by the analysis of protein stability. TNF-induced degradation of p65 was less efficient in the presence of overexpressed p50 (Fig. 4.13). This suggests that the stability of p65 is enhanced within the p50/p65 complex. Furthermore, this experiment also showed that Flag-tagged p50 was not degraded after TNF induction.

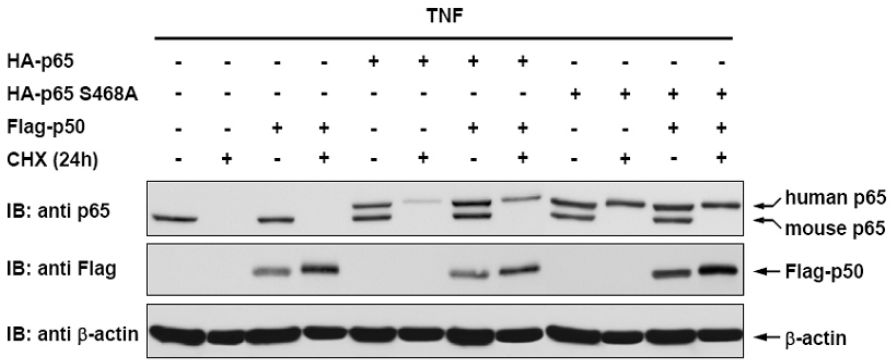

Figure 4.13 p50 can enhance p65 stability.

IκBα$^{-/-}$ MEFs were transiently transfected with HA-tagged p65 plasmids either alone or together with Flag-tagged p50 as shown. 36 h later, cells were stimulated with a 15 min pulse of TNF, and then incubated with CHX at indicated time points. Total cell extracts were further analyzed by immunoblotting to detect p65, p50 and β-actin, respectively.

4.2.4 p65 degradation occurs in a proteasome-dependent manner

TNF triggers multiple signaling pathways and transcription factors, thus raising the question whether gene expression is required for p65 destabilization. Blockage of transcription by actinomycin D prior to TNF treatment also allowed full degradation of p65 (Fig 4.14A), revealing that this process does not depend on *de novo* gene expression. Similarly, p65 degradation also occurred when CHX was added prior to TNF stimulation (Fig. 4.14B). These data indicate that p65 degradation is independent from TNF-induced gene expression or new protein synthesis.

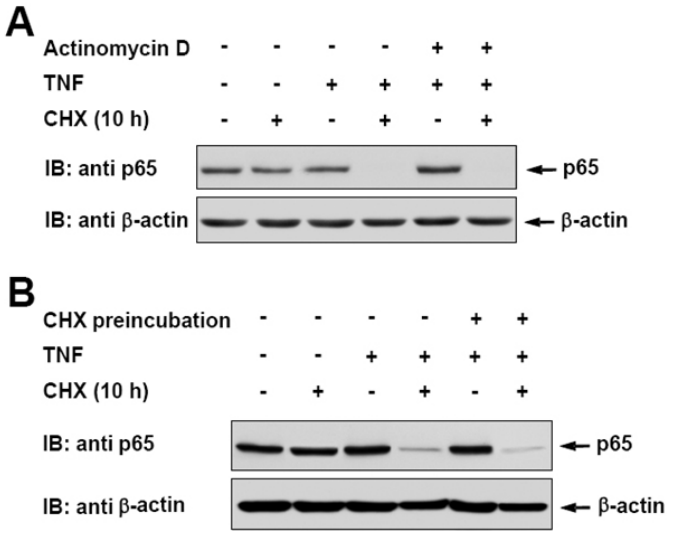

Figure 4.14 p65 degradation occurs independent from TNF-induced gene expression.

(A) IκBα$^{-/-}$ MEFs were pre-incubated with actinomycin D (1 μg/ml) for 1 h, pulsed for 15 min with TNF, and after wash-out, further incubated for 10 h in the presence of CHX. The protein levels of p65 and β-actin were analyzed by immunoblotting as shown. (B) The experiment was performed as in (A) with the exception that cells were pretreated with CHX for 1 h before TNF stimulation.

The stability of p65 can be controlled by caspases (Ravi et al., 1998), serine proteases (Franzoso et al., 1994) and the proteasome (Saccani et al., 2004). In order to reveal the pathway involved in TNF-induced p65 elimination, cells were preincubated with various inhibitors targeting distinct kinase signaling pathways (MG132, proteasome inhibitor; AS602868, IKK inhibitor; PD98059, ERK inhibitor; SB203580, p38 MAPK inhibitor; SP600125, JNK inhibitor; Wortmannin, PI3K inhibitor; and LiCl, GSK3 inhibitor). While inhibition of the kinase signaling pathways remained without any impact on p65 stability, inducible degradation of p65 was largely blocked by the proteasome inhibitor MG132 (Fig. 4.15). These data confirm that TNF-induced p65 degradation is mediated by the proteasome.

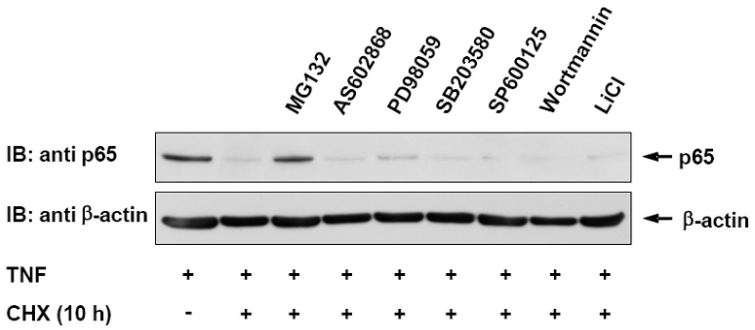

Figure 4.15 p65 is degraded by the proteasome.

TNF-induced elimination of the endogenous p65 protein was triggered in IκBα$^{-/-}$ MEFs as described above, but cells were pretreated for 1 h with the following inhibitors: MG132 (10 μM), AS602868 (12 μg/ml), PD98059 (50 μM), SB203580 (20 μM), SP600125 (20 μM), Wortmannin (2 μM) and LiCl (25 mM) as shown. Total cell extracts were further analyzed by immunoblotting using the indicated antibodies.

4.2.5 Phosphorylation at Ser 468 is important for p65 ubiquitination

Given the relevance of the proteasome for the control of p65 stability, the wildtype transcription factor and the phosphorylation and DNA-binding mutants were compared for their ubiquitination ability. 293T cells were transfected with various p65 expression plasmids either alone or together with a vector encoding His-tagged ubiquitin. In order to detect ubiquitination, cells were directly lyzed in 1 x SDS sample buffer, which allows the maintenance of various modified protein forms. Immunoblotting revealed the occurrence of high molecular weight forms of p65. This modification was further augmented by coexpression of ubiquitin (Fig. 4.16A), suggesting these upshifted bands represent ubiquitin-conjugated p65. Also the DNA-binding mutant showed largely intact ubiquitination, whereas the p65 S468A mutant displayed a strongly impaired pattern of ubiquitination.

To explore whether the multiple upshifted bands really correspond to ubiquitinated p65, the transfected cells were lyzed under denaturing conditions and His-tagged ubiquitin was enriched on Ni-NTA columns. Subsequent immunoblotting with either HA or p65 antibodies clearly identified the upshifted bands as ubiquitinated p65 and also confirmed the robustly diminished ubiquitination of the p65 Ser 468 mutant

(Fig. 4.16B). These results show that phosphorylation of p65 at Ser 468 also controls its ubiquitination.

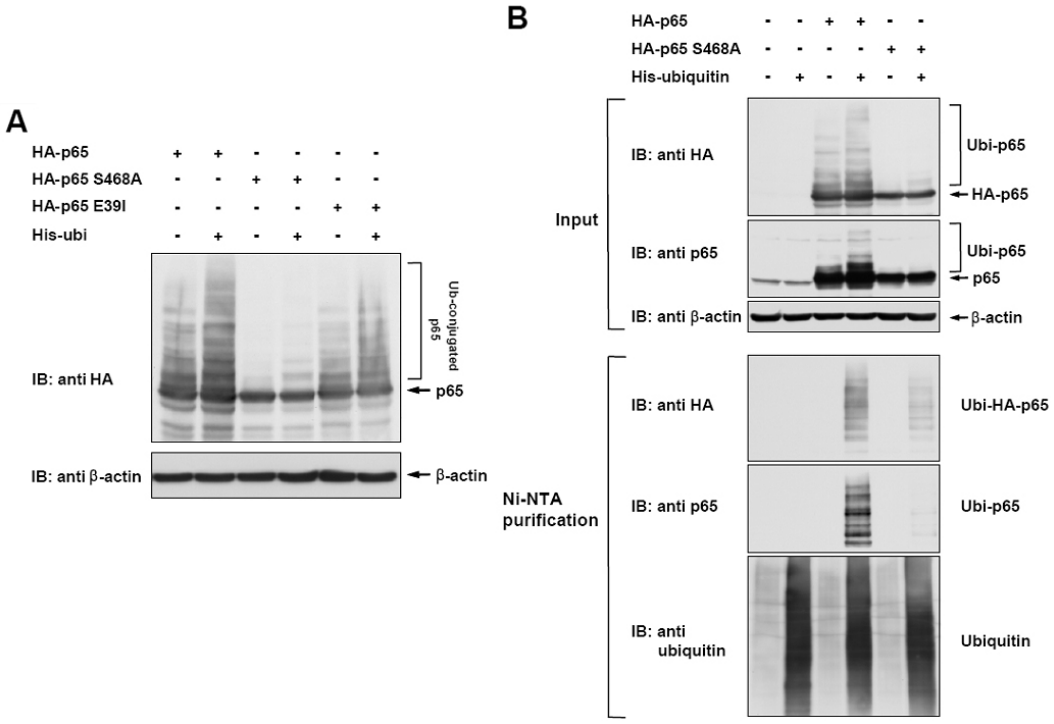

Figure 4.16 p65 ubiquitination depends on Ser 468.

(A) The different HA-tagged p65 proteins were expressed either alone or together with His-tagged ubiquitin in 293T cells. Cells were directly lyzed in 1 x SDS sample buffer and analyzed by immunoblotting to reveal p65 ubiquitination. (B) 293T cells were transfected as shown. An aliquot was lyzed in 1 x SDS sample buffer and tested by Western blotting (upper). Another aliquot was lyzed under denaturing conditions, followed by purification of His-tagged ubiquitin on Ni-NTA agarose columns. The eluted proteins were revealed by immunoblotting using specific antibodies as indicated (lower).

4.2.6 Various ubiquitin modifiers interact with p65 and regulate its proteasome-dependent degradation

An increasing number of enzymes from the ubiquitination machinery have been identified in the NF-κB signaling pathways (Chen, 2005; Krappmann and Scheidereit, 2005; Wullaert et al., 2006). It has been reported that ubiquitination of p65 is controlled by several ubiquitin E3 ligases, including SOCS1, PDLIM2 and COMMD1 (Maine et al., 2007; Ryo et al., 2003; Tanaka et al., 2007). Some ubiquitin-modifying enzymes, such as β-TrCP act on different proteins within the NF-κB pathway (Lang

et al., 2003; Yaron et al., 1998). Under the assumption that also p65 ubiquitination could be regulated by already identified NF-κB ubiquitinating enzymes, a large set of enzymes with relevance for NF-κB signaling were screened for binding to p65. Co-immunoprecipitation experiments were performed to check the association of p65 with the following ubiquitin-modifying enzymes involved in NF-κB signaling: A20, ABIN1, ABIN2, COMMD1, Cul2, CYLD, c-IAP1, Itch, Nedd4, PDLIM2, SOCS1, β-TrCP, TRAF2 and TRAF6. HA-tagged p65 together with various ubiquitin modifiers was expressed in 293T cells, and then tested for protein-protein interaction by co-immunoprecipitation experiments under buffer conditions maintaining ubiquitination. The results confirmed published interactions, such as the association of p65 with PDLIM2, and also revealed some novel p65 interaction partners. The novel p65 binding proteins are Itch, Nedd4, CYLD, βTrCP, and TRAF2 (Fig. 4.17A, B).

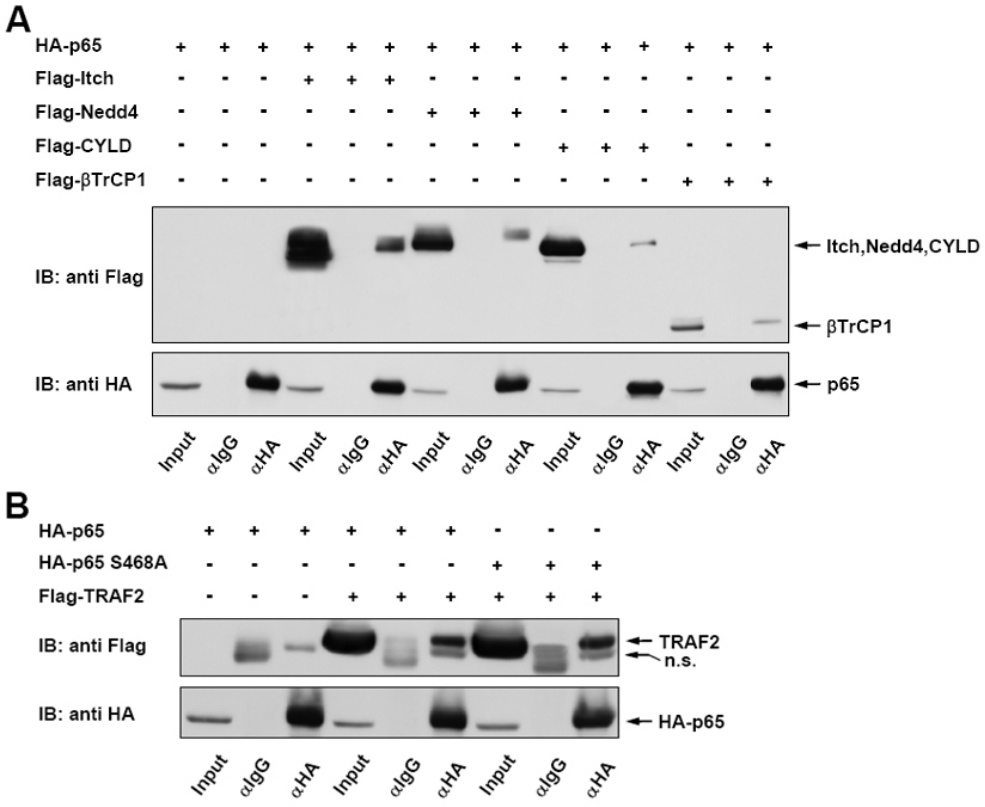

Figure 4.17 p65 interacts with various ubiquitin modifiers.

(A) 293T cells were transiently transfected with HA-tagged p65 either alone or together with the indicated epitope-tagged proteins as shown. Following immunoprecipitation (IP) with either HA or control antibodies, co-precipitated proteins were revealed by immunoblotting. (B) Cells were transfected to express wildtype or Ser 468 mutated p65 either alone or with Flag-tagged TRAF2 as shown. After IP, co-precipitated proteins were revealed by immunoblotting.

All these p65 interacting proteins were then systematically compared for potential differences in binding to p65 wildtype and the S468A mutant. Most interactors including these five new partners showed no differences in binding affinities, as exemplified for TRAF2 (Fig. 4.17B).

In addition, the contribution of the p65 interacting proteins on p65 ubiquitination and degradation were also investigated in 293T cells. Very low amounts of p65 protein were expressed to allow sensitive detection of the differences between basal and induced ubiquitination. All of these five enzymes can trigger subtle changes in the ubiquitination pattern of p65 (Fig. 4.18A). However, only TRAF2 overexpression resulted in a significant degradation of p65 (Fig. 4.18 B).

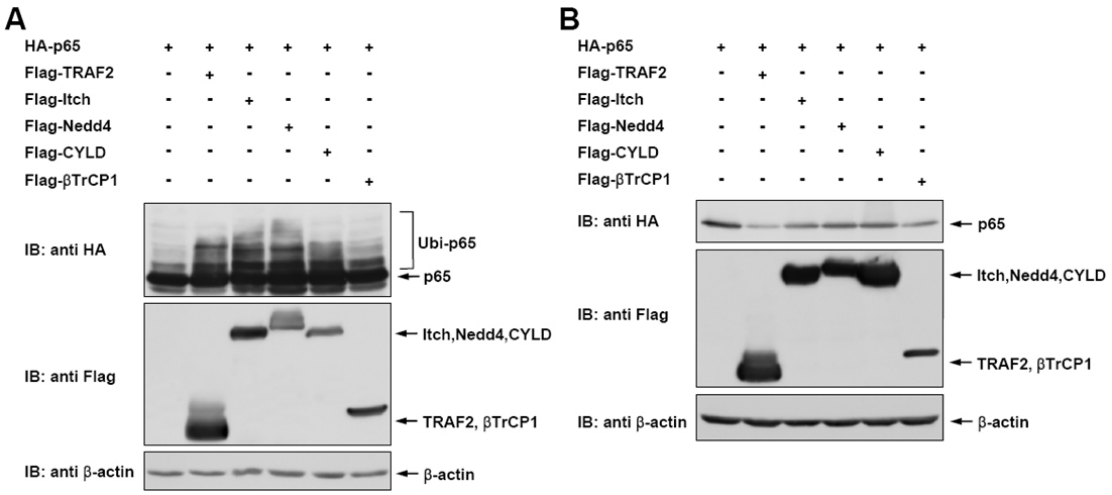

Figure 4.18 p65-associated ubiquitin modifiers change its ubiquitination pattern.

(A) 293T cells were transfected to express limited amounts of p65 protein along with different ubiquitin modifiers as shown. After denaturing lysis, p65 ubiquitination was revealed by immunoblotting. (B) The experiments were performed as in (A) with the exception of extracting proteins in NP-40 lysis buffer.

4.2.7 p65 Ser 468 controls its binding with COMMD1 and Cullin-2

A previous study revealed that COMMD1 promoted the ubiquitination of p65 through its interaction with a multisubunit ubiquitin E3 ligase complex containing Elongin B/C, Cullin-2 and SOCS1 (Maine et al., 2007).

The components of this multisubunit ubiquitin ligase complex, COMMD1, SOCS1 and Cul2 were also compared for the association between p65 wildtype and the phosphorylation mutant. 293T cells were transiently transfected to express HA-tagged wildtype and S468A p65 either alone or together with one member of this complex. Following immunoprecipitation with either HA or control antibodies, co-precipitated proteins were revealed by immunoblotting. In agreement with the published data, SOCS1, COMMD1 and Cul2 all interacted with p65 wildtype protein (Fig. 4.19A-C), whereas they showed different binding affinities to the S468A mutant. SOCS1 also bound to the Ser 468 mutated p65 (Fig. 4.19A), while COMMD1 and Cul2 had lost most of their p65 binding abilities (Fig. 4.19B, C).

To investigate the consequences of this differential binding for p65 ubiquitination, limited amounts of p65 wildtype or the phosphorylation mutant were expressed together with different components of this COMMD1-containing E3 ligase complex in 293T cells. After denaturing lysis in 1 x SDS sample buffer, p65 ubiquitination was revealed by immunoblotting. Consistent with previous reports (Maine et al., 2007), expression of SOCS1, COMMD1 or Cul2 increased p65 ubiquitination. Again, they differed in the ability to trigger ubiquitination of Ser 468-mutated p65. SOCS1 mediated the ubiquitination of p65 and p65 S468A to the same extent. In contrast, COMMD1 and Cul2 showed strongly diminished ubiquitination activity for the phosphorylation mutant (Fig. 4.19D).

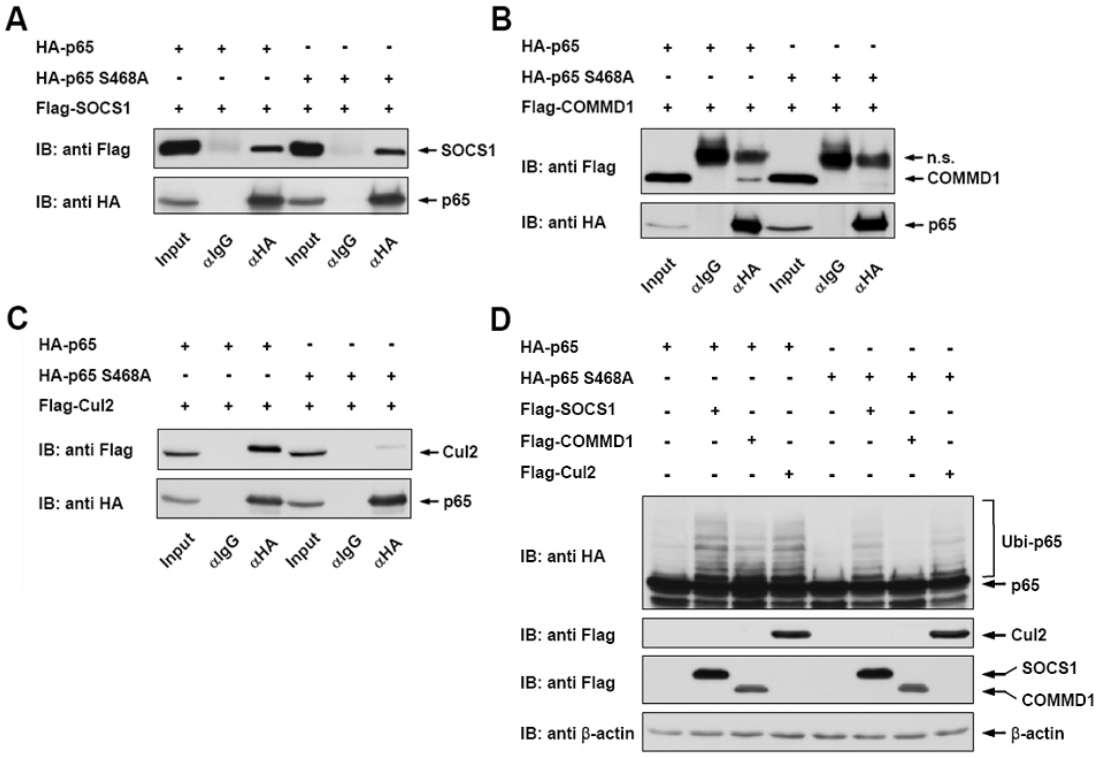

Figure 4.19 p65 Ser 468 directs the interaction with COMMD1 and Cul2.

(A) 293T cells were transiently transfected with HA-tagged p65 either alone or together with Flag-tagged SOCS1 as shown. Following immunoprecipitation (IP) with either HA or control antibodies, co-precipitated proteins were revealed by immunoblotting. (B and C) The experiments were performed as in (A) with the exception that COMMD1 and Cul2 were tested for p65 binding. (D) 293T cells were transfected to express limited amounts of HA-p65 protein along with different component of the COMMD1-containing ubiquitin ligase complex as shown. After denaturing lysis, p65 ubiquitination and protein expression were revealed by immunoblotting.

Overall, these data firmly establish the role of p65 Ser 468 for the binding to COMMD1 and Cul2. Furthermore, diminished interactions correlate with impaired p65 ubiquitination.

4.2.8 Phosphorylation-dependent p65 degradation occurs at a subset of NF-κB target genes

To identify the NF-κB target genes at which p65 elimination occurs, gene array experiments were performed. p65 deficient MEFs were retransfected with p65 wildtype or the S468A point mutant and were left untreated or stimulated with TNF

for different periods. Western blotting experiments confirmed the similar expression of various p65 proteins (Fig. 4.20).

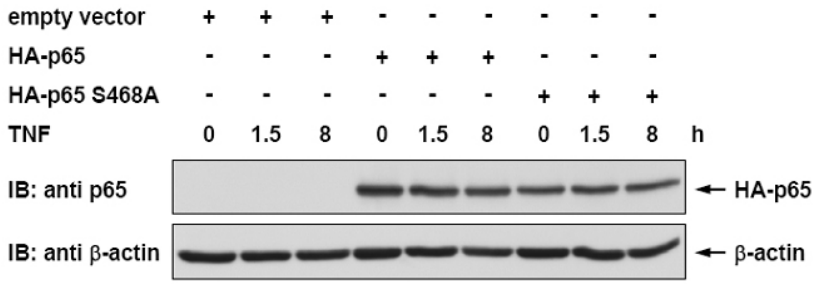

Figure 4.20 Expression of p65 proteins for gene array experiments.

$p65^{-/-}$ MEFs were transfected with empty vector, p65 wildtype or the S468A mutant. The next day, cells were left untreated or stimulated with TNF for 1.5 h and 8 h. Total cell extracts were tested by immunoblotting for p65 and β-actin as shown.

Gene expression was monitored by a low density microarray (MWG Biotech), covering 136 highly regulated inflammatory genes and 19 housekeeping genes (Winzen et al., 2007). Eleven genes were up-regulated by p65 reconstitution. These genes can be divided into six groups, according to their different transcriptional activities in response to reintroduced p65 wildtype or the S468A mutant, TNF stimulation, and kinetics during TNF treatment (Table 4.1 and Fig. 4.21).

Table 4.1 Microarray results of up-regulated genes by reconstituted p65

Group	Induction by p65 reconstitution	Induction by TNF	Kinetics during stimulation	Gene
A	p65 wt ≈ p65 S468A	yes	wt ≈ S468A 8 h ≈ 1.5 h	CXCL2 (MIP-2)
B	p65 wt ≈ p65 S468A	yes	wt ≈ S468A 8 h < 1.5 h	CCL2, CXCL10 (IP-10), CXCL1 and NFKBIA
C	p65 wt > p65 S468A	yes	wt ≈ S468A 8 h > 1.5 h	MMP3 and MMP13
D	p65 wt > p65 S468A	no	wt ≈ S468A 8 h ≈ 1.5 h	SAA3
E	p65 wt < p65 S468A	yes	wt ≈ S468A 8 h > 1.5 h	VCAM-1 and CSF2
F	p65 wt < p65 S468A	yes	wt: 8 h < 1.5 h S468A: 8 h ≈ 1.5 h	ICAM-1

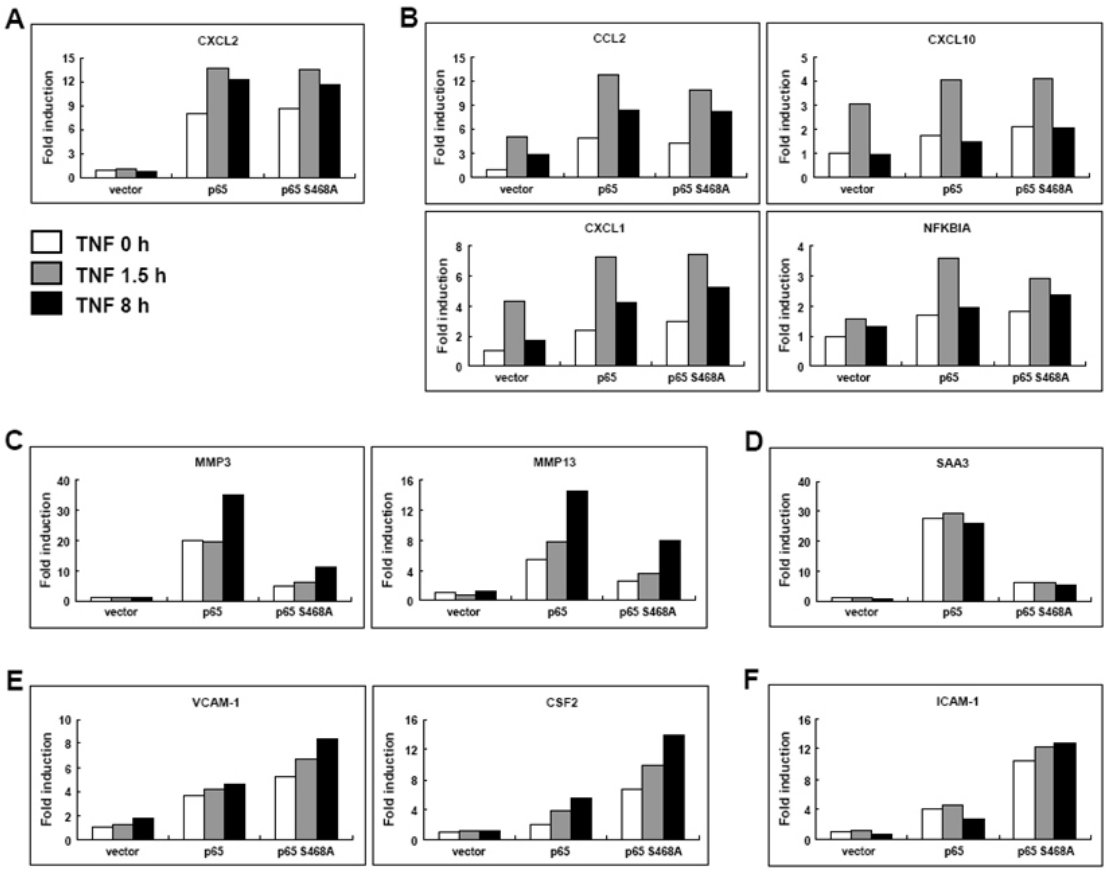

Figure 4.21 Different kinetics of p65-induced genes.

$p65^{-/-}$ MEFs were transfected and treated as in Fig. 4.20. Total RNA was isolated using the RNeasy kit. Microarray experiments were performed using the second version of the mouse inflammation microarray, which contains 136 probes for inflammatory genes and 19 probes for housekeeping genes. The p65-induced genes fall into 6 groups as shown. Fold induction relative to unstimulated cells transfected with empty vector is shown.

Collectively, these results allow several conclusions: (1) the gene regulating capacity of p65 wildtype or the S468A mutant is strictly dependent on the individual target gene; (2) the Ser 468 phosphorylation of p65 can remain without impact on gene expression, but can also inhibit or augment the mRNA production of target genes.

NF-κB p65-triggered induction of the ICAM-1 gene was reduced 8 h after TNF stimulation, whereas p65 S468A activated ICAM-1 expression was largely unchanged at this time point. This raises the possibility that p65 might be removed from the ICAM-1 promoter. In contrast, the transcription of other genes, such as MIP-2 did not show any difference between p65 and the S468A mutant.

Gene expression of ICAM-1 and MIP-2 as a control gene was quantified by real-time PCR analysis. This approach confirmed the different transcriptional induction of ICAM-1 and MIP-2 by p65 or the S468A mutant. Both genes were largely triggered by p65 reconstitution and their p65-incuded gene expression was further enhanced by TNF stimulation. For ICAM-1, the p65-dependent gene expression was diminished 8 h after TNF treatment, while p65 S468A-mediated transcription was not impaired (Fig. 4.22A). In contrast, MIP-2 gene expression was triggered to the same extent by p65 wildtype and the phosphorylation mutant (Fig. 4.22B).

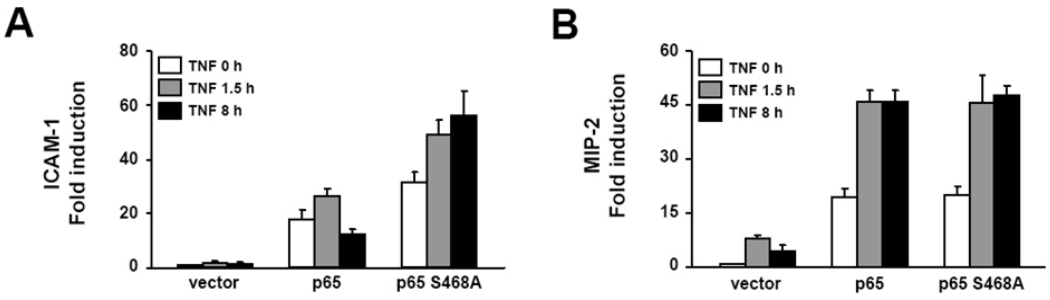

Figure 4.22 Real-time PCR of selective NF-κB target genes.

(A) $p65^{-/-}$ MEFs were transfected as shown. The next day, cells were left untreated or stimulated with TNF for 1.5 h and 8 h. Gene expression of ICAM-1 was assessed by real-time PCR, fold activation relative to unstimulated cells transfected with empty expression vector is shown. Data were analyzed from at least 3 independent experiments and error bars showed standard deviations. Values were normalized to the expression of β-actin and the relative abundance of transcripts was calculated by the comparative ΔΔCT method. (B) The same experiment was performed as in (A) and shows MIP-2 gene expression.

4.2.9 Phosphorylation-induced elimination of p65 only occurs at selective promoters

To investigate whether these differences in target gene expression are reflected by p65 promoter occupancy, chromatin immunoprecipitation (ChIP) assays were employed. $p65^{-/-}$ MEFs were transfected to express either p65 wildtype or S468A mutant, followed by TNF stimulation for the indicated time points and further analyzed for p65 binding to target promoters by ChIP experiments. Expression of p65 was sufficient to cause some basal binding of p65 to the ICAM-1 promoter which was further enhanced after 1 h of TNF treatment. In contrast, the amount of

promoter-associated p65 was strongly diminished 5 h after TNF induction (Fig. 4.23A). Also the p65 S468A mutant was recruited to the ICAM-1 promoter 1 h after TNF stimulation, but stayed there even after a prolonged period of TNF treatment. The association of both p65 proteins with the promoter region of MIP-2 showed similar kinetics, and the binding affinities were unchanged even at the late time point after TNF stimulation (Fig. 4.23A). These data indicate that p65 Ser 468 determines the removal of p65 from selective promoters.

It has been previously demonstrated that p65 clearance at some NF-κB target genes is proteasome-dependent (Saccani et al., 2004). To reveal whether p65 elimnation at the ICAM-1 promoter depends on proteasome activity, the ChIP experiments were repeated in the presence of MG132. The induced removal of p65 from this promoter at 5 h after TNF stimulation did not occur in the presence of this proteasome inhibitor (Fig. 4.23B). These results reveal the importance of ubiquitin/proteasome-mediated events for the removal of p65 from its cognate binding site at the ICAM-1 promoter.

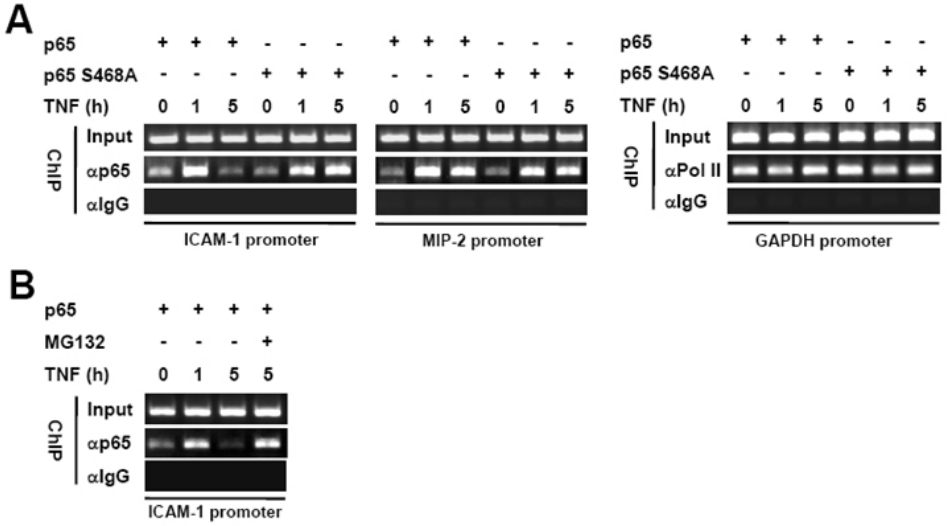

Figure 4.23 Phosphorylation-dependent p65 degradation occurs at selective promoters.

(A) $p65^{-/-}$ MEFs were transfected as shown, followed by TNF stimulation for the indicated time points and ChIP analysis using the indicated specific and control antibodies. Immunoprecipitates from each sample were analyzed by PCR with specific primers for the indicated genes. Input represents the PCR product from chromatin obtained before immunoprecipitation. PCR products were separated by agarose gel electrophoresis. The binding of GAPDH promoter to Pol II is shown as a specificity control. (B) The experiment was performed as in (A) with the exception that cells were pretreated for 1 h with MG132 (10 μM) as shown.

5 Discussion

In order to achieve a properly controlled NF-κB response, the induction, amplitude and duration of this transcription factor are tightly regulated. Post-translational modifications of the DNA-binding subunits represent a second level of regulating its activity. It has been shown that several NF-κB subunits, including p65, can undergo phosphorylation, acetylation and ubiquitination, which may regulate several features, such as nuclear import and transactivation. This study has provided evidence that p65 is phosphorylated by IKKε at Ser 468 in response to T cell costimulation, and this phosphorylation event is important for transactivation in a target gene-specific way. Ser 468 phosphorylation also controls TNF-induced p65 ubiquitination and degradation and allows its association with the ubiquitin ligase components COMMD1 and Cullin-2. The phosphorylation-dependent p65 elimination only occurs at selective promoters, thus allowing termination of the late transcriptional response at distinct target genes.

5.1 Function of IKKε as a p65 kinase

This study allowed to identify IKKε as a kinase phosphorylating the p65 protein at Ser 468 and Ser 536, as revealed by *in vivo* and *in vitro* experiments. Each of these two serines is still phosphorylated by IKKε when the other serine is mutated to alanine, showing that IKKε can phosphorylate these sites also individually. IKKε failed to induce an upshifted band for GFP-p65 that is mutated in either Ser 536 or Ser 468 to alanine. Therefore, both serine residues are required to induce the slower migrating p65 form. As phosphorylation can also occur without the induction of slower migrating upshifted bands, it cannot be excluded that IKKε can phosphorylate p65 at additional sites, a possibility that remains to be examined in future studies. IKKε-mediated phosphorylation of p65 helps to explain data from a previous study that described unchanged inducible IκBα phosphorylation and DNA-binding in IKKε$^{-/-}$ cells (Kravchenko et al., 2003). However, these cells showed selective defects

in the LPS-induced expression of some late NF-κB target genes, including COX-2, RANTES and IP-10, which may now be well explained by effects due to IKKε-mediated p65 phosphorylation. In a line with this finding, the kinase activity of IKKε is triggered at late time points after LPS stimulation (Solis et al., 2007). IKKε also contributes in the alternative NF-κB activation pathway through a direct interaction with p52 in complex with p65, which promotes transactivation of p52-dependent genes (Wietek et al., 2006). In addition, IKKε is important for the induction of the antiviral response and phosphorylates IRF3 and IRF7 (Fitzgerald et al., 2003; Sharma et al., 2003). These transcription factors assemble together with p65 at the enhanceosome of the interferon-β (IFN-β) gene (Maniatis et al., 1998). A recently published atomic model of the interferon-β enhanceosome revealed that IRF, p65 and further factors assemble to create a continuous surface for recognizing a composite DNA-binding element (Panne et al., 2007). In such a situation, IKKε can phosphorylate both assembled IRF and p65 proteins that would result in enhanced recruitment of CBP/p300 coactivators and synergistic regulation of target gene expression. The homologous kinase TBK1 performs similar functions as IKKε in various biological events, including the regulation of IRF3/7 activation and p65 Ser 536 phosphorylation (Buss et al., 2004b; Fitzgerald et al., 2003; Sharma et al., 2003). Also TBK1$^{-/-}$ MEFs show normal IκBα degradation and DNA-binding, but defects in the transactivation of specific NF-κB target genes (Bonnard et al., 2000). However, the evidence for a role of TBK1 in p65 Ser 468 phosphorylation is yet missing and needs to be addressed in the future.

The kinase activity of IKKε can be induced upon T cell costimulation and the induction of IKKε kinase activity parallels p65 Ser 468 phosphorylation. As inducible Ser 468 phosphorylation is lost in the presence of a shRNA down-regulating IKKε levels or a dominant negative IKKε mutant, these results suggest that IKKε is the kinase mainly responsible for p65 Ser 468 phosphorylation induced by T cell costimulation. While GSK3β mediates basal phosphorylation of p65 at Ser 468 in unstimulated cells (Buss et al., 2004a), IKKβ has been shown to trigger Ser 468

phosphorylation in response to TNF or IL-1 stimulation (Schwabe and Sakurai, 2005). However, both TNF- and IL-1 induce p65 Ser 468 phosphorylation with a very fast kinetics and this p65 modification is not detectable even 15 min after stimulation. In costimulated T cells, Ser 468 phosphorylation occurs with a significantly delayed kinetics and stays even after 45 min post-stimulation. As the activity of IKKβ already drops 30 min after induction (Delhase et al., 1999), a contribution of this kinase for Ser 468 phosphorylation is rather unlikely. Altogether, these results demonstrate that the involved kinase for p65 Ser 468 phosphorylation is dependent on the employed stimulus. The notion that various stimuli employ distinct kinases for a given p65 phosphorylation site also holds true for the Ser 536 phosphorylation site. Ser 536 phosphorylation triggered by TNF or T cell costimulation is chiefly mediated by IKKβ (Mattioli et al., 2004b; Sakurai et al., 1999). IL-1-induced phosphorylation is regulated by multiple kinases, including IKKα/β, IKKε and TBK1 (Buss et al., 2004b), whereas DNA damage employs RSK1 to modify the same site (Bohuslav et al., 2004). Additionally, IKKε has also been found to phosphorylate p65 at the C-terminal transactivation domain during TNF induction (Wietek et al., 2006). The precise role of IKKε for TNF- and IL-1-triggered p65 Ser 468 phosphorylation should be tested in future experiments using IKKε$^{-/-}$ MEFs.

It has been shown that the p65 protein can activate the transcription of IKKε (Wang et al., 2005). This study provides evidence that IKKε in turn can mediate the phosphorylation of p65, thus establishing a positive feedback loop. Indeed, IKKε overexpression was able to enhance the expression of various NF-κB target genes, including CCND1, MYC, COX-2, IL-1, MMP9, VEGF, c-IAP1, c-IAP2 and BCL2 (Boehm et al., 2007). The requirement of IKKε-mediated p65 phosphorylation for these effects remains to be explored in the future work. A previous study revealed that IKKε also increases the DNA-binding activity of C/EBPδ, thus affecting the expression of target genes, such as IP-10 and RANTES, which often rely on the coordinate binding of NF-κB and C/EBP (Kravchenko et al., 2003). IKKε gene expression was found to be regulated by C/EBP, suggesting that an autoactivation

mechanism also exists between IKKε and this transcription factor. Since IKKε deficiency only partially affects C/EBPδ DNA-binding affinity, but completely abolishes transcription of individual target genes, it is reasonable to assume that IKKε will employ additional mechanisms to contribute to NF-κB-dependent gene expression. The changed transcriptional activity of phosphorylated p65 shows a new insight of IKKε-dependent control of gene expression, in addition to the integration of C/EBP and NF-κB pathways.

Multiple experimental approaches showed that IKKε-mediated p65 Ser 468 phosphorylation only occurs after its release from IκBα, but IKKα/β-induced degradation of IκBα is still a prerequisite for this IKKε-mediated modification of p65 under physiological conditions. Subcellular fractionation experiments revealed that Ser 468 phosphorylated p65 mainly occurs in the nucleus. However, there is no direct evidence to exclude the possibility that IKKε-mediated p65 phosphorylation can also take place in the cytoplasm, as the distribution of IKKε was found in both the cytoplasm and the nucleus. A mutated and dominant negative IKKε delayed the kinetics of p65 nuclear import, thus revealing its importance for the regulation of this process. This effect is not linked to p65 Ser 468 phosphorylation, as this site is not relevant for the subcellular distribution of p65 (Schwabe and Sakurai, 2005). Consequently, this kinase may phosphorylate p65 at additional sites or modify further substrate proteins. Moreover, endogenous IKKε can mediate p65 phosphorylation at Ser 468 in response to T cell costimulation even in the absence of NEMO, showing that the inducible kinase activity of IKKε is independent from the functional IKK complex. Therefore, the function of IKKε as a p65 kinase provides a mechanistic clue to explain the relevance of IKKε for the expression of a subset of NF-κB target genes without affecting IKK activity. In addition, specific inhibitors for the kinases GSK3, p38, ERK, JNK and PI3K did not influence p65 Ser 468 phosphorylation after T cell costimulation, excluding a role of these kinases for inducible Ser 468 phosphorylation in T cells. These results are consistent with a previous study reporting that none of these kinases are involved in the TNF- or IL-1-induced p65 Ser 468 phosphorylation

(Schwabe and Sakurai, 2005). Similar to the classical IKK complex, kinase activity of IKKε and TBK1 may also require the activation of upstream adaptor proteins. NAK-associated protein 1 (NAP1) was identified to interact with TBK1 and enhance its ability to phosphorylate p65 at Ser 536 (Fujita et al., 2003). Moreover, the scaffold protein TANK is involved in the LPS-induced, IKKε- and TBK1-mediated IRF3/7 phosphorylation (Gatot et al., 2007). The responsible adaptor protein for IKKε-induced p65 phosphorylation remains to be explored.

5.2 Functional consequences of Ser 468 phosphorylation

The p65 subunit is responsible for the strong transactivation potential and can be phosphorylated in both TAD1 (521-551) and TAD2 (439-520) (Schmitz et al., 1995). Ser 468 within TAD2 is located at the position homologous to Ser 536 within TAD1 (Fig. 4.1), which suggests these two serines may exert similar or overlapping functions. Furthermore, both serine sites are evolutionary conserved from mammals to amphibians (Fig. 5.1), suggesting that they are functionally important.

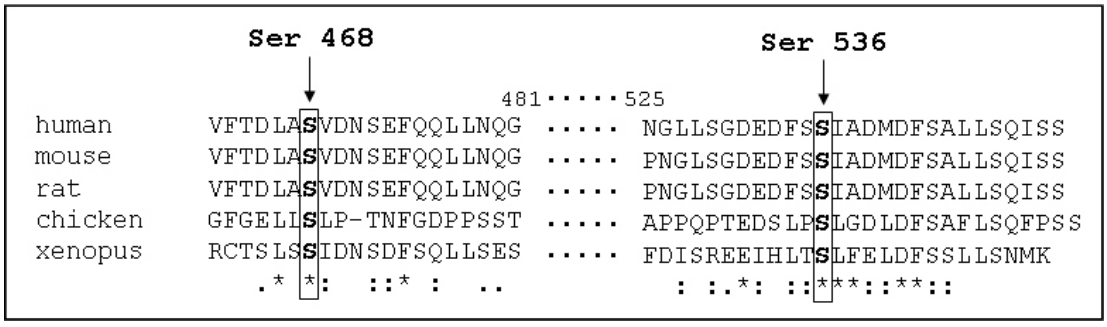

Figure 5.1 p65 Ser 468 and Ser 536 are evolutionary conserved.

NF-κB p65 proteins from the indicated organisms are compared for the conservation of Ser 468 and Ser 536. Homologous amino acids are indicated by stars and related amino acids are indicated by dots.

Ser 536 is one of the best-characterized p65 phosphorylation sites and it can be phosphorylated by multiple kinases via various signaling pathways. In most cases, these phosphorylations serve to regulate NF-κB-dependent transcription (Viatour et al., 2005). This study demonstrates that this also holds true for p65 phosphorylation at Ser 468. First, the Ser 468-phosphorylated p65 occurs mainly in the nucleus in

response to various stimuli, including T cell costimulation, thus suggesting a function for transactivation. Second, reconstitution of $p65^{-/-}$ cells with either wildtype p65 or point mutated p65 variants showed that inducible phosphorylation of p65 at Ser 468 indicates an enhanced capacity to trigger expression of a NF-κB reporter gene. However, gene array experiments revealed that the impact of Ser 468 phosphorylation strictly depends on the target genes. While inducible expression of MMP3, MMP13 and SAA3 depends on an intact serine, transcription of the MIP-2, CCL2, CXCL10, CXCL1 and NFKBIA genes is not affected by this phosphorylation site. Moreover, the p65 S468A mutant triggers production of VCAM-1, CSF2 and ICAM-1 mRNA even more potently when compared to the p65 wildtype protein. How can these differences be explained mechanistically? One model compatible with this finding would reflect the fact that only a subfraction of p65 is phosphorylated at Ser 468. Thus, target genes could be differentially activated in dependence of differentially phosphorylated p65 subpools. In addition to its effects on transactivation, this study reveals that Ser 468 phosphorylation controls the ubiquitination and stability of this transcription factor. Ser 468 phosphorylation controls TNF-triggered p65 degradation and proteasomal elimination from specific target genes, thus contributing to the termination of the NF-κB response. Also phosphorylation of Ser 536 has been linked to the promotion of stimulus-induced p65 degradation (Lawrence et al., 2005), suggesting that both sites collaborate in the regulation of p65 stability.

Several pieces of evidence have revealed that Ser 536 phosphorylation bears further functions. In addition to the association with TAFII31 (Buss et al., 2004b), phosphorylation at Ser 536 has been suggested to change the conformation of the C-terminal region of p65, which should promote its interaction with the coactivator p300, thus resulting in the regulation of p65 Lys 310 acetylation (Chen et al., 2005). Ser 468 is adjacent to the CBP/p300 binding region within p65, which locates between amino acids 477 and 503 (Zhong et al., 1998). Therefore, inducible phosphorylation of this site may also affect the interaction between p65 and coregulators. The Ser 536-contained TAD1 region can form an inducible α-helix upon binding to other proteins (Schmitz et al., 1994). Accordingly secondary structure

predictions suggest that the homologous TAD1' region containing Ser 468 could fold in such an α-helix, as well (Fig 4.1) (Combet et al., 2000). In such a conformation, phosphorylation of Ser 468 would increase the negative charge on one helix surface, thus potentially affecting the binding to coactivators or corepressors. Phosphorylation of p65 at Ser 468 does not occur alone and is accompanied by further p65 modifications. As a result, distinct p65 modification patterns control subsets of induced target genes as well as the duration and amplitude of the NF-κB response. The transcription of target genes also depends on the oscillation persistence, involving cycles of p65 phosphorylation and dephosphorylation. The oscillation of p65 Ser 536 phosphorylation appears to be a consequence of its shuttling between the cytoplasm and the nucleus (Nelson et al., 2004). It will be interesting to explore a potential contribution of oscillatory p65 Ser 468 phosphorylations for its subcellular distribution in the future.

5.3 Ubiquitin/proteasome-mediated mechanisms terminating the NF-κB response

Given the central function of NF-κB activation for key cellular processes, various pathways have evolved to ensure a tight regulation of the NF-κB response. These mechanisms include feedback loops and post-inductive degradation of the DNA-binding subunits (Maine and Burstein, 2007; Natoli and Chiocca, 2008). Many NF-κB target genes can generate negative feedback loops to influence the function of NF-κB and switch off the transcription program. IκBα is one of the master terminators of NF-κB response. After NF-κB activation, rapidly resynthesized IκBα can enter the nucleus, associate with the DNA-binding subunits and shuttle them back to the cytoplasm (Brown et al., 1993; Zabel and Baeuerle, 1990). IκBα$^{-/-}$ cells were not only defective in limiting the NF-κB activity in response to pulse stimulation, but also expressed the gene for the chemokine RANTES, a hallmark for persistent NF-κB activity (Hoffmann et al., 2002). Other NF-κB target genes, such as A20, Cezanne and CYLD, encode deubiquitinating enzymes and can therefore inhibit and limit the NF-κB response. These ubiquitin modifiers serve to shut off NF-κB transactivation

through disassembling the Lys 63-linked polyubiquitination chains from IKK upstream adaptors and receptors, such as TRAF proteins (Evans et al., 2001; Jono et al., 2004; Kovalenko et al., 2003; Wertz et al., 2004). Additionally, Bcl10, a key scaffold protein upstream from the IKK complex and downstream from protein kinase C (PKC) provides another example for a negative feedback mechanism in the activated T cells. A previous study revealed that TCR/PKC signaling initially activates Bcl10 to turn on the NF-κB response, but later on these signals promote Bcl10 degradation to selectively turn off the signal transduction process (Scharschmidt et al., 2004). Two current reports suggested that IKKβ can also negative regulate TCR signal production through phosphorylating Bcl10 at several C-terminal serines, thus leading to the inactivation of Bcl10. This event results in the limited duration and degree of IKK and NF-κB activation (Lobry et al., 2007; Wegener et al., 2006).

Ubiquitin- and proteasome-dependent degradation of NF-κB is also important to prevent prolonged target gene expression. The stability of DNA-binding subunits p50 and p65 is controlled by the ubiquitin proteasome system in a highly regulated manner. Ubiquitination of p50 is inhibited by Bcl3, whereas the p65 subunit is ubiquitinated by various ubiquitin E3 ligases, including SOCS1, PDLIM2 and COMMD1 (Carmody et al., 2007; Maine et al., 2007; Ryo et al., 2003; Tanaka et al., 2007). This study has provided evidence that Ser 468 phosphorylation controls the ubiquitination and stability of p65, thus identifying a novel phosphorylation/ ubiquitination switch in the NF-κB network. Only a limited subfraction of the p65 protein undergoes this phosphorylation-dependent proteasomal degradation, showing that the turnover of p65 is firmly controlled by regulatory mechanisms. The TNF signaling pathway was chosen in this study to investigate p65 stability, as only TNF triggers p65 degradation in both MEFs and Hela cells. Since other groups have reported that LPS can induce p65 destabilization in macrophages (Lawrence et al., 2005; Tanaka et al., 2007), signal-induced control of p65 stability may occur in a stimulus- and cell type-specific fashion. In future studies, it will be interesting to

examine whether p65 degradation also occurs in further cell types and in response to other stimuli.

As one of the most common regulatory processes, ubiquitination affects a wide variety of proteins, and controls their stability and/or activity. Degradative ubiquitination regulates at least four steps in the NF-κB pathway, including the proteolysis of IκB proteins, the processing of NF-κB precursors, the degradation of IKK upstream adaptors TAB2/3 and the diminishment of DNA binding subunits (Chen, 2005; Marienfeld et al., 2001; Saccani et al., 2004; Tian et al., 2007). In most of these events, it has been shown that phosphorylation is a prerequisite for ubiquitination. The signal-induced site-specific phosphorylation targets IκBs for polyubiquitination by the $SCF^{\beta\text{-}TrCP}$ ubiquitin ligase complex and subsequent degradation by the proteasome, thereby releasing NF-κB (Chen et al., 1995). Again, phosphorylation of p100 at the C-terminal serine residues leads to the selective degradation of its IκB-like domain by the proteasome, thus generating mature p52 subunit (Xiao et al., 2001). Furthermore, TCR-induced RelB phosphorylation can also target this DNA-binding subunit to undergo subsequent proteolysis (Marienfeld et al., 2001). This study established a novel phosphorylation-dependent ubiquitination mechanism for the degradation of nuclear p65. Ser 468 phosphorylation of p65 is the prerequisite for its association with COMMD1 and Cul2, components of a multisubunit ubiquitin ligase complex. In addition, this phosphorylation-dependent p65 degradation only occurs at a subset of promoters. While p65 and the Ser 468 defective mutant did not show any difference in binding to the MIP-2 promoter, Ser 468 phosphorylation allowed p65 removal from the ICAM-1 promoter. This inducible p65 elimination was notably blocked by the proteasome inhibitor MG132, confirming the importance of the proteasome for p65 diminishment from its cognate binding sites (Saccani et al., 2004). Therefore, the phosphorylation-dependent elimination of p65 contributes to the selective termination of late NF-κB-dependent gene expression. Consistent with the finding that Ser 468 controls p65 removal from the ICAM-1 promoter, COMMD1 deficiency resulted in the enhanced ICAM-1

transcription in response to TNF stimulation (Maine et al., 2007). The relative contribution of COMMD1 for the removal of p65 from the ICAM-1 promoter remains to be examined in the future.

This study has shown that p65 ubiquitination also occurs without stimulation or proteasome blockage. Various ubiquitin mutants defective in branching at Lys 48, Lys 63 or Lys 29 can be attached to p65, suggesting that p65 can also be modified by non-degradative, regulatory ubiquitination. The specificity of ubiquitination is mainly controlled by E3 ligases, as they selectively bind to target proteins and promote transfer of the polyubiquitin chain to a specific substrate. E3 ligases often harbor specific domains, such as the HECT (homologous to E6-associated protein C-terminus), RING (really interesting new gene) or U-box (a modified RING motif without the full complement of Zn^{2+}-binding ligands) domain. The RING type E3 can be further divided into single- and multisubunit enzymes (Ben-Neriah, 2002; Liu, 2004). The p65 protein is ubiquitinated by a multisubunit complex termed as COMMD1-ECS^{SOCS1} complex, which contains Elongins B and C, Cullin-2, the RING finger protein Rbx1, the SOCS-box ligase SOCS1 and the COMM domain-containing protein COMMD1. A previous study revealed that the interaction between COMMD1 and Cul2 is TNF inducible and COMMD1 in turn facilitates the binding of p65 to SOCS1 (Maine et al., 2007). Therefore, SOCS1 is a major component of this E3 ligase complex targeting p65 for ubiquitination. However, the interaction between this multisubunit complex and p65 has not been clearly mapped. The group of Burstein showed that both SOCS1 and COMMD1 mainly interacts with the N-ternimal portion of p65 between amino acids 1 and 180 (Burstein et al., 2005; Maine et al., 2007), whereas Ryo et al. revealed SOCS1 association with a p65 fragment from amino acids 220 to 335 (Ryo et al., 2003). Further work should clarify this discrepancy. In addition, it will also be necessary to map the p65 ubiquitination sites induced by the SOCS1/COMMD1 complex. Besides this COMMD1-containing complex, various ubiquitin-modifying enzymes involved in NF-κB signaling, including TRAF2, β-TrCP, Itch, Nedd4, and CYLD, were identified to interact with p65 and enhance

p65 ubiquitination. TRAF2 is RING type ubquitin ligase and is involved in the TNF-induced NF-κB activation upon catalyzing the Lys 63-linked polyubiquitination of RIP (Shi and Kehrl, 2003). The F-box WD repeat enzyme β-TrCP is one of the best-characterized E3 ligase, which plays a critical role in both canonical and alternative NF-κB activations, including the degradation of IκBs and the generation of mature p52 subunit (Chen, 2005; Yaron et al., 1998). The E3 ligases Itch and Nedd4 belong to the HECT domain family. Both of them can catalyze ubiquitination and degradation of Bcl10, PLCγ1 and PKCθ in TCR-induced NF-κB activation, thus leading to the termination of NF-κB response (Heissmeyer et al., 2004; Scharschmidt et al., 2004). Surprisingly, the de-ubiquitinating enzyme CYLD slightly enhanced basal p65 ubiquitination. Thus CYLD might be able to mediate Lys 48-linked polyubiquitination, although this hypothesis definitively requires further experimental support. Such a situation occurs in the case of the A20 protein, which is known to have a dual role as a deubiquitinating and a ubiquitinating enzyme (Wertz et al., 2004). Among these five novel p65 ubiquitination modifiers, only TRAF2 overexpression results in a significant degradation of p65, assuming a possible role for TRAF2 in p65 decay. The ability to trigger p65 degradation depends on the presence of the RING finger domain of TRAF2. However, TRAF2 binding to p65 was independent from Ser 468. While degradative ubiquitination can only be revealed in the presence of proteasome inhibitors, basal p65 ubiquitination was also frequently detected in the absence of MG132. The functional role of this ubiquitin modification and the involved enzymes remain to be investigated in the future.

How can phosphorylation of a single amino acid control the binding to a multisubunit ubiquitin ligase complex? It may be assumed that the phosphorylation of Ser 468 affects the overall conformation of p65. In the unphosphorylated state, the reported intramolecular interaction between its C-terminal TAD and N-terminal portion (Zhong et al., 1998) may lock it in a closed conformation. A former study revealed that Ser 276 phosphorylation could disrupt this intramolecular binding and allow accessibility to the CBP protein (Zhong et al., 1998). Also Ser 468 might contribute to

p65 confirmation and its phosphorylation may alter the stucture/accessibility of the p65 protein. The proposed phosphorylation/conformation switch is schematically displayed in Fig 5.2. In this model, the relief of intramolecular masking of p65 by Ser 468 phosphorylation would facilitate binding to the COMMD1-containing E3 ligase complex. The COMMD1 complex can mediate p65 ubiquitination and allow it subsequent proteasomal degradation by nuclear proteasomes, thus resulting in the termination of late NF-κB response.

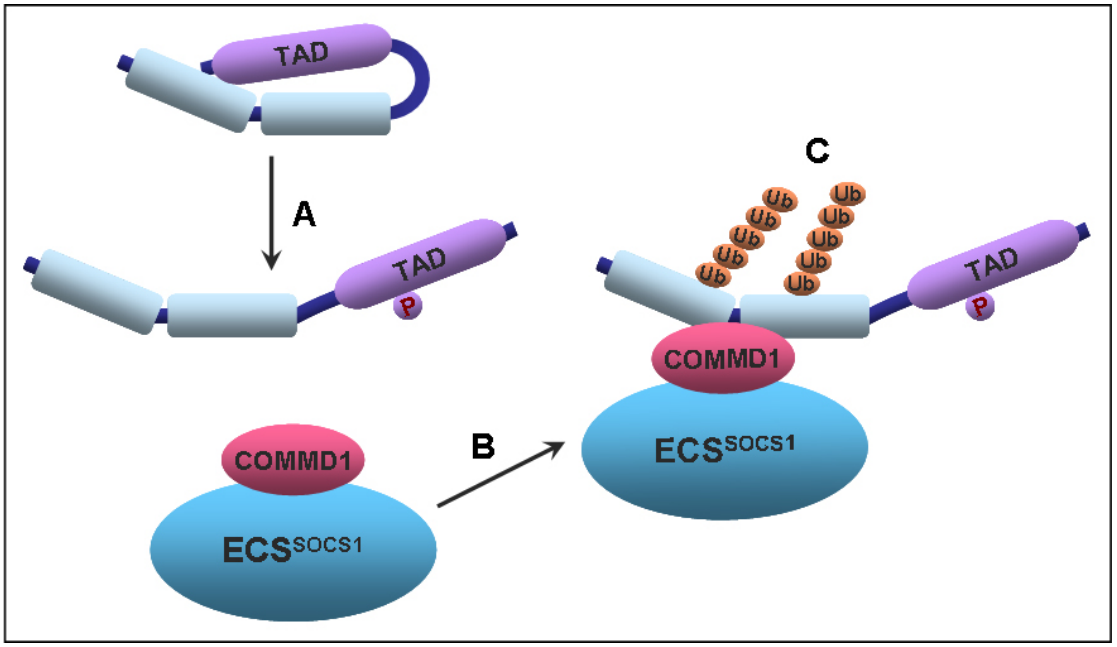

Figure 5.2 A model for p65 Ser 468 phosphorylation-dependent ubiquitination.

In the unphosphorylated state, p65 shows an intramolecular interaction between the C-terminal region and the N-terminal portion (closed conformation). Upon TNF stimulation, p65 is phosphorylated at Ser 468 (step A) which weakens its intramolecular binding and facilitates the docking with the COMMD1-containing ubiquitin ligase complex (step B). This event allows inducible ubiquitination and subsequent degradation of p65 (step C).

In conclusion, this study reveals the importance of p65 Ser 468 phosphorylation for its induced transactivation, ubiquitination and degradation. In the activation phase, phoshorylation at this serine site serves to regulate the expression of a subset of p65-dependent target genes. In the termination phase, Ser 468-phosphorylated p65 might be recognized by a COMMD1-containing multisubunit ubiquitin ligase complex which in turn allows for p65 elimination from distinct target promoters, thus ensuring irreversible termination of the p65 response. While the early NF-κB

response is terminated by IκBα-mediated removal of promoter-bound p65, termination of the late response involves proteasomal elimination of p65 subunit. A complete and timely termination of the pro-inflammatory NF-κB response will be necessary to avoid residual NF-κB activity that is frequently associated with chronic inflammatory processes and other diseases.

6 References

Adli, M. and Baldwin, A.S. (2006) IKK-i/IKKepsilon controls constitutive, cancer cell-associated NF-kappaB activity via regulation of Ser-536 p65/RelA phosphorylation. *J Biol Chem*, **281**, 26976-26984.

Anrather, J., Racchumi, G. and Iadecola, C. (2005) cis-acting, element-specific transcriptional activity of differentially phosphorylated nuclear factor-kappa B. *J Biol Chem*, **280**, 244-252.

Arenzana-Seisdedos, F., Turpin, P., Rodriguez, M., Thomas, D., Hay, R.T., Virelizier, J.L. and Dargemont, C. (1997) Nuclear localization of I kappa B alpha promotes active transport of NF-kappa B from the nucleus to the cytoplasm. *J Cell Sci*, **110 (Pt 3)**, 369-378.

Bae, J.S., Jang, M.K., Hong, S., An, W.G., Choi, Y.H., Kim, H.D. and Cheong, J. (2003) Phosphorylation of NF-kappa B by calmodulin-dependent kinase IV activates anti-apoptotic gene expression. *Biochem Biophys Res Commun*, **305**, 1094-1098.

Baldwin, A.S., Jr. (1996) The NF-kappa B and I kappa B proteins: new discoveries and insights. *Annu Rev Immunol*, **14**, 649-683.

Ben-Neriah, Y. (2002) Regulatory functions of ubiquitination in the immune system. *Nat Immunol*, **3**, 20-26.

Betts, J.C. and Nabel, G.J. (1996) Differential regulation of NF-kappaB2(p100) processing and control by amino-terminal sequences. *Mol Cell Biol*, **16**, 6363-6371.

Birbach, A., Gold, P., Binder, B.R., Hofer, E., de Martin, R. and Schmid, J.A. (2002) Signaling molecules of the NF-kappa B pathway shuttle constitutively between cytoplasm and nucleus. *J Biol Chem*, **277**, 10842-10851.

Boehm, J.S., Zhao, J.J., Yao, J., Kim, S.Y., Firestein, R., Dunn, I.F., Sjostrom, S.K., Garraway, L.A., Weremowicz, S., Richardson, A.L., Greulich, H., Stewart, C.J., Mulvey, L.A., Shen, R.R., Ambrogio, L., Hirozane-Kishikawa, T., Hill, D.E., Vidal, M., Meyerson, M., Grenier, J.K., Hinkle, G., Root, D.E., Roberts, T.M., Lander, E.S., Polyak, K. and Hahn, W.C. (2007) Integrative genomic approaches identify IKBKE as a breast cancer oncogene. *Cell*, **129**, 1065-1079.

Bohuslav, J., Chen, L.F., Kwon, H., Mu, Y. and Greene, W.C. (2004) p53 induces NF-kappaB activation by an IkappaB kinase-independent mechanism involving phosphorylation of p65 by ribosomal S6 kinase 1. *J Biol Chem*, **279**, 26115-26125.

Bonizzi, G. and Karin, M. (2004) The two NF-kappaB activation pathways and their role in innate and adaptive immunity. *Trends Immunol*, **25**, 280-288.

Bonnard, M., Mirtsos, C., Suzuki, S., Graham, K., Huang, J., Ng, M., Itie, A., Wakeham, A., Shahinian, A., Henzel, W.J., Elia, A.J., Shillinglaw, W., Mak, T.W., Cao, Z. and Yeh, W.C. (2000) Deficiency of T2K leads to apoptotic liver degeneration and impaired NF-kappaB-dependent gene transcription. *Embo J*, **19**, 4976-4985.

Bours, V., Franzoso, G., Azarenko, V., Park, S., Kanno, T., Brown, K. and Siebenlist, U. (1993) The oncoprotein Bcl-3 directly transactivates through kappa B motifs via association with DNA-binding p50B homodimers. *Cell*, **72**, 729-739.

Bracken, C.P., Whitelaw, M.L. and Peet, D.J. (2005) Activity of hypoxia-inducible factor 2alpha is regulated by association with the NF-kappaB essential modulator. *J Biol Chem*, **280**, 14240-14251.

Brown, K., Gerstberger, S., Carlson, L., Franzoso, G. and Siebenlist, U. (1995) Control of I kappa B-alpha proteolysis by site-specific, signal-induced phosphorylation. *Science*, **267**, 1485-1488.

Brown, K., Park, S., Kanno, T., Franzoso, G. and Siebenlist, U. (1993) Mutual regulation of the transcriptional activator NF-kappa B and its inhibitor, I kappa B-alpha. *Proc Natl Acad Sci U S A*, **90**, 2532-2536.

Buerki, C., Rothgiesser, K.M., Valovka, T., Owen, H.R., Rehrauer, H., Fey, M., Lane, W.S. and Hottiger, M.O. (2008) Functional relevance of novel p300-mediated lysine 314 and 315 acetylation of RelA/p65. *Nucleic Acids Res*, **36**, 1665-1680.

Burstein, E., Hoberg, J.E., Wilkinson, A.S., Rumble, J.M., Csomos, R.A., Komarck, C.M., Maine, G.N., Wilkinson, J.C., Mayo, M.W. and Duckett, C.S. (2005) COMMD proteins, a novel family of structural and functional homologs of MURR1. *J Biol Chem*, **280**, 22222-22232.

Buss, H., Dorrie, A., Schmitz, M.L., Frank, R., Livingstone, M., Resch, K. and Kracht, M. (2004a) Phosphorylation of serine 468 by GSK-3beta negatively regulates basal p65 NF-kappaB activity. *J Biol Chem*, **279**, 49571-49574.

Buss, H., Dorrie, A., Schmitz, M.L., Hoffmann, E., Resch, K. and Kracht, M. (2004b) Constitutive and interleukin-1-inducible phosphorylation of p65 NF-{kappa}B at serine 536 is mediated by multiple protein kinases including I{kappa}B kinase (IKK)-{alpha}, IKK{beta}, IKK{epsilon}, TRAF family member-associated (TANK)-binding kinase 1 (TBK1), and an unknown kinase and couples p65 to TATA-binding protein-associated factor II31-mediated interleukin-8 transcription. *J Biol Chem*, **279**, 55633-55643.

Campbell, K.J. and Perkins, N.D. (2006) Regulation of NF-kappaB function. *Biochem Soc Symp*, 165-180.

Campbell, K.J., Witty, J.M., Rocha, S. and Perkins, N.D. (2006) Cisplatin mimics ARF tumor suppressor regulation of RelA (p65) nuclear factor-kappaB transactivation. *Cancer Res*, **66**, 929-935.

Carmody, R.J., Ruan, Q., Palmer, S., Hilliard, B. and Chen, Y.H. (2007) Negative regulation of toll-like receptor signaling by NF-kappaB p50 ubiquitination blockade. *Science*, **317**, 675-678.

Chen, L.F. and Greene, W.C. (2004) Shaping the nuclear action of NF-kappaB. *Nat Rev Mol Cell Biol*, **5**, 392-401.

Chen, L.F., Mu, Y. and Greene, W.C. (2002) Acetylation of RelA at discrete sites regulates distinct nuclear functions of NF-kappaB. *Embo J*, **21**, 6539-6548.

Chen, L.F., Williams, S.A., Mu, Y., Nakano, H., Duerr, J.M., Buckbinder, L. and Greene, W.C. (2005) NF-kappaB RelA phosphorylation regulates RelA acetylation. *Mol Cell Biol*, **25**, 7966-7975.

Chen, Z., Hagler, J., Palombella, V.J., Melandri, F., Scherer, D., Ballard, D. and Maniatis, T. (1995) Signal-induced site-specific phosphorylation targets I kappa B alpha to the ubiquitin-proteasome pathway. *Genes Dev*, **9**, 1586-1597.

Chen, Z.J. (2005) Ubiquitin signalling in the NF-kappaB pathway. *Nat Cell Biol*, **7**, 758-765.

Chien, Y., Kim, S., Bumeister, R., Loo, Y.M., Kwon, S.W., Johnson, C.L., Balakireva, M.G., Romeo, Y., Kopelovich, L., Gale, M., Jr., Yeaman, C., Camonis, J.H., Zhao, Y. and White, M.A. (2006) RalB GTPase-mediated activation of the IkappaB family kinase TBK1 couples innate immune signaling to tumor cell survival. *Cell*, **127**, 157-170.

Claudio, E., Brown, K., Park, S., Wang, H. and Siebenlist, U. (2002) BAFF-induced NEMO-independent processing of NF-kappa B2 in maturing B cells. *Nat Immunol*, **3**, 958-965.

Cohen, P. and Goedert, M. (2004) GSK3 inhibitors: development and therapeutic potential. *Nat Rev Drug Discov*, **3**, 479-487.

Combet, C., Blanchet, C., Geourjon, C. and Deleage, G. (2000) NPS@: network protein sequence analysis. *Trends Biochem Sci*, **25**, 147-150.

Coope, H.J., Atkinson, P.G., Huhse, B., Belich, M., Janzen, J., Holman, M.J., Klaus, G.G., Johnston, L.H. and Ley, S.C. (2002) CD40 regulates the processing of NF-kappaB2 p100 to p52. *Embo J*, **21**, 5375-5385.

Dejardin, E., Droin, N.M., Delhase, M., Haas, E., Cao, Y., Makris, C., Li, Z.W., Karin, M., Ware, C.F. and Green, D.R. (2002) The lymphotoxin-beta receptor induces different patterns of gene expression via two NF-kappaB pathways. *Immunity*, **17**, 525-535.

Delhase, M., Hayakawa, M., Chen, Y. and Karin, M. (1999) Positive and negative regulation of IkappaB kinase activity through IKKbeta subunit phosphorylation. *Science*, **284**, 309-313.

DiDonato, J., Mercurio, F., Rosette, C., Wu-Li, J., Suyang, H., Ghosh, S. and Karin, M. (1996) Mapping of the inducible IkappaB phosphorylation sites that signal its ubiquitination and degradation. *Mol Cell Biol*, **16**, 1295-1304.

DiDonato, J.A., Hayakawa, M., Rothwarf, D.M., Zandi, E. and Karin, M. (1997) A cytokine-responsive IkappaB kinase that activates the transcription factor NF-kappaB. *Nature*, **388**, 548-554.

Duran, A., Diaz-Meco, M.T. and Moscat, J. (2003) Essential role of RelA Ser311 phosphorylation by zetaPKC in NF-kappaB transcriptional activation. *Embo J*, **22**, 3910-3918.

Ea, C.K., Deng, L., Xia, Z.P., Pineda, G. and Chen, Z.J. (2006) Activation of IKK by TNFalpha requires site-specific ubiquitination of RIP1 and polyubiquitin binding by NEMO. *Mol Cell*, **22**, 245-257.

Evans, P.C., Taylor, E.R., Coadwell, J., Heyninck, K., Beyaert, R. and Kilshaw, P.J. (2001) Isolation and characterization of two novel A20-like proteins. *Biochem J*, **357**, 617-623.

Fitzgerald, K.A., McWhirter, S.M., Faia, K.L., Rowe, D.C., Latz, E., Golenbock, D.T., Coyle, A.J., Liao, S.M. and Maniatis, T. (2003) IKKepsilon and TBK1 are essential components of the IRF3 signaling pathway. *Nat Immunol*, **4**, 491-496.

Franzoso, G., Biswas, P., Poli, G., Carlson, L.M., Brown, K.D., Tomita-Yamaguchi, M., Fauci, A.S. and Siebenlist, U.K. (1994) A family of serine proteases expressed exclusively in myelo-monocytic cells specifically processes the nuclear factor-kappa B subunit p65 in vitro and may impair human immunodeficiency virus replication in these cells. *J Exp Med*, **180**, 1445-1456.

Franzoso, G., Bours, V., Park, S., Tomita-Yamaguchi, M., Kelly, K. and Siebenlist, U. (1992) The candidate oncoprotein Bcl-3 is an antagonist of p50/NF-kappa B-mediated inhibition. *Nature*, **359**, 339-342.

Fujita, F., Taniguchi, Y., Kato, T., Narita, Y., Furuya, A., Ogawa, T., Sakurai, H., Joh, T., Itoh, M., Delhase, M., Karin, M. and Nakanishi, M. (2003) Identification of NAP1, a regulatory subunit of IkappaB kinase-related kinases that potentiates NF-kappaB signaling. *Mol Cell Biol*, **23**, 7780-7793.

Gatot, J.S., Gioia, R., Chau, T.L., Patrascu, F., Warnier, M., Close, P., Chapelle, J.P., Muraille, E., Brown, K., Siebenlist, U., Piette, J., Dejardin, E. and Chariot, A. (2007) Lipopolysaccharide-mediated interferon regulatory factor activation involves TBK1-IKKepsilon-dependent Lys(63)-linked polyubiquitination and phosphorylation of TANK/I-TRAF. *J Biol Chem*, **282**, 31131-31146.

Ghosh, S. and Karin, M. (2002) Missing pieces in the NF-kappaB puzzle. *Cell*, **109 Suppl**, S81-96.

Ghosh, S., May, M.J. and Kopp, E.B. (1998) NF-kappa B and Rel proteins: evolutionarily conserved mediators of immune responses. *Annu Rev Immunol*, **16**, 225-260.

Gringhuis, S.I., Garcia-Vallejo, J.J., van Het Hof, B. and van Dijk, W. (2005) Convergent actions of I kappa B kinase beta and protein kinase C delta modulate mRNA stability through phosphorylation of 14-3-3 beta complexed with tristetraprolin. *Mol Cell Biol*, **25**, 6454-6463.

Hacker, H. and Karin, M. (2006) Regulation and function of IKK and IKK-related kinases. *Sci STKE*, **2006**, re13.

Hatakeyama, S., Kitagawa, M., Nakayama, K., Shirane, M., Matsumoto, M., Hattori, K., Higashi, H., Nakano, H., Okumura, K., Onoe, K., Good, R.A. and Nakayama, K. (1999) Ubiquitin-dependent degradation of IkappaBalpha is

mediated by a ubiquitin ligase Skp1/Cul 1/F-box protein FWD1. *Proc Natl Acad Sci U S A*, **96**, 3859-3863.

Hayden, M.S. and Ghosh, S. (2008) Shared principles in NF-kappaB signaling. *Cell*, **132**, 344-362.

Hayden, M.S., West, A.P. and Ghosh, S. (2006) SnapShot: NF-kappaB signaling pathways. *Cell*, **127**, 1286-1287.

Heissmeyer, V., Macian, F., Im, S.H., Varma, R., Feske, S., Venuprasad, K., Gu, H., Liu, Y.C., Dustin, M.L. and Rao, A. (2004) Calcineurin imposes T cell unresponsiveness through targeted proteolysis of signaling proteins. *Nat Immunol*, **5**, 255-265.

Hemmi, H., Takeuchi, O., Sato, S., Yamamoto, M., Kaisho, T., Sanjo, H., Kawai, T., Hoshino, K., Takeda, K. and Akira, S. (2004) The roles of two IkappaB kinase-related kinases in lipopolysaccharide and double stranded RNA signaling and viral infection. *J Exp Med*, **199**, 1641-1650.

Hershko, A. and Ciechanover, A. (1998) The ubiquitin system. *Annu Rev Biochem*, **67**, 425-479.

Hinz, M. and Scheidereit, C. (2007) Striking back at the activator: how IkappaB kinase terminates antigen receptor responses. *Sci STKE*, **2007**, pe19.

Hoberg, J.E., Popko, A.E., Ramsey, C.S. and Mayo, M.W. (2006) IkappaB kinase alpha-mediated derepression of SMRT potentiates acetylation of RelA/p65 by p300. *Mol Cell Biol*, **26**, 457-471.

Hoffmann, A., Levchenko, A., Scott, M.L. and Baltimore, D. (2002) The IkappaB-NF-kappaB signaling module: temporal control and selective gene activation. *Science*, **298**, 1241-1245.

Hoffmann, A., Natoli, G. and Ghosh, G. (2006) Transcriptional regulation via the NF-kappaB signaling module. *Oncogene*, **25**, 6706-6716.

Hu, M.C., Lee, D.F., Xia, W., Golfman, L.S., Ou-Yang, F., Yang, J.Y., Zou, Y., Bao, S., Hanada, N., Saso, H., Kobayashi, R. and Hung, M.C. (2004) IkappaB kinase promotes tumorigenesis through inhibition of forkhead FOXO3a. *Cell*, **117**, 225-237.

Huang, T.T., Kudo, N., Yoshida, M. and Miyamoto, S. (2000) A nuclear export signal in the N-terminal regulatory domain of IkappaBalpha controls cytoplasmic

localization of inactive NF-kappaB/IkappaBalpha complexes. *Proc Natl Acad Sci U S A*, **97**, 1014-1019.

Huang, T.T., Wuerzberger-Davis, S.M., Wu, Z.H. and Miyamoto, S. (2003) Sequential modification of NEMO/IKKgamma by SUMO-1 and ubiquitin mediates NF-kappaB activation by genotoxic stress. *Cell*, **115**, 565-576.

Huang, W.C., Ju, T.K., Hung, M.C. and Chen, C.C. (2007) Phosphorylation of CBP by IKKalpha promotes cell growth by switching the binding preference of CBP from p53 to NF-kappaB. *Mol Cell*, **26**, 75-87.

Huxford, T., Huang, D.B., Malek, S. and Ghosh, G. (1998) The crystal structure of the IkappaBalpha/NF-kappaB complex reveals mechanisms of NF-kappaB inactivation. *Cell*, **95**, 759-770.

Israel, A. (1995) A role for phosphorylation and degradation in the control of NF-kappa B activity. *Trends Genet*, **11**, 203-205.

Jacobs, M.D. and Harrison, S.C. (1998) Structure of an IkappaBalpha/NF-kappaB complex. *Cell*, **95**, 749-758.

Jacque, E., Tchenio, T., Piton, G., Romeo, P.H. and Baud, V. (2005) RelA repression of RelB activity induces selective gene activation downstream of TNF receptors. *Proc Natl Acad Sci U S A*, **102**, 14635-14640.

Janssens, S., Tinel, A., Lippens, S. and Tschopp, J. (2005) PIDD mediates NF-kappaB activation in response to DNA damage. *Cell*, **123**, 1079-1092.

Janssens, S. and Tschopp, J. (2006) Signals from within: the DNA-damage-induced NF-kappaB response. *Cell Death Differ*, **13**, 773-784.

Jiang, X., Takahashi, N., Matsui, N., Tetsuka, T. and Okamoto, T. (2003) The NF-kappa B activation in lymphotoxin beta receptor signaling depends on the phosphorylation of p65 at serine 536. *J Biol Chem*, **278**, 919-926.

Jimi, E. and Ghosh, S. (2005) Role of nuclear factor-kappaB in the immune system and bone. *Immunol Rev*, **208**, 80-87.

Jono, H., Lim, J.H., Chen, L.F., Xu, H., Trompouki, E., Pan, Z.K., Mosialos, G. and Li, J.D. (2004) NF-kappaB is essential for induction of CYLD, the negative regulator of NF-kappaB: evidence for a novel inducible autoregulatory feedback pathway. *J Biol Chem*, **279**, 36171-36174.

Karin, M. and Ben-Neriah, Y. (2000) Phosphorylation meets ubiquitination: the control of NF-[kappa]B activity. *Annu Rev Immunol*, **18**, 621-663.

Karin, M. and Delhase, M. (2000) The I kappa B kinase (IKK) and NF-kappa B: key elements of proinflammatory signalling. *Semin Immunol*, **12**, 85-98.

Kato, T., Jr., Delhase, M., Hoffmann, A. and Karin, M. (2003) CK2 Is a C-Terminal IkappaB Kinase Responsible for NF-kappaB Activation during the UV Response. *Mol Cell*, **12**, 829-839.

Kiernan, R., Bres, V., Ng, R.W., Coudart, M.P., El Messaoudi, S., Sardet, C., Jin, D.Y., Emiliani, S. and Benkirane, M. (2003) Post-activation turn-off of NF-kappa B-dependent transcription is regulated by acetylation of p65. *J Biol Chem*, **278**, 2758-2766.

Kim, H.J., Hawke, N. and Baldwin, A.S. (2006) NF-kappaB and IKK as therapeutic targets in cancer. *Cell Death Differ*, **13**, 738-747.

Kishore, N., Huynh, Q.K., Mathialagan, S., Hall, T., Rouw, S., Creely, D., Lange, G., Caroll, J., Reitz, B., Donnelly, A., Boddupalli, H., Combs, R.G., Kretzmer, K. and Tripp, C.S. (2002) IKK-i and TBK-1 are enzymatically distinct from the homologous enzyme IKK-2: comparative analysis of recombinant human IKK-i, TBK-1, and IKK-2. *J Biol Chem*, **277**, 13840-13847.

Korherr, C., Gille, H., Schafer, R., Koenig-Hoffmann, K., Dixelius, J., Egland, K.A., Pastan, I. and Brinkmann, U. (2006) Identification of proangiogenic genes and pathways by high-throughput functional genomics: TBK1 and the IRF3 pathway. *Proc Natl Acad Sci U S A*, **103**, 4240-4245.

Kovalenko, A., Chable-Bessia, C., Cantarella, G., Israel, A., Wallach, D. and Courtois, G. (2003) The tumour suppressor CYLD negatively regulates NF-kappaB signalling by deubiquitination. *Nature*, **424**, 801-805.

Krappmann, D. and Scheidereit, C. (2005) A pervasive role of ubiquitin conjugation in activation and termination of IkappaB kinase pathways. *EMBO Rep*, **6**, 321-326.

Kravchenko, V.V., Mathison, J.C., Schwamborn, K., Mercurio, F. and Ulevitch, R.J. (2003) IKKi/IKKepsilon plays a key role in integrating signals induced by pro-inflammatory stimuli. *J Biol Chem*, **278**, 26612-26619.

Lang, V., Janzen, J., Fischer, G.Z., Soneji, Y., Beinke, S., Salmeron, A., Allen, H., Hay, R.T., Ben-Neriah, Y. and Ley, S.C. (2003) betaTrCP-mediated

proteolysis of NF-kappaB1 p105 requires phosphorylation of p105 serines 927 and 932. *Mol Cell Biol*, **23**, 402-413.

Lawrence, T., Bebien, M., Liu, G.Y., Nizet, V. and Karin, M. (2005) IKKalpha limits macrophage NF-kappaB activation and contributes to the resolution of inflammation. *Nature*, **434**, 1138-1143.

Li, Q., Lu, Q., Bottero, V., Estepa, G., Morrison, L., Mercurio, F. and Verma, I.M. (2005) Enhanced NF-kappaB activation and cellular function in macrophages lacking IkappaB kinase 1 (IKK1). *Proc Natl Acad Sci U S A*, **102**, 12425-12430.

Li, Q. and Verma, I.M. (2002) NF-kappaB regulation in the immune system. *Nat Rev Immunol*, **2**, 725-734.

Ling, L., Cao, Z. and Goeddel, D.V. (1998) NF-kappaB-inducing kinase activates IKK-alpha by phosphorylation of Ser-176. *Proc Natl Acad Sci U S A*, **95**, 3792-3797.

Liu, Y.C. (2004) Ubiquitin ligases and the immune response. *Annu Rev Immunol*, **22**, 81-127.

Lobry, C., Lopez, T., Israel, A. and Weil, R. (2007) Negative feedback loop in T cell activation through IkappaB kinase-induced phosphorylation and degradation of Bcl10. *Proc Natl Acad Sci U S A*, **104**, 908-913.

Maine, G.N. and Burstein, E. (2007) COMMD proteins and the control of the NF kappa B pathway. *Cell Cycle*, **6**, 672-676.

Maine, G.N., Mao, X., Komarck, C.M. and Burstein, E. (2007) COMMD1 promotes the ubiquitination of NF-kappaB subunits through a cullin-containing ubiquitin ligase. *EMBO J*, **26**, 436-447.

Makris, C., Roberts, J.L. and Karin, M. (2002) The carboxyl-terminal region of IkappaB kinase gamma (IKKgamma) is required for full IKK activation. *Mol Cell Biol*, **22**, 6573-6581.

Maniatis, T., Falvo, J.V., Kim, T.H., Kim, T.K., Lin, C.H., Parekh, B.S. and Wathelet, M.G. (1998) Structure and function of the interferon-beta enhanceosome. *Cold Spring Harb Symp Quant Biol*, **63**, 609-620.

Marienfeld, R., Berberich-Siebelt, F., Berberich, I., Denk, A., Serfling, E. and Neumann, M. (2001) Signal-specific and phosphorylation-dependent RelB

degradation: a potential mechanism of NF-kappaB control. *Oncogene*, **20**, 8142-8147.

Martone, R., Euskirchen, G., Bertone, P., Hartman, S., Royce, T.E., Luscombe, N.M., Rinn, J.L., Nelson, F.K., Miller, P., Gerstein, M., Weissman, S. and Snyder, M. (2003) Distribution of NF-kappaB-binding sites across human chromosome 22. *Proc Natl Acad Sci U S A*, **100**, 12247-12252.

Mattioli, I., Dittrich-Breiholz, O., Livingstone, M., Kracht, M. and Schmitz, M.L. (2004a) Comparative analysis of T-cell costimulation and CD43 activation reveals novel signaling pathways and target genes. *Blood*, **104**, 3302-3304.

Mattioli, I., Geng, H., Sebald, A., Hodel, M., Bucher, C., Kracht, M. and Schmitz, M.L. (2006) Inducible phosphorylation of NF-kappa B p65 at serine 468 by T cell costimulation is mediated by IKK epsilon. *J Biol Chem*, **281**, 6175-6183.

Mattioli, I., Sebald, A., Bucher, C., Charles, R.P., Nakano, H., Doi, T., Kracht, M. and Schmitz, M.L. (2004b) Transient and selective NF-kappa B p65 serine 536 phosphorylation induced by T cell costimulation is mediated by I kappa B kinase beta and controls the kinetics of p65 nuclear import. *J Immunol*, **172**, 6336-6344.

May, M.J., Marienfeld, R.B. and Ghosh, S. (2002) Characterization of the Ikappa B-kinase NEMO binding domain. *J Biol Chem*, **277**, 45992-46000.

McWhirter, S.M., Fitzgerald, K.A., Rosains, J., Rowe, D.C., Golenbock, D.T. and Maniatis, T. (2004) IFN-regulatory factor 3-dependent gene expression is defective in Tbk1-deficient mouse embryonic fibroblasts. *Proc Natl Acad Sci U S A*, **101**, 233-238.

Mercurio, F., Zhu, H., Murray, B.W., Shevchenko, A., Bennett, B.L., Li, J., Young, D.B., Barbosa, M., Mann, M., Manning, A. and Rao, A. (1997) IKK-1 and IKK-2: cytokine-activated IkappaB kinases essential for NF-kappaB activation. *Science*, **278**, 860-866.

Natoli, G. and Chiocca, S. (2008) Nuclear ubiquitin ligases, NF-kappaB degradation, and the control of inflammation. *Sci Signal*, **1**, pe1.

Nelson, D.E., Ihekwaba, A.E., Elliott, M., Johnson, J.R., Gibney, C.A., Foreman, B.E., Nelson, G., See, V., Horton, C.A., Spiller, D.G., Edwards, S.W., McDowell, H.P., Unitt, J.F., Sullivan, E., Grimley, R., Benson, N., Broomhead, D., Kell, D.B. and White, M.R. (2004) Oscillations in NF-kappaB signaling control the dynamics of gene expression. *Science*, **306**, 704-708.

Neumann, M. and Naumann, M. (2007) Beyond IkappaBs: alternative regulation of NF-kappaB activity. *Faseb J*, **21**, 2642-2654.

Nolan, G.P., Ghosh, S., Liou, H.C., Tempst, P. and Baltimore, D. (1991) DNA binding and I kappa B inhibition of the cloned p65 subunit of NF-kappa B, a rel-related polypeptide. *Cell*, **64**, 961-969.

O'Mahony, A.M., Montano, M., Van Beneden, K., Chen, L.F. and Greene, W.C. (2004) Human T-cell lymphotropic virus type 1 tax induction of biologically Active NF-kappaB requires IkappaB kinase-1-mediated phosphorylation of RelA/p65. *J Biol Chem*, **279**, 18137-18145.

Palombella, V.J., Rando, O.J., Goldberg, A.L. and Maniatis, T. (1994) The ubiquitin-proteasome pathway is required for processing the NF-kappa B1 precursor protein and the activation of NF-kappa B. *Cell*, **78**, 773-785.

Panne, D., Maniatis, T. and Harrison, S.C. (2007) An atomic model of the interferon-beta enhanceosome. *Cell*, **129**, 1111-1123.

Park, S.W., Huq, M.D., Hu, X. and Wei, L.N. (2005) Tyrosine nitration on p65: a novel mechanism to rapidly inactivate nuclear factor-kappaB. *Mol Cell Proteomics*, **4**, 300-309.

Paz, S., Sun, Q., Nakhaei, P., Romieu-Mourez, R., Goubau, D., Julkunen, I., Lin, R. and Hiscott, J. (2006) Induction of IRF-3 and IRF-7 phosphorylation following activation of the RIG-I pathway. *Cell Mol Biol (Noisy-le-grand)*, **52**, 17-28.

Perkins, N.D. (2006) Post-translational modifications regulating the activity and function of the nuclear factor kappa B pathway. *Oncogene*, **25**, 6717-6730.

Perkins, N.D. (2007) Integrating cell-signalling pathways with NF-kappaB and IKK function. *Nat Rev Mol Cell Biol*, **8**, 49-62.

Perkins, N.D. and Gilmore, T.D. (2006) Good cop, bad cop: the different faces of NF-kappaB. *Cell Death Differ*, **13**, 759-772.

Perry, A.K., Chow, E.K., Goodnough, J.B., Yeh, W.C. and Cheng, G. (2004) Differential requirement for TANK-binding kinase-1 in type I interferon responses to toll-like receptor activation and viral infection. *J Exp Med*, **199**, 1651-1658.

Peters, R.T., Liao, S.M. and Maniatis, T. (2000) IKKepsilon is part of a novel PMA-inducible IkappaB kinase complex. *Mol Cell*, **5**, 513-522.

Peters, R.T. and Maniatis, T. (2001) A new family of IKK-related kinases may function as I kappa B kinase kinases. *Biochim Biophys Acta*, **1471**, M57-62.

Pomerantz, J.L. and Baltimore, D. (1999) NF-kappaB activation by a signaling complex containing TRAF2, TANK and TBK1, a novel IKK-related kinase. *Embo J*, **18**, 6694-6704.

Ravi, R., Bedi, A., Fuchs, E.J. and Bedi, A. (1998) CD95 (Fas)-induced caspase-mediated proteolysis of NF-kappaB. *Cancer Res*, **58**, 882-886.

Regnier, C.H., Song, H.Y., Gao, X., Goeddel, D.V., Cao, Z. and Rothe, M. (1997) Identification and characterization of an IkappaB kinase. *Cell*, **90**, 373-383.

Rothwarf, D.M., Zandi, E., Natoli, G. and Karin, M. (1998) IKK-gamma is an essential regulatory subunit of the IkappaB kinase complex. *Nature*, **395**, 297-300.

Rudolph, D., Yeh, W.C., Wakeham, A., Rudolph, B., Nallainathan, D., Potter, J., Elia, A.J. and Mak, T.W. (2000) Severe liver degeneration and lack of NF-kappaB activation in NEMO/IKKgamma-deficient mice. *Genes Dev*, **14**, 854-862.

Ryo, A., Suizu, F., Yoshida, Y., Perrem, K., Liou, Y.C., Wulf, G., Rottapel, R., Yamaoka, S. and Lu, K.P. (2003) Regulation of NF-kappaB signaling by Pin1-dependent prolyl isomerization and ubiquitin-mediated proteolysis of p65/RelA. *Mol Cell*, **12**, 1413-1426.

Saccani, S., Marazzi, I., Beg, A.A. and Natoli, G. (2004) Degradation of promoter-bound p65/RelA is essential for the prompt termination of the nuclear factor kappaB response. *J Exp Med*, **200**, 107-113.

Saccani, S., Pantano, S. and Natoli, G. (2003) Modulation of NF-kappaB activity by exchange of dimers. *Mol Cell*, **11**, 1563-1574.

Sakurai, H., Chiba, H., Miyoshi, H., Sugita, T. and Toriumi, W. (1999) IkappaB kinases phosphorylate NF-kappaB p65 subunit on serine 536 in the transactivation domain. *J Biol Chem*, **274**, 30353-30356.

Scharschmidt, E., Wegener, E., Heissmeyer, V., Rao, A. and Krappmann, D. (2004) Degradation of Bcl10 induced by T-cell activation negatively regulates NF-kappa B signaling. *Mol Cell Biol*, **24**, 3860-3873.

Scherer, D.C., Brockman, J.A., Chen, Z., Maniatis, T. and Ballard, D.W. (1995) Signal-induced degradation of I kappa B alpha requires site-specific ubiquitination. *Proc Natl Acad Sci U S A*, **92**, 11259-11263.

Schmid, J.A., Birbach, A., Hofer-Warbinek, R., Pengg, M., Burner, U., Furtmuller, P.G., Binder, B.R. and de Martin, R. (2000) Dynamics of NF kappa B and Ikappa Balpha studied with green fluorescent protein (GFP) fusion proteins. Investigation of GFP-p65 binding to DNa by fluorescence resonance energy transfer. *J Biol Chem*, **275**, 17035-17042.

Schmitz, M.L. and Baeuerle, P.A. (1991) The p65 subunit is responsible for the strong transcription activating potential of NF-kappa B. *Embo J*, **10**, 3805-3817.

Schmitz, M.L., dos Santos Silva, M.A., Altmann, H., Czisch, M., Holak, T.A. and Baeuerle, P.A. (1994) Structural and functional analysis of the NF-kappa B p65 C terminus. An acidic and modular transactivation domain with the potential to adopt an alpha-helical conformation. *J Biol Chem*, **269**, 25613-25620.

Schmitz, M.L., dos Santos Silva, M.A. and Baeuerle, P.A. (1995) Transactivation domain 2 (TA2) of p65 NF-kappa B. Similarity to TA1 and phorbol ester-stimulated activity and phosphorylation in intact cells. *J Biol Chem*, **270**, 15576-15584.

Schwabe, R.F. and Sakurai, H. (2005) IKKbeta phosphorylates p65 at S468 in transactivaton domain 2. *Faseb J*, **19**, 1758-1760.

Senftleben, U., Cao, Y., Xiao, G., Greten, F.R., Krahn, G., Bonizzi, G., Chen, Y., Hu, Y., Fong, A., Sun, S.C. and Karin, M. (2001) Activation by IKKalpha of a second, evolutionary conserved, NF-kappa B signaling pathway. *Science*, **293**, 1495-1499.

Sharma, S., tenOever, B.R., Grandvaux, N., Zhou, G.P., Lin, R. and Hiscott, J. (2003) Triggering the interferon antiviral response through an IKK-related pathway. *Science*, **300**, 1148-1151.

Shi, C.S. and Kehrl, J.H. (2003) Tumor necrosis factor (TNF)-induced germinal center kinase-related (GCKR) and stress-activated protein kinase (SAPK) activation depends upon the E2/E3 complex Ubc13-Uev1A/TNF receptor-associated factor 2 (TRAF2). *J Biol Chem*, **278**, 15429-15434.

Shimada, T., Kawai, T., Takeda, K., Matsumoto, M., Inoue, J., Tatsumi, Y., Kanamaru, A. and Akira, S. (1999) IKK-i, a novel lipopolysaccharide-inducible kinase that is related to IkappaB kinases. *Int Immunol*, **11**, 1357-1362.

Siebenlist, U., Franzoso, G. and Brown, K. (1994) Structure, regulation and function of NF-kappa B. *Annu Rev Cell Biol*, **10**, 405-455.

Sil, A.K., Maeda, S., Sano, Y., Roop, D.R. and Karin, M. (2004) IkappaB kinase-alpha acts in the epidermis to control skeletal and craniofacial morphogenesis. *Nature*, **428**, 660-664.

Sizemore, N., Lerner, N., Dombrowski, N., Sakurai, H. and Stark, G.R. (2002) Distinct roles of the Ikappa B kinase alpha and beta subunits in liberating nuclear factor kappa B (NF-kappa B) from Ikappa B and in phosphorylating the p65 subunit of NF-kappa B. *J Biol Chem*, **277**, 3863-3869.

Solis, M., Romieu-Mourez, R., Goubau, D., Grandvaux, N., Mesplede, T., Julkunen, I., Nardin, A., Salcedo, M. and Hiscott, J. (2007) Involvement of TBK1 and IKKepsilon in lipopolysaccharide-induced activation of the interferon response in primary human macrophages. *Eur J Immunol*, **37**, 528-539.

Tanahashi, M., Yokoyama, T., Kobayashi, Y., Yamakawa, Y., Maeda, M. and Fujii, Y. (2001) Effect of phorbol ester and calcium ionophore on human thymocytes. *Hum Immunol*, **62**, 771-781.

Tanaka, T., Grusby, M.J. and Kaisho, T. (2007) PDLIM2-mediated termination of transcription factor NF-kappaB activation by intranuclear sequestration and degradation of the p65 subunit. *Nat Immunol*, **8**, 584-591.

Tegethoff, S., Behlke, J. and Scheidereit, C. (2003) Tetrameric oligomerization of IkappaB kinase gamma (IKKgamma) is obligatory for IKK complex activity and NF-kappaB activation. *Mol Cell Biol*, **23**, 2029-2041.

tenOever, B.R., Sharma, S., Zou, W., Sun, Q., Grandvaux, N., Julkunen, I., Hemmi, H., Yamamoto, M., Akira, S., Yeh, W.C., Lin, R. and Hiscott, J. (2004) Activation of TBK1 and IKKvarepsilon kinases by vesicular stomatitis virus infection and the role of viral ribonucleoprotein in the development of interferon antiviral immunity. *J Virol*, **78**, 10636-10649.

Tergaonkar, V., Bottero, V., Ikawa, M., Li, Q. and Verma, I.M. (2003) IkappaB kinase-independent IkappaBalpha degradation pathway: functional NF-kappaB activity and implications for cancer therapy. *Mol Cell Biol*, **23**, 8070-8083.

Tian, Y., Zhang, Y., Zhong, B., Wang, Y.Y., Diao, F.C., Wang, R.P., Zhang, M., Chen, D.Y., Zhai, Z.H. and Shu, H.B. (2007) RBCK1 negatively regulates tumor necrosis factor- and interleukin-1-triggered NF-kappaB activation by targeting TAB2/3 for degradation. *J Biol Chem*, **282**, 16776-16782.

Tojima, Y., Fujimoto, A., Delhase, M., Chen, Y., Hatakeyama, S., Nakayama, K., Kaneko, Y., Nimura, Y., Motoyama, N., Ikeda, K., Karin, M. and Nakanishi, M. (2000) NAK is an IkappaB kinase-activating kinase. *Nature*, **404**, 778-782.

Toledano, M.B., Ghosh, D., Trinh, F. and Leonard, W.J. (1993) N-terminal DNA-binding domains contribute to differential DNA-binding specificities of NF-kappa B p50 and p65. *Mol Cell Biol*, **13**, 852-860.

Torrado, M., Senatorov, V.V., Trivedi, R., Fariss, R.N. and Tomarev, S.I. (2004) Pdlim2, a novel PDZ-LIM domain protein, interacts with alpha-actinins and filamin A. *Invest Ophthalmol Vis Sci*, **45**, 3955-3963.

Udalova, I.A., Mott, R., Field, D. and Kwiatkowski, D. (2002) Quantitative prediction of NF-kappa B DNA-protein interactions. *Proc Natl Acad Sci U S A*, **99**, 8167-8172.

Verma, I.M., Stevenson, J.K., Schwarz, E.M., Van Antwerp, D. and Miyamoto, S. (1995) Rel/NF-kappa B/I kappa B family: intimate tales of association and dissociation. *Genes Dev*, **9**, 2723-2735.

Vermeulen, L., De Wilde, G., Van Damme, P., Vanden Berghe, W. and Haegeman, G. (2003) Transcriptional activation of the NF-kappaB p65 subunit by mitogen- and stress-activated protein kinase-1 (MSK1). *Embo J*, **22**, 1313-1324.

Viatour, P., Merville, M.P., Bours, V. and Chariot, A. (2005) Phosphorylation of NF-kappaB and IkappaB proteins: implications in cancer and inflammation. *Trends Biochem Sci*, **30**, 43-52.

Wang, D., Westerheide, S.D., Hanson, J.L. and Baldwin, A.S., Jr. (2000) Tumor necrosis factor alpha-induced phosphorylation of RelA/p65 on Ser529 is controlled by casein kinase II. *J Biol Chem*, **275**, 32592-32597.

Wang, N., Ahmed, S. and Haqqi, T.M. (2005) Genomic structure and functional characterization of the promoter region of human IkappaB kinase-related kinase IKKi/IKKvarepsilon gene. *Gene*, **353**, 118-133.

Wegener, E., Oeckinghaus, A., Papadopoulou, N., Lavitas, L., Schmidt-Supprian, M., Ferch, U., Mak, T.W., Ruland, J., Heissmeyer, V. and Krappmann, D. (2006) Essential role for IkappaB kinase beta in remodeling Carma1-Bcl10-Malt1 complexes upon T cell activation. *Mol Cell*, **23**, 13-23.

Welchman, R.L., Gordon, C. and Mayer, R.J. (2005) Ubiquitin and ubiquitin-like proteins as multifunctional signals. *Nat Rev Mol Cell Biol*, **6**, 599-609.

Wertz, I.E., O'Rourke, K.M., Zhou, H., Eby, M., Aravind, L., Seshagiri, S., Wu, P., Wiesmann, C., Baker, R., Boone, D.L., Ma, A., Koonin, E.V. and Dixit, V.M. (2004) De-ubiquitination and ubiquitin ligase domains of A20 downregulate NF-kappaB signalling. *Nature*, **430**, 694-699.

Whiteside, S.T. and Israel, A. (1997) I kappa B proteins: structure, function and regulation. *Semin Cancer Biol*, **8**, 75-82.

Wietek, C., Cleaver, C.S., Ludbrook, V., Wilde, J., White, J., Bell, D.J., Lee, M., Dickson, M., Ray, K.P. and O'Neill, L.A. (2006) IkappaB kinase epsilon interacts with p52 and promotes transactivation via p65. *J Biol Chem*, **281**, 34973-34981.

Wietek, C. and O'Neill, L.A. (2007) Diversity and regulation in the NF-kappaB system. *Trends Biochem Sci*, **32**, 311-319.

Willems, A.R., Schwab, M. and Tyers, M. (2004) A hitchhiker's guide to the cullin ubiquitin ligases: SCF and its kin. *Biochim Biophys Acta*, **1695**, 133-170.

Winzen, R., Thakur, B.K., Dittrich-Breiholz, O., Shah, M., Redich, N., Dhamija, S., Kracht, M. and Holtmann, H. (2007) Functional analysis of KSRP interaction with the AU-rich element of interleukin-8 and identification of inflammatory mRNA targets. *Mol Cell Biol*, **27**, 8388-8400.

Woronicz, J.D., Gao, X., Cao, Z., Rothe, M. and Goeddel, D.V. (1997) IkappaB kinase-beta: NF-kappaB activation and complex formation with IkappaB kinase-alpha and NIK. *Science*, **278**, 866-869.

Wu, C.J., Conze, D.B., Li, T., Srinivasula, S.M. and Ashwell, J.D. (2006) Sensing of Lys 63-linked polyubiquitination by NEMO is a key event in NF-kappaB activation [corrected]. *Nat Cell Biol*, **8**, 398-406.

Wullaert, A., Heyninck, K., Janssens, S. and Beyaert, R. (2006) Ubiquitin: tool and target for intracellular NF-kappaB inhibitors. *Trends Immunol*, **27**, 533-540.

Xiao, G., Harhaj, E.W. and Sun, S.C. (2001) NF-kappaB-inducing kinase regulates the processing of NF-kappaB2 p100. *Mol Cell*, **7**, 401-409.

Yamaoka, S., Courtois, G., Bessia, C., Whiteside, S.T., Weil, R., Agou, F., Kirk, H.E., Kay, R.J. and Israel, A. (1998) Complementation cloning of NEMO, a component of the IkappaB kinase complex essential for NF-kappaB activation. *Cell*, **93**, 1231-1240.

Yaron, A., Hatzubai, A., Davis, M., Lavon, I., Amit, S., Manning, A.M., Andersen, J.S., Mann, M., Mercurio, F. and Ben-Neriah, Y. (1998) Identification of the receptor component of the IkappaBalpha-ubiquitin ligase. *Nature*, **396**, 590-594.

Yeh, P.Y., Yeh, K.H., Chuang, S.E., Song, Y.C. and Cheng, A.L. (2004) Suppression of MEK/ERK signaling pathway enhances cisplatin-induced NF-kappaB activation by protein phosphatase 4-mediated NF-kappaB p65 Thr dephosphorylation. *J Biol Chem*, **279**, 26143-26148.

Yeung, F., Hoberg, J.E., Ramsey, C.S., Keller, M.D., Jones, D.R., Frye, R.A. and Mayo, M.W. (2004) Modulation of NF-kappaB-dependent transcription and cell survival by the SIRT1 deacetylase. *Embo J*, **23**, 2369-2380.

Zabel, U. and Baeuerle, P.A. (1990) Purified human I kappa B can rapidly dissociate the complex of the NF-kappa B transcription factor with its cognate DNA. *Cell*, **61**, 255-265.

Zandi, E., Chen, Y. and Karin, M. (1998) Direct phosphorylation of IkappaB by IKKalpha and IKKbeta: discrimination between free and NF-kappaB-bound substrate. *Science*, **281**, 1360-1363.

Zandi, E., Rothwarf, D.M., Delhase, M., Hayakawa, M. and Karin, M. (1997) The IkappaB kinase complex (IKK) contains two kinase subunits, IKKalpha and IKKbeta, necessary for IkappaB phosphorylation and NF-kappaB activation. *Cell*, **91**, 243-252.

Zhong, H., May, M.J., Jimi, E. and Ghosh, S. (2002) The phosphorylation status of nuclear NF-kappa B determines its association with CBP/p300 or HDAC-1. *Mol Cell*, **9**, 625-636.

Zhong, H., Voll, R.E. and Ghosh, S. (1998) Phosphorylation of NF-kappa B p65 by PKA stimulates transcriptional activity by promoting a novel bivalent interaction with the coactivator CBP/p300. *Mol Cell*, **1**, 661-671.

Acknowledgements

First and foremost, I would like to thank my supervisor Prof. Dr. M. Lienhard Schmitz for giving me the opportunity to work in his group, for proposing the projects, for his constant support, excellent guidance and creative discussion. It was his invaluable encouragement and suggestions that have given me the motivation and the inspiration to advance the projects. In addition, I am extremely grateful for his careful and critical review of this thesis.

Many thanks to Prof. Dr. Michael Martin for being my doctoral thesis supervisor in the faculty of Biology, as well as for his kind support and review of this thesis.

Furthermore, I would like to thank Prof. Dr. Michael Kracht for his critical discussion and supportive advice during my PhD study.

A special thank goes to Dr. Roger Dennis for his kind help to correct this thesis.

Additionally, I would like to express my sincere thanks to all my colleagues, not only for creating a nice working atmosphere, but also for translating many German documents. It was a great pleasure to work with them.

In particular, I would like to say “Vielen, vielen, vielen Dank” to Stefanie Ritterhoff, Florian Renner, Dr. Marco Antonio Calzado and Dr. Ana Roscic, for their great help, for their invaluable advice, and above all for being very good friends.

I would like to thank Dr. Ivan Mattioli, who gave me a lot of help at the beginning of my PhD study, for his supervision and cooperation.

I am grateful to Tobias Wittwer for cloning siRNA constructs and to Dr. Oliver Dittrich-Breiholz for microarray analyses.

To Dr. Julia Sevilla, Dr. Laureano de la Vega, Rita Moreno, Dr. Katrin Thamm, Dr. Dietmar von der Ahe, Dr. Ekaterina Gresko, Dr. Andrea Sebald, Michael Hodel, Dr. Nadine Schracke and Aysegül Dalmizrak, many thanks for sharing their experience, as well as for providing kind suggestions. To Ines Höfliger and Gabriele Schmidt, sincere thanks for helping me deal with the German administration. To Daniela Stock, Stephanie Wack, Rosel Engel and Katharina Schmid Lüdi, I would like to express my gratitude for their technical assistance.

In addition, extra special thanks to my parents for their never-ending support and love.

Last, but not least, I would like to thank all my friends from different parts of the world, whom I did not mention above.

Erklärung

Hiermit erkläre ich, dass ich die vorliegende Arbeit selbstständig verfasst habe und dabei keine anderen als die angegebenen Quellen und Hilfsmittel verwendet habe. Zitate sind als solche gekennzeichnet.

Giessen, den 28.04.2008

Hui Geng